Control of gene expression in *E. coli* using light induction.

By Maithili Krishnan





Control of gene expression in *E. coli* using light induction.

Ву

Maithili Krishnan

in partial fulfilment of the requirements for the degree of

Master of Science

in Life science and Technology

at the Delft University of Technology, to be defended publicly on Wednesday August 20th, 2014 at 10:00 am.

Supervisor: Dr. Anne S Meyer, BN, TU Delft (Assistant Prof.)

Thesis committee: Dr. Fred Hagen, BT, TU Delft (Prof.)

Dr. Marie-Eve Aubin-Tam, BN, TU Delft (Assistant Prof.)

This thesis is confidential and cannot be made public until December 31, 2014.

An electronic version of this thesis is available at http://repository.tudelft.nl/.



Preface

Synthetic biology has become far more interesting and attractive during the recent decades. After participating in iGEM (International Genetically Engineered Machines) in 2013, I was very keen to work in the field of synthetic biology. And, this project description seemed very innovative and new to me. Using microorganisms to produce enzymes, bio-diesel, biosensor is already giving competition to the convectional production of substances which are leading to a polluted Earth. Green production of materials using light as a source from microorganisms provides a sustainable method for production compared to the current manufacturing sector.

Imagine controlling bacteria and asking it to do what you like!

Controlling the production of biomaterials using light, though seemed like a very easy idea has not been successfully accomplished yet. Producing a complex structure like nacre using light as a control mechanism is the prime challenge.

Analysing different sensor systems, their response circuit and output signals under different intensities of light was the scope of this project. Of course, trying to set up the sensor systems and their light source set-ups in the lab was quite some challenge. Co-ordinating between various experts from field of physics and biology, then trying to bridge their understanding for the experiments was challenging yet thought provoking.

Science is a never-ending quest for answers. And this was something, I learnt during the course of this project. Trying to understand why the experiments didn't work and then formulate several other strategies to make it work, is I think the real magic. One must always be creative when working with science. And I hope that I would continue my quest in understanding nature, that has amazed mankind since the very beginning.

I would like to thank Dr. Anne Meyer for giving me her valuable guidance and support during the course of my project. My special thanks to Michela De Martino, for guiding me and without whom this project could not have been successful. I would like to thank Dr. Roland Kieffer, for building all the devices used in this project. My thanks to Ilja Westerlaken for helping me with a lot of stuff in the lab.

I would like to acknowledge my parents and thank them for always believing in me. My brother, Arvind for always being there whenever I needed support and guidance. I would also like to thank my long list of friends and relatives who have been very understanding during my project duration.

Oh! And not to forget, coffee and the Dutch weather! ©

Finally, I would like to contemplate about that supreme power existing somewhere in this universe for making this lovely earth. I hope we can always preserve and nurture mother earth, the way it is.

Maithili Krishnan Delft, August 2014

Abstract

Biomaterials in nature provide abundant source of inspiration for the design and synthesis of novel high-performance materials. Nacre, a bio-mineralized material found in the inner lining of seashells has recently gained attraction due to its impressive material properties and eco-friendly nature. This ultratough coating could become inexpensive and can be the next-generation technology in aerospace and civil engineering if produced synthetically. The biological production of nacre can make building bio-concrete on Moon and several architectural applications possible.

Controllability in the production of such biomaterials using photo-induction of different wavelengths of light, still remains a challenge. Light is an ideal tool to control living cells since it induces output through an external stimulus¹. This provides great flexibility in controlling cells without having to manipulate the cell at genetic and metabolic level¹. Light-mediated control of gene expression has various applications in the field of functional genomics, systems biology and biotechnology¹.

Previously a recombinant red light-sensor in *Escherichia coli* was engineered by Tabor et.al (2005) by combining Cph1, a red/far-red light switchable cyanobacterial phytochrome and EnvZ/OmpR two-component signalling pathway natively present in *E. coli*. Thereafter, they reported the development of a green sensor in *E. coli* from CcaS-CcaR, a green/red photoswitchable two-component system found in cyanobacteria *Synechocystis*².

This project will study the expression of both red and green sensors in *E. coli* to construct spatial patterning of layers of output, with further purpose of producing bio-layers of nacre. Study of the two-optical control of transcription across a layer of engineered cells will be the prime aim. Creation of patterns using these engineered cells can be helpful in designing the production of alternate output layers. The transfer function (the relationship between input strength and output strength) of each sensor individually and in combination will be studied, as well as tuning the output through different durations of light application. Fine tuning of the circuit to improve the background output is of high consideration for such a light-switch based application. Therefore, an attempt to create a random RBS library in order to reduce the background output signal given by the sensors under dark will be carried out.

Contents

List of	jures	9
List of	bles	11
List of	breviations	12
	uction	
	ontrol of gene expression using light	
	cope of the project	
1.3.	pecifications of sensor system	17
1.4.	oal of the project	20
1.5.	oject Overview	22
2. Mat	als and Methods	23
2.1.	eliminary set-up	23
	1.1. Properties of plasmids and strains	23
	1.2. Expression of red and green sensors in <i>E. coli</i>	24
	1.3. Wavelength and intensity of light	25
2.2.	naracterize sensors by pattern creation	26
	2.1. Light Induction Device (LID) Set-Up	26
	2.2. β-galactosidase/S-gal reporter system	27
	2.3. Quantifying signal intensity using ImageJ	27
2.3.	naracterize sensors by quantification of LacZ	28
	3.1. Array Tube Illuminator set up	28
	3.2. Miller assay	30
2.4.	ne tuning the sensor system	31
	4.1. RBS library generation	31
	S	
	verview	
	reliminary results	
3.3.	naracterization of sensors by pattern creation	
	3.1. Pattern creation	
	3.2. Scope of pattern creation	
	3.3. Comparison of sensors	
	3.4. Gradient experiment	
	naracterization of sensors by quantification of LacZ	
3.5.	ne tuning the sensor system5.1. Using site-directed mutagenesis by randomised primers (method I)	
	5.2. Using error prone PCR coupled with randomized primers (method II)	
4 D:	5.3. Using synthetically designed oligonucleotide with random base pairs (method III)	
	sion	
	k рhy	
_	pny	

List of Figures

Figure 1 Circuit of red, green and green-red sensor systems (adapted from Tabor et al., 2010)1
Figure 2 Schematic diagram of nacre showing calcium carbonate (CaCO ₃) layers with biopolymers in between
them (top); Nacre in sea shells (bottom-left); Electron microscopy image of nacre (bottom-right). 25
Figure 3 Preliminary set-up of light induction at room temperature (left) and on heat block at 37 °C (right)2
Figure 4 Light Induction Device (LID) shown diagrammatically (left) and real device (right)2
Figure 5 The glycosidic bond of S-gal which is cleaved by β -galactosidase (a); Two esculetins bonded by ferr
iron, which forms the black pigment (b). (Adapted from Tabor et al., 2010)
Figure 6 Circuit of green and red sensor systems with activation and deactivation wavelengths of light; Design of
Light tube array ³
Figure 7 Design and set-up of Array Tube Illuminator; A - design specifications; B - Different components of
Array Tube Illuminator; C - set-up after assembling; D - Array Tube Illuminator kept inside 37 °C shakir
incubator
Figure 8 Chemical reaction of Miller assay
Figure 9 Plasmid map of pJT106b indicating the site of RBS library generation
Figure 10 Diagrammatic view of RBS library creation using method I
Figure 11 Insert containing RBS and cI for error prone PCR
Figure 12 Diagrammatic view of RBS library creation using method III
Figure 13 Light induction of all sensors and control under room temp and 37 °C
Figure 14 All sensors and control under dark, red, green and green + far-red light - 12 hr and 24 hr (edited image
Appendix III-1 shows the original plates
Figure 15 Different pattern examples used for analysis
Figure 16 Pattern creation on petri dish containing red, green and green-red sensor by red, green and green + fa
red light (edited images) Appendix III-1 show original images.
$Figure\ 17\ Pattern\ creation\ using\ red\ sensor\ under\ red\ light\ 0.06\ W/m2\ after\ 12-15\ hours\ (both\ grey\ scale\ (original original ori$
coloured version)
Figure 18 Examples of pattern development using the sensor systems (both grey scale (original) and coloured)
picture image of a person on a petri dish (left); TU Delft logo (middle); TU delft written on petri dish (right); Th
bacterial image can be clearly distinguished till ~ 1.5 mm, which was measured by a red line on the design on the
flame holder in TU Delft logo (middle - bottom plate).
Figure 19 Comparison of all sensor systems and control strain under red, green and green + far-red light with
pattern 2 using LID after 24 hours (edited images). Appendix III-1 shows the original image of plates4
Figure 20 Output signals of different sensor systems under red, green and green + far-red light; Bg: background
output of GR (green-red sensor), G(green sensor), R (red sensor)
Figure 21 Gradient of green, green + far-red and red light intensity on green and red sensors (original)

Figure 22 Gradient plate showing different intensities for green light and bands which were quanti	fied using
ImageJ software	45
Figure 23 Output signals of green sensor with respect to gradient intensities of green and green + far-red l	light46
Figure 24 Output signals of red sensor with respect to gradient intensities of red light	46
Figure 25 Miller Unit output for red sensor with respect to different intensities of red light (a), green light	ght (b) and
green + red light (c) induction over time.	49
Figure 26 Miller Unit output for green sensor with respect to different intensities of red light (a), green light	ght (b) and
green + red light (c) induction over time.	51
Figure 27 Miller Unit output for green - red sensor with respect to different intensities of red light (a),	green light
(b) and green + red light (c) induction over time	52
Figure 28 Light controlled gene expression in $E. coli$, (a) Under different intensities of green light -0 ,	2, 4 and 6
W/m^2 ; (b) Under different intensities of red light -0 , 0.5, 1 and 2 W/m^2 after \sim 8 hours of induction;	Green and
green-red sensors correspond to the left axis, red sensor corresponds to the right axis.	54
Figure 29 Screening of RBS library colonies created from Method I.	55
Figure 30 Screening of RBS library colonies created from Method II.	56
Figure 31 Screening of 63 colonies of RBS library from Method III for less black output generation und	der dark at
37 °C (b3:pJT106b3 plasmid; JT2: E. coli strain; G-R: green-red sensor)	57
Figure 32 Miller assay on RBS library colonies after 7 hours of under dark	58
Figure 33 Spectrum of green and far-red 731 LEDs, the supply intensity of each LED has been adjusted	d for same
power intensity.	72
Figure 34 Holder for LED and filters which fit on PVC tube of 95mm inner diameter	73
Figure 35 Design of Array Tube Illuminator	74
Figure 36 Electronic driver for one line of LED	75
Figure 37 Transient regime simulation of circuit; green line represents a PWM signal at 50% duty of	cycle from
Arduino; red line represents the current in the LED branch.	75
Figure 38 Calibration of LEDs used in six rows of Array Tube Illuminator	76
Figure 39 Integrated graphs of Miller unit output vs. time of induction for all sensors under different int	tensities of
light	80
Figure 40 Fold induction over dark for red and green sensor exposed to different wavelengths of light	81
Figure 41 Miller units for green and red sensors under dark, green and red light with and without presen	ce of PCB
molecules	81
Figure 42 Calibration for each sensor for Miller assay.	83
Figure 43 Calibration of pattern 3 using ImageJ software	83

List of Tables

Table 1 Description of plasmids used in the generation of sensor systems.	19
Table 2 Properties of light sensing strains	24
Table 3 Overview of results	34
Table 4 List of experiments carried out on Array Tube Illuminator	48
Table 5 Sequencing results of colonies in method I	55
Table 6 Sequencing results of colonies in method II	56
Table 7 Sequencing results of colonies in method III	57

List of Abbreviations

DNA	Deoxyribonucleic acid
E. coli	Escherichia coli
PCB	Phycocyanacobilin
LID	Light induction device
UV	Ultra violet
IPTG	Isopropyl β-D-1-thiogalactopyranoside
FAD	Flavin adenine dinucleotide
BLUF	Blue-Light Using FAD
Pr	Red light absorbing ground state
Pfr	Far-red light absorbing activated state
LED	Light emitting diode
RBS	Ribosome binding site
S-gal	3,4-cyclohexenoesculetin-ß-D-galactopyranoside
Psuffix	Promoter gene
Cm	Chloramphenicol
Amp	Ampicillin
Spec	Spectinomycin
LB	Lysogeny broth/ Luria-Bertani
PCR	Polymerase chain reaction
TetR	Tetracycline repressor protein
OD ₆₀₀	Optical density measured at 600 nm
W/m ²	Watt per square metre, measure of intensity of light
mL	Milli litre
μL	Micro litre
Rpm	Revolutions per minute
KCl	Potassium chloride
dNTP	Deoxynucleotide triphosphates
mM	Millimolar [1Molar = 1 mol/L]
DTT	Dithiothreitol
NAD	Nicotinamide adenine dinucleotide
PEG	Polyethylene glycol
PVC tube	Polyvinyl chloride tube

Introduction

"It always seems impossible until it's done." – Nelson Mandela

The idea of building bio-concrete on Moon to build new ventures for the future seems like the most impossible notion. Mankind has yet achieved a lot in the 21st century that seemed difficult earlier. For example, creating artificial organs like heart (Abiocor), liver and pancreas has been made possible by AbioMed and Alin foundation. 3D-printing of food items like cookies and carrots for healthy and sustainable life has been demonstrated by scientists at Netherlands Organization for Applied Scientific Research TNO.

Similarly, engineering bacteria to produce bio materials like nacre is one such futuristic goal in the Department of Bionanoscience at Delft University of technology. The high toughness of nacre has vast application in architecture and civil engineering.

Genetic circuits which regulate the input signal to output signals are driven by the cellular environment and its changes. Dynamic characterization of some gene circuits have been done to create step changes in the extracellular molecules while measuring the intracellular responses³. However, the complexity of using chemical signalling limits their application to a certain level. Diffusion and transportation of chemicals across cellular membranes bring delay and slows down the output signal³. Using light to control gene expression can by-pass these limitations and allow for dynamic characterization of any gene pathway. In this project we expect to gain better understanding of light sensor systems and hope to use it for more applications in synthetic biology.

1.1. Control of gene expression using light

There are several light sensors existing in nature which differ in structure but are able to respond to changing light conditions. Thomas Drepper et al., 2010 summarised various light induction of biological reactions done by photo-caged molecules, enzymes or photoreceptors. A brief introduction to the various photoreceptors used in the control of gene expression is given below¹:

1) Chemical caging:

UV radiation can activate biological functions in caged inactive effectors which are inactive due to the presence of a caging group⁴. There are many small effectors molecules that control gene expression by binding to proteins involved in that pathway¹. For example, it has been revealed that caged IPTG 1 and doxycycline assist in the control of gene expression⁵. Induction with UV light makes the caged IPTG active by releasing the caged group thus allowing it to bind to LacI-repressor. This initiates the gene expression which was earlier repressed by LacI. These caging groups can also be integrated into a protein structure¹. For example, caged tyrosine introduced in the T7 polymerase, made the enzyme inactive, whereas on decaging, it restored the enzyme activity¹.

However, these caged compounds are rather complex. This limits their use in a wide range of organisms¹. Targeting of specific compounds *in vivo* through light induction can also be tricky.

However in nature, there are different photo-receptor families, chromophore-binding input domains and light induced output domains. Microorganisms use a combination of different sensors, input domains and output domains in a systematic manner to sense light¹.

2) Natural microbial photoreceptors:

Natural photoreceptors contain chromophores embedded inside their structure, which are small light-absorbing molecules. Different chromophores react to light thus enabling the photoreceptor to respond to different wavelengths of light⁶. This light absorption then triggers the excitation of chromophore leading to conformational changes of the nearby proteins⁶. Many organisms have different chromophores responding to different wavelengths of light¹. In order to control the gene expression it is necessary to understand the sensory event and the signal transduction mechanism of the photoreceptors.

Some examples of the signal transduction methods of photoreceptors seen in nature are:

- a) Signal transduction via protein-protein interaction:
 - The most well characterised sensor is the red/far-red light-sensitive phytochromes of *Bradhyrhizobium* and phototrophic bacterium *Rhodopseudomonas palustris*⁷. These sensors react by protein-protein interactions and are directly linked to the photosynthetic mechanism⁷. Another popular sensor system is the blue sensor light-oxidative-voltage (LOV). It uses flavin adenine dinucleotide (FAD) and BLUF domain containing photoreceptors to absorb light^{1,8}. *E. coli* also contains YcgF protein which acts like a blue-light sensor using BLUF as a sensory domain⁹. The protein-protein interactions show an effective means to control the metabolic reactions. But such systems are very complex and this could be difficult to engineer into other organisms. Therefore, its application in synthetic biology is limited¹.
- b) Signal transduction via two-component system:

Cph1 of *Synechocystis* sp. PCC6803¹, RcaE of *Fremyella diplosiphon* ^{10,11} and CcaS of *Synechocystis* sp. PCC6803^{12,13} are some of the examples of two-component cyanobacterial phytochrome systems. They are well studied sensor systems both, structurally and functionally. Cph1, RcaE and CcaS are light dependent sensor histidine kinases. The genes for the response regulators are located immediately downstream of their respective phytochrome genes^{12,13}. It is therefore a much less complex system for control of gene expression than a cascade response. However, some cross-talks between the sensory kinases and response regulators has been observed¹. This can lead to a reduced target specificity at cellular levels. Most natural sensor systems are too complex to identify the response regulators or promoters involved in the circuit, thus limiting the direct use of natural two-component systems in synthetic biology.

c) Signal transduction via secondary messengers:

Light can also induce a change in an enzymatically active effector module¹. This can lead to synthesis or degradation of secondary messengers responsible for gene expression¹. 3',5'-cyclic adenosine monophosphate (cAMP) and cyclic-di-guanosine monophosphate (c-di-GMP) are the most important secondary messengers in bacteria. They bind to respective receptors and can induce or repress transcription based on the promoters involved 14,15.

However, this signal transduction is very complex and unwanted cross-talks may occur due to delayed response to intracellular concentration of the individual secondary messengers. This regulation happens on a global regulatory level which may lead to off-target effects¹. These intrinsic limitations can be overcome by developing artificial light sensing systems.

3) Recombinant photoreceptors:

In order to overcome the limitations of naturally occurring photoreceptors, many recombinant photoreceptors have been engineered. They have a well characterized light sensor domain and a regulatory output domain. The design has a sensor module taken from a natural sensor as input domain linked to the intracellular response module from either bacteria or yeast as an output domain. The sensor domains and the response modules which can be used in combination are quite limited. This allows for a specific response by the organism to a given light induction ¹⁶. Some of the artificial photoreceptors made from natural sensor systems and response regulators are described below:

a) Phytochrome based two component bacterial systems:

Cph8 was the first engineered bacterial light sensor by Levskaya et al., in 2005 to control gene expression of LacZ¹⁷. It has a sensory kinase which contains the light absorbing domain phytochrome Cph1 from cyanobacterial *Synechocystis*. This was fused to a histidine kinase domain EnvZ which is native to *E. coli* and acts as the output domain⁹.

Phycocyanobilin (PCB) is the red light absorbing chromophore present inside the phytochrome Cph1. Upon activation by light Cph1 switches from red light absorbing ground state (Pr) to far-red light absorbing active state (Pfr) due to conformational changes triggered by the PCB molecules¹. This allows for phosphorylation of the EnvZ component in the sensor. EnvZ is a well-characterised dimeric transmembrane osmosensor found in $E.\ coli$, which regulates OmpR to bind to P_{OmpC} for transcription of genes downstream to begin¹.

A similar green light sensor was developed using CcaS-CcaR system from cyanobacteria *Synechocystis*, which gets activated at 535 nm (green light)². This sensor was quite successful when engineered in *E. coli*.

b) LOV – based two component bacterial systems:

Bradyrhizobium japonicum contains FixL, an oxygen sensor kinase with a PAS domain. This domain was replaced by YtvA, a photoreceptor from *B. subtilis* to create YF1, a recombinant blue light sensor. YtvA is a blue light sensing photoreceptor from the LOV family which binds to flavin mononucleotide (FMN) as a chromophore¹⁸. α-helix was used as a natural linker to create YF1 as well as Cph8. This linker distance plays a vital role in determining the efficiency of most recombinant photoreceptors.

c) LOV – based photo-controlled DNA-binding protein systems:

Another interesting chimera between LOV2 domain from *Arvena sativa* and TrpR repressor from *E. coli* was engineered¹⁹. AsLOV2 binds to FMN and allows for a photocycle upon activation/deactivation by blue light¹. Trp repressor is a small protein which specifically binds to DNA and blocks transcription¹. The TrpR aporepressor is natively inactive, but in the presence of tryptophan, it can bind to several promoters like P_{trp} and inactivate it²⁰. This controls the transcription of genes which are downstream of the promoter trp.

d) PYP – based photo-controlled DNA-binding protein systems:

PYP is a photoactive yellow protein from *Halorhodospira halophile*. It is a blue light photoreceptor from the family of xanthopsins²¹ and was used to create a light sensitive bZIP activator²¹. bZIP is a DNA binding domain in GCN4 which generally controls amino acid repression in yeast. Therefore the recombinant photoreceptor GCN4-PYP, has the PYP domain which binds to the p-coumaric acid²¹. This acts like a chromophore and is induced by light. Under blue light conditions, GCN4-PYP can control the DNA-binding capacity with almost 2 fold specific binding towards AP1 site as compared to under dark state²¹.

1.2. Scope of the project

Of the various sensor systems mentioned in Section 1.1, the phytochrome based two component system developed in 2005 by Levskaya et al., are most interesting sensor systems as they can be used in optical control of gene expression by both red and green light. Exposure of blue light wavelength can cause DNA damage to E. coli cells, so green and red light renders best for light induction experiments under long time periods. Cph8 regulator designed from native Cph1 from Synechocystis phytochrome and EnvZ, a transmembrane protein from E. coli is highly compatible in the E. coli cellular system¹⁷. It is also a well characterized and the most studied sensor system. Cph8, red sensor system, together with CcaS/R, green sensor system induced a controlled gene expression in E. coli resulting in development of patterns across a lawn of engineered cells². The same system was also used to create genetically encoded edge detection algorithm that allowed E. coli to sense light-dark edges and communicate through different conditions²². In a recent paper by Tabor et al., (2014), these two sensor systems - green and red, were used to characterize the dynamics of a gene circuit under varying intensities of light³. These features make them suitable for the motivation of this project, i.e., to produce alternate layers of CaCO₃ and bio elastic to manufacture nacre. Different outputs can be controlled using red and green light in a controlled fashion. Therefore, for this project, Cph8 and CcaS-CcaR sensor systems were selected for further analysis and to explore their potential in controlling the production of biomaterials such as nacre.

1.2.1. Assumptions

Light Source:

The light source used during this project was measured using a spectrometer Ocean Optics QE65 Pro. However, this can only measure light intensity at the surface of a petri dish or at the bottom of a test-tube. The exact light intensity inside the agarose slab or culture medium will be lower than what is measure by the spectrometer. But, we assumed the light intensity measured at the surface of petri-dish or test tube to be the light intensity applied on the cells and all the intensities mentioned in this project were calculated from the spectrometer.

Wavelength of LEDs used:

The far-red light wavelength which reverses the gene output for red sensor system is mentioned as 705 nm². However, we assume the far-red LEDs having emission peaks at 700 nm and 731 nm to give the same effect as 705 nm on the red sensor. The reason for such as assumption was the unavailability of LEDs with emission peak 705 nm from the manufacturer.

Light intensities used:

Several devices were built during this project to help induce the sensors. However, the intensities of light used are not exactly what is mentioned in the literature, as some LEDs purchased were of low power. The maximum intensity which could be achieved while building the devices were used throughout this project and new intensities of light were also used to induce the sensors, apart from the ones mentioned in literature.

1.2.2. Exclusions

Production of nacre

Production of the biomaterial nacre is a futuristic goal and a motivation for this project. However, its production is not in the scope of this project and has been excluded. Instead, the output product is LacZ which can be later replaced for production of any biomaterial.

Mutating the sensor proteins

For fine tuning the background output of the sensor systems, a synthetic biology approach like RBS library creation was employed instead of a molecular biology approach like mutating the sensor proteins.

A library can generate wide range of RBS mutations and tweak the circuit for desired output compared to mutations on the sensor proteins. The structure of sensor proteins are highly complex and not entirely understood²³. Many mutations on the sensor domains were not successful in producing efficient sensors²³. Therefore, in this project, an attempt to create RBS library seemed more feasible.

JW3367-3 strain

The strain JW3367-3 ($\Delta envZ \Delta P_{ompC}$) containing all three sensor systems was developed for this project. They were tested for their sensor activation under light, but no activation was observed. A reason for this could be that the dynamic range of P_{ompC} is much lower in JW3367-3 than in JT2 strain²⁴. Therefore, JW3367-3 was not used for any analysis during this project and was excluded.

1.3. Specifications of the sensor circuits

Red sensor

As mentioned earlier, the recombinant red light sensor Cph8 was engineered by fusing Cph1 from cyanobacteria Synechocystis and EnvZ from $E.\ coli^{17}$. Cph1 consists of a membrane-bound, extracellular sensor that responds to light and an intracellular response regulator. But the response regulators cannot bind to DNA in order to control gene expression. To overcome this, the response domain was fused with the intracellular histidine kinase domain, EnvZ present in $E.\ coli$. Under hyperosmotic conditions, this two component system EnvZ-OmpR, regulates the porin expression and activates P_{OmpC} leading to the transcription of genes downstream. The strain used to express this system has $\Delta envZ$. As noticed in Figure 1, the red sensor gives black output when induced by red light (650 nm) and this process reverses when far-red light (750 nm) is applied. The red sensor circuit contains a repressor switch cI- P_{cI} , which was introduced to generate output signal when red light is applied on the system. Application of far-red light can reverse the red sensor system's output. It is suggested to induce the red sensor system with far-red light for some amount of time before inducing with red light for better gene output².

Green sensor

Similarly, green light sensor was engineered from CcaS-CcaR system present in cyanobacteria *Synechocystis* in *E. coli*. CcaS is a membrane associated histidine kinase and CcaR is a response regulator. CcaS is autophosphorylated when it induced by green light. This leads to phoshotransfer to CcaR domain which triggers the activation of P_{cpcG2} and transcription takes place. Red light (672nm) induction can reverse this process^{2,13}. Inducing with far-red light (705 nm) has also been proposed to inactivate the green sensor system².

Chromophore Synthesis

Chromophore – Phycocynanobilin (PCB) producing genes *ho1* and *pcyA* is introduced as plasmid pPL-PCB into the *E. coli* strain to convert haem into phycocyanobilin. This chromophore is an essential part of the photoreceptor which responds to light.

Output Signal

The light activation and control is measured by gene expression of output lacZ, which when reacts with S-gal (3,4-cyclohexenoesuletin- β -D-galactopyranoside) present in the medium produces a stable, insoluble black coloured pigment. The output genes are integrated along with the genes encoding for the sensor proteins for the green sensor system (pJT118) and integrated as a separate plasmid (pJT106b/b3) for the red sensor system.

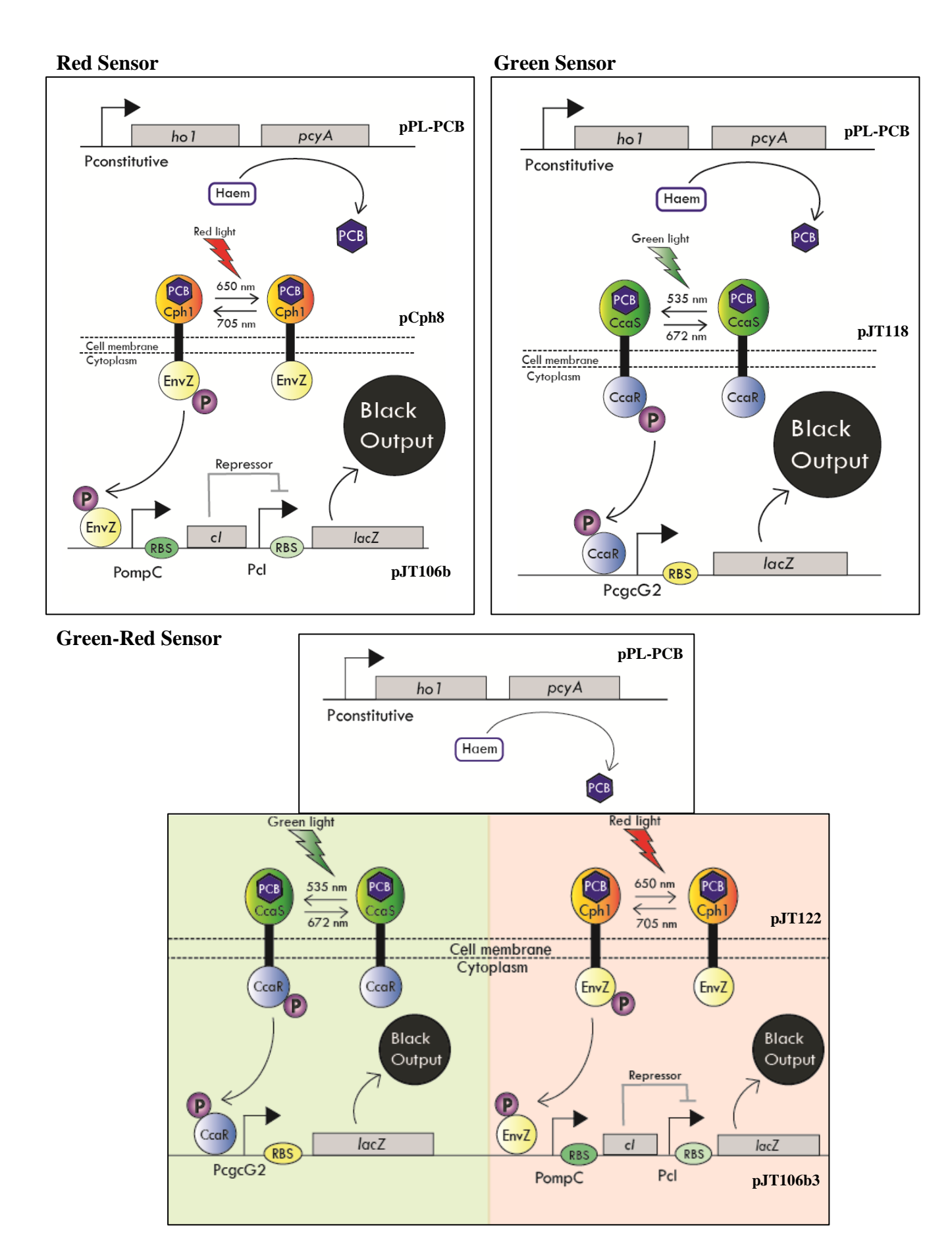


Figure 1 Circuit of red, green and green-red sensor systems (adapted from Tabor et al., 2010).

In Figure 1, schematics of the gene circuit of red, green and green-red sensors are shown (adapted from Tabor et al., 2010). Red and green sensors were expressed in *E. coli* both separately and together to control gene expression. Several plasmids had to be co-transformed in order to express a whole sensor system.

The PCB synthesis genes *ho1* and *pcyA* were in plasmid pPL-PCB. The genes encoding for sensor proteins were in pCph8 (red sensor), pJT118 (green sensor) and pJT122 (green-red sensor)². The output for green sensor was embedded in pJT118 and pJT122. The output for red sensor was kept in a separate plasmid pJT106b having a strong RBS upstream of *lacZ* (used in red sensor system) and in pJT106b3 having a weak RBS upstream of *lacZ* (used in green-red sensor system)^{2,24}.

Each set of sensors (red, green and green-red) were engineered by co-transforming the required plasmids into *E. coli* strains JT2 ($\Delta lacZ \Delta P_{ompC}$) and JW3367-3 ($\Delta envZ \Delta P_{ompC}$). Plasmids used for the development of the strains are listed in Table 1 and described in detail in Section 2.1.1.

Table 1 Description of plasmids used in the generation of sensor systems. ^{2,17}

Plasmid	Size(bp)	Origin	Antibiotic	Properties
pCph8	4231	ColE1	Ст	Red Sensor expression ¹⁷
<i>pJT118</i>	8780	ColE1	Ст	Green sensor – LacZ Output ²
pJT122	11,112	ColE1	Cm	pJT118 + Red sensor expression ²
pJT106b	7728	pSC101	Amp	Red light inverter – LacZ output ²
pJT106b3	7735	pSC101	Amp	Red light inverter – LacZ output (weak) ²
pPL-PCB	3946	P15A	Spec	PCB synthesis ²

The strain JW3367-3 ($\Delta envZ \Delta P_{ompC}$) containing all three sensor systems were developed and tested for its activation under light, but since, no activation under light was seen, it was not used for any analysis during this project. A reason for the strains being inactive under light could be that the dynamic range of P_{ompC} is much lower in JW3367-3 than in JT2 strain²⁴.

1.4. Goal of the project

Light sensing bacteria can be specifically used in controlling the synthesis of biomaterials such as nacre. Nacre is found in inner lining of sea shells and comprises of alternating layers of calcium carbonate (CaCO₃) and bio-elastin layers like chitin, as shown in Figure 2.

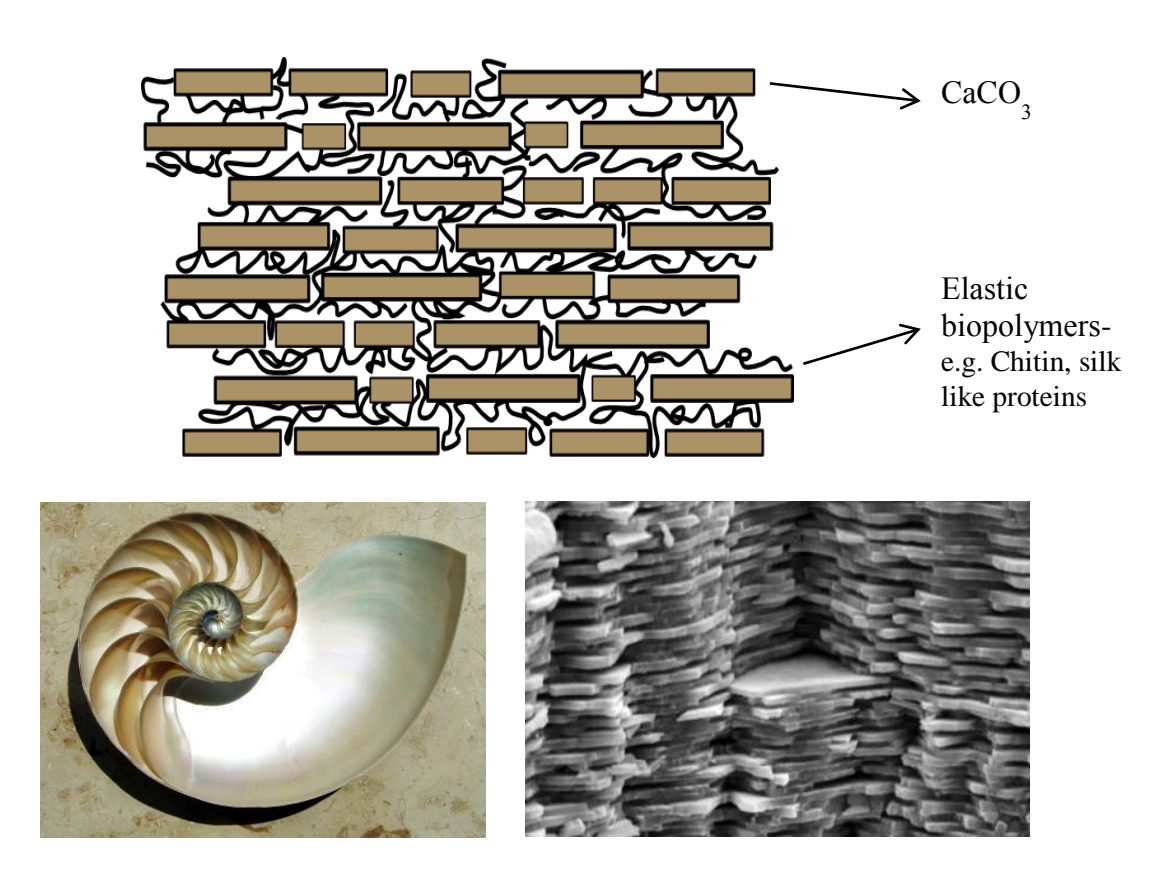


Figure 2 Schematic diagram of nacre showing calcium carbonate (CaCO₃) layers with biopolymers in between them (top); Nacre in sea shells (bottom-left); Electron microscopy image of nacre (bottom-right).²⁵

This project will focus on the controllability of *E. coli* cells using light as an input to generate LacZ as an output. LacZ reacts with S-gal present in the medium to give a black precipitate, which can be clearly seen by eye as a distinct output.

Since, these sensor systems are relatively complex and have not been engineered at Delft University of Technology, it was a challenge to set-up proper light conditions for these sensor systems. Several devices had to be built in order to achieve the right light induction on the sensor systems.

Following are the research objectives of this project:

- The first step will be to engineer the red, green and green-red sensors into *E. coli* in order to sense wavelengths of red and green light, thus answering a fundamental question Are the sensor systems effectively sensitive to wavelengths of light when engineered into *E. coli* and can they be used for future application in production of nacre?
- All the sensor systems will be induced with different light intensities to analyse the input strength vs. the output strength. Different patterns will be created using the sensor systems. This will be carried out to analyse if we can create patterns or layers of output using these sensor systems, which could be helpful in creating layers of CaCO₃ for nacre production.

- ➤ The sensor systems are shown to be deactivated at certain wavelength of light³. It will be interesting to analyse the activation and deactivation of sensors by applying desired wavelengths of light while quantifying of output. Miller assay will be carried out with the help of a special device built to induce liquid cultures. Quantification of output signal vs. input signal can indicate about the sensor efficiencies under particular intensities of light and their potential in a light sensor application.
- ➤ Since the background output is too high for these systems², an attempt to fine tune the circuit by creating library of RBSs will be carried out. They will be then screened for the best phenotypically desired output. Later cloning into sensor system will be carried out to develop a sensor with better efficiency.

Detailed description of each research goal with appropriate approaches and planning is given in:

1) Preliminary set-up – Section 2.1

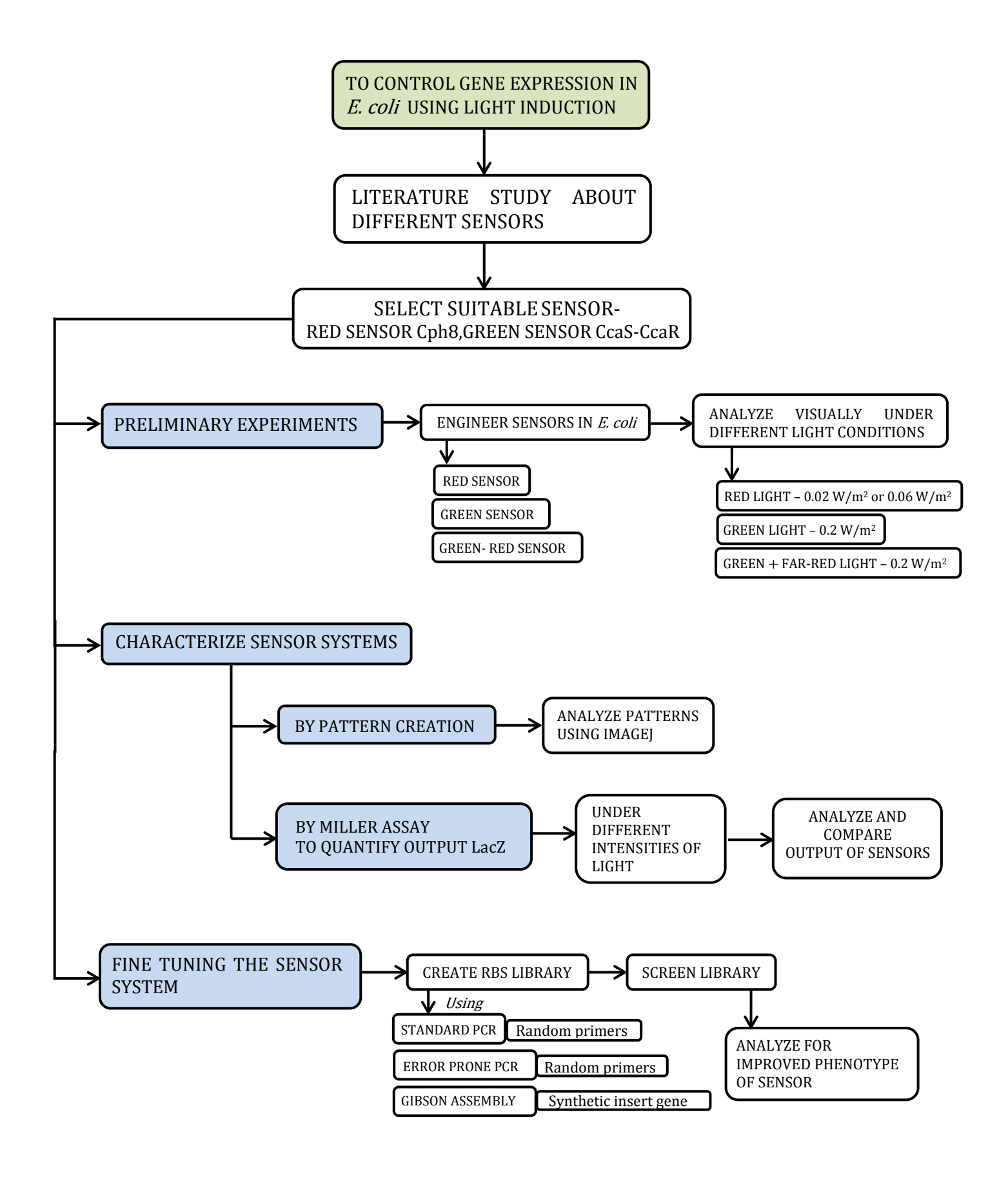
2) Characterize sensors by pattern creation – **Section 2.2**

3) Characterize sensors by quantification of output (LacZ) – Section 2.3

4) Fine tuning the sensor system – **Section 2.4**

A schematic flow of the project has been shown in *Project Overview*.

1.5. Project Overview



Materials and Methods

2.1. Preliminary set-up

2.1.1. Properties of plasmids and strains

Plasmids: All necessary plasmids engineered by Tabor et al., 2010 were acquired from Addgene (https://www.addgene.org/).

• pPL-PCB

This plasmid encodes for ho1 and pcyA for the synthesis of chromophore - phycocyanobilin. It carries Spectinomycin resistance marker and p15A origin of replication. Gene encoding for ho1 and pcyA are under the control of $P_{lac/ara-1}$ promoter. This can be induced by $E.\ coli$ strains carrying AraC. AraC is a repressor that binds to promoter in the presence of L(+)-arabinose and allows for transcription to occur. JT2 and JW3367-3 strains contain AraC²⁴. As this plasmid has been reported to be unstable in $E.\ coli$, long propagation for many generations should be avoided. Transformation of this plasmid in the last can avoid unwanted mutations²⁴.

• pCph8

Originally developed by Levskaya *et al.*, 2005, the plasmid pCph8 encodes for red sensing protein Cph8, which was created by fusing Cph1 from *Synechocystis* PCCC6803 and C-terminal 229 amino acids of *E. coli* EnvZ²⁴. Cph1 is the light receptor part and EnvZ is the histidine kinase domain. pCph8 plasmid has TetR-repressible $P_{LTetO-1}$ promoter followed by *cph8*. As TetR protein knockout strains of *E. coli* are used, the expression of Cph8 becomes constitutive²⁴.

• pJT118

This plasmid has the green/red photoswitchable histidine kinase CcaS and its response regulator CcaR. The native cyanobacterial promoters control the expression of ccaS and ccaR. The lacZ gene is downstream to ccaR and under the control of promoter cpcG2, which gets activated by CcaR binding upon light activation²⁴.

pJT122

This plasmid is created by adding *cph8* from pCph8 to pJT118 in order to construct a plasmid with both green and red sensor domain expression. *lacZ* for output of green sensor remains downstream of *ccaR*.

• pJT106 and pJT106b3

These two plasmids carry the output gene lacZ for the red sensor system. pJT106b has a much stronger RBS upstream lacZ output compared to pJT106b3. The two plasmids have pSB4A3 backbone, with pSC101* origin of replication. cI is under the control of P_{ompC} . cI in turn represses P_{cI} and lacZ. cI has a weak RBS in front since very low concentration of cI is enough to repress P_{cI}^{24} .

Plasmid maps for each are shown in Appendix III-2.

Strains: The *E. coli* strain JT2 was acquired from Dr. Christopher Voigt's lab, where they were originally engineered. Another strain JW3367-3 was ordered from Keio collection (CGSC#10509). Properties of the two strains are described below:

JT2

This strain is derived from RU1012, which comes from MC4100. MC4100 has been used commonly to study the EnvZ/OmpR pathway. It is a derivative of K12 with at least 123 genetic mutations²⁶. RU1012 was used by Levskaya et al., 2005 to create patterns on bacterial plates as this strain has 10-fold reduced P_{ompC} transcription. Later JT2 strain was constructed by knocking out P_{ompC} - lacZ from the genome of RU1012². JT2 strain is proved to be very successful in plate-based assays using LacZ as output. This strain is Kanamycin resistant.

· JW3367-3

This strain was created by knocking out *envZ* from K12 *E. coli* strain²⁷. It lacks *lacZ* and promoter *ompC* (red sensor response regulator). Although this strain has less mutations compared to RU1012, the dynamic range of the promoter *ompC* is much lower²⁴. For this project JW3367-3 which is Kanamycin resistant was used.

Since the green sensor system does not integrate any components from *E. coli* genome, it can be expressed in any strain of *E. coli*.

2.1.2. Expression of red and green sensors in *E. coli*

The sensor systems are a combination of different plasmids expressing genes for PCB chromophore synthesis, sensor proteins and output lacZ which encodes for enzyme β -galactosidase.

The red-light sensing strain was generated by transforming pCph8, pPL-PCB and pJT106b (strong RBS upstream of *lacZ*) in *E. coli* strain.

The green light sensing strain was generated by transforming pJT118 and pPL-PCB in *E. coli* cells. The green and red light sensing strain was generated by transforming pJT122, pPL-PCB and pJT106b3 (weak RBS upstream of *lacZ*) in *E. coli* cells.

Table 2 shows different strains which were engineered in JT2 and JW3367-3 E. coli cells.

Table 2 Properties of light sensing strains

Strain	Plasmids	Antibiotics	Properties ²⁴
	pPL-PCB, pCph8, pJT106b	Spec, Cm, Amp, Kan	Red light ON
JT2	pPL-PCB, pJT118	Spec, Cm, Kan	Green light ON
	pPL-PCB, pJT122, pJT106b3	Spec, Cm, Amp, Kan	Green OR red ON
	pPL-PCB, pCph8, pJT106b	Spec, Cm, Amp, Kan	Red light ON
JW3367-3	pPL-PCB, pJT118	Spec, Cm, Kan	Green light ON
	pPL-PCB, pJT122, pJT106b3	Spec, Cm, Amp, Kan	Green OR red ON

The transformed cells were then plated on LB agar with appropriate antibiotics and incubated at 37 °C overnight. A single colony from the plate was recovered next day and grown in 5mL LB media with appropriate antibiotics. The culture was kept at 250 rpm 37 °C until it reached mid-log phase $(OD_{600} \sim 0.4 - 0.7)^{24}$. Appropriate glycerol stocks were made.

2.1.3. Wavelength and intensity of light

The engineered sensor systems were tested for their characteristic outputs by inducing with wavelengths of red (650 nm), green (535 nm) and green (535 nm) + far-red (750 nm) light. Literature proposes that the red sensor system can be inactivated or reversed by applying far-red light 2 . However, this has never been confirmed experimentally. Therefore, in this project, it was decided to check for the influence of far-red light on all three sensor systems. Far-red light at intensity of 0.2 W/m^2 was applied to test its influence on output of sensors.

The suitable range of red light intensity suggested is $0.15~\text{W/m}^2$ for the red sensor. Green light intensity of $0.15~\text{W/m}^2$ is required for green sensor to get activated. Whereas for the green-red sensor system, green light of $0.002~\text{to}~0.1~\text{W/m}^2$ is suggested. The green light should be applied at very low intensities since the red sensor present in green-red sensor is sensitive to green light. So in order to activate the green sensor and keep the red sensor inactive in cells containing both the sensor systems, very low intensities of green light must be applied. Red light <0.01~\text{W/m}^2 is required for green-red sensor.

Figure 3 shows the preliminary set-up containing light source of a particular wavelength. This was the first set-up built for this project. Individual devices for red and green wavelengths (far-red light as switch) were built (Appendix II-2). The intensity of light can be adjusted using filter to block the light. The maximum intensity for green light was 0.12 W/m² and 0.06 W/m² for red light. These are different intensities from what was mentioned in the literature, as it is the maximum intensity of light which could be achieved while building these devices. Since the LEDs used for light source have a certain power input, the maximum intensity achieved was 0.06 W/m² for red light and 0.12 W/m² for green light. The device can be used both at room temperature or on a heat block to provide 37 °C as shown in Figure 3.





Figure 3 Preliminary set-up of light induction at room temperature (left) and on heat block at 37 °C (right).

Initial experiments to characterize the sensor systems were done. The protocol for plate based assay is given in Appendix I-1. Results are shown in Section 3.2. Since strain JW3367-3 is not recommended for pattern creation as its dynamic range of P_{ompC} (red sensor system) is much lower than in JT2 *E. coli* strain²⁴, only results for JT2 cells are shown for all experiments and throughout this project. Experiments with JW3367-3 were not successful in activation of sensors, hence it was excluded for this project.

2.2. Characterize sensors by pattern creation

Generation of spatially patterned *E. coli* using light induction was carried out by triggering the sensor systems (mentioned in Section 1.3). Special agarose plates containing S-gal (3,4-cyclohexenoesculetin- β -D-galactopyranoside) medium were used to visualize the patterns as β -galactosidase (output LacZ) hydrolyzes the S-gal to enzymatically produce a black pigment²⁴. Ferric irons are required as a co-factor to carry out this reaction. A detailed description of the β -galactosidase/S-gal reporter system is given in Section 2.2.2. The protocol to prepare the agarose slab is described in Appendix I-1.

The different sensors were characterized by comparing their pattern formation under varying light conditions. Quantification of black output through ImageJ was done to determine the difference in light induction as compared to under dark. This can help us analyse if these sensor systems are suitable for making of several layers of CaCO₃ and bio-polymer for the production of nacre.

The black output expressed on the petri-dish does not diffuse away and can be stored in fridge even after the bacterial cells have died²⁴. Very clear crisp stable images were seen.

A special device called *Light Induction Device (LID)* was built in order to create patterns. A brief description is as follows:

2.2.1. Light Induction Device (LID) Set-Up

The agarose slabs have to be activated by particular wavelength of light in a controlled environment. This set-up can be constructed in a variety of ways. Light Induction Device (LID) was developed at Department of Bionanoscience particularly for this project, which allows for simple control of light intensity on the surface of a petri-dish.

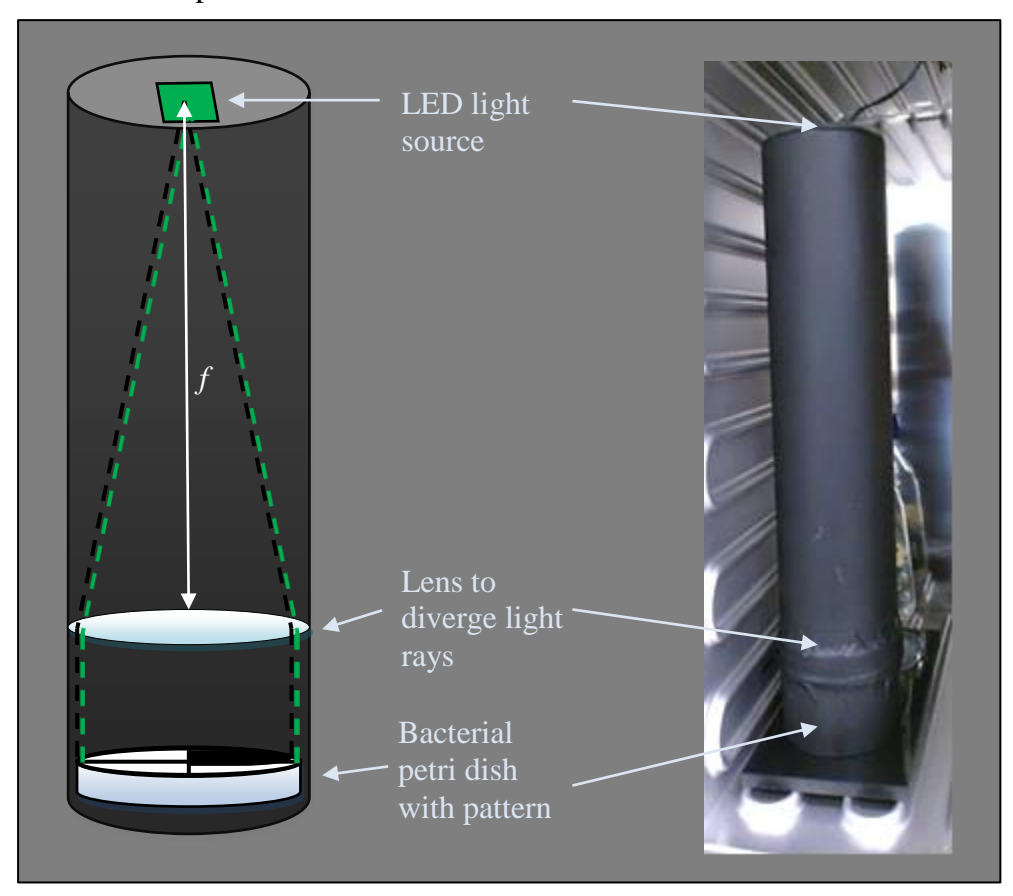


Figure 4 Light Induction Device (LID) shown diagrammatically (left) and real device (right)

LID shown in Figure 4, was made out of a cylindrical black tube with LEDs as light source on the top of the tube. A convex lens is located inside the cylindrical tube to diverge the light rays to fall exactly on the bacterial petri dish which was kept at the bottom of the tube. The light source was placed exactly at distance equal to the focal length of the lens. Thus the light rays fall as parallel uniformed rays on the petri dish. This whole set-up was placed inside the incubator at 37 °C. Therefore, the petri dish was kept in dark and only desired wavelength of light was reflected upon it to activate the sensor system. Desired patterns can be printed on laser paper and placed upon the petri dish as a mask. The amount of time for creating a pattern depends on the intensity of the light source.

LEDs with green (535 nm), far-red (750 nm) and red wavelengths (650 nm) were used in the above set-up. Two different devices were built for red light of intensity (0.026 W/m² upgrade to 0.06 W/m²) and green and far-red (750 nm) light of intensity 0.2 W/m². These were the intensities of LEDs which could be achieved while building the device, since it is the maximum power of the LEDs. Far-red light was built-in with a switch to on/off when necessary.

Specifications about making the device is described in Appendix II - 2.

2.2.2. β-galactosidase/S-gal reporter system

For quantification of output LacZ, the β -galactosidase/S-gal reporter system was used. It is a very successful assay compared to fluorescent protein assays. The sugar analog, S-gal (3,4-cyclohexenoesculetin- β -D-galactopyranoside) is hydrolyzed by β -galactosidase and converted to galactose and esculetin²⁴. Ferric iron, added as ammonium iron (III) sulphate dodecahydrate in the medium, is required as a co-factor for this reaction to take place. An insoluble black precipitate is formed which is the esuletin-coordinated iron.

X-gal is a similar reporter system, but since X-gal is sensitive to light and heat, it makes the use of the blue colour producing X-gal substrate inappropriate. S-gal is insensitive to light and is heat resistant allowing it to be autoclaved along with nutrient media²⁴.

Figure 5 The glycosidic bond of S-gal which is cleaved by β -galactosidase (a); Two esculetins bonded by ferric iron, which forms the black pigment (b). (Adapted from Tabor et al., 2010)

2.2.3. Quantifying signal intensity using ImageJ

Output of the sensors after induction by light is a black pigment which can be clearly seen by eye. A better quantification for this output can be done by capturing a grey image of the bacterial petri dish on Molecular Imager® Gel-DocTM (http://www.bio-rad.com/en-us/product/gel-doc-xr-system) and later the signal intensity across the plate can then be analysed using ImageJ software (NIH). This can give a rough estimate of the grey value on the petri dish image.

Several experiments were carried out using the LID and then analysed using ImageJ. Experiments under red and green wavelengths of light were carried out to characterize the sensor systems. Result are shown in Section 3.3. Appendix III-7 shows calibration done for ImageJ software.

2.3. Characterize sensors by quantification of LacZ

The black output LacZ was quantified using ImageJ software. However, accurate quantification of LacZ can be done by Miller assay for better characterization of the sensors. Miller assay can be done using liquid culture and measuring the cell density at each point of growth and light incubation. Therefore, the Array Tube Illuminator was built in order to induce cell culture with light. Another motivation in building such a device was to deactivate and activate the liquid culture containing *E. coli* cells with appropriate wavelengths of light, a concept used in characterizing the circuit dynamics by Tabor et al., 2014³. Better controllability of the sensors can be attained by applying various intensities of light on the liquid cultures.

The relationship between the input and output signals of a genetic circuit is called transfer function. Here, the light intensity is the input and gene expression of lacZ is the output measured by Miller assay.

2.3.1. Array Tube Illuminator set up

The engineered sensors containing the output promoters are controlled by different activating and inhibitory light wavelengths. A successful attempt was made by Tabor et al., (2014) to characterize the relationship between light input and protein expression output for green and red sensors using sfGFP as an output³. A light tube array (LTA) was used to send increasing and decreasing signals of light³. This is shown in Figure 6. A design adaption of LTA was built for this project in order to analyze the sensor systems in liquid culture and to quantify the output LacZ through Miller assay. This device is named Array Tube Illuminator and has green, red and far-red LEDs at calibrated intensities of each wavelength and can accommodate 12 test tubes. The intensities of LEDs can be controlled by programming through the Arduino software (http://arduino.cc/en/Main/Software). Array Tube Illuminator can be kept in shaking incubator, and sampled for quantification of output signal during the exponential growth of the bacteria while being induced by light. The design specification are shown in Appendix II-3.

In the green sensor system, CcaS is generally in Pg (ground state), which allows it to absorb green light³. When green light induction is done, the CcaS moves to Pr (red-absorbing state)³. This leads to the phosphorylation of CcaR which activated promoter *cpcG2*. This initiates the transcription of genes downstream of promoter *cpcG2*. However, when red light is applied, the CcaS turns from Pr to Pg state³. This will dephosphorylate the CcaR and turn the transcription off.

In the red sensor system, Cph8 which is in Pr state switches to Pfr, when induced with red light³. This will dephosphorylate the phosphor-OmpR and turn the transcription of lacZ 'on', due to the presence of a invertor in the red sensor system (P_{ompR} - cI - term - P_{cI} - lacZ - term). However in dark, Pr state is achieved, which leads to phospho-OmpR activating the P_{ompR} then turning the transcription 'off'. (Figure 6)

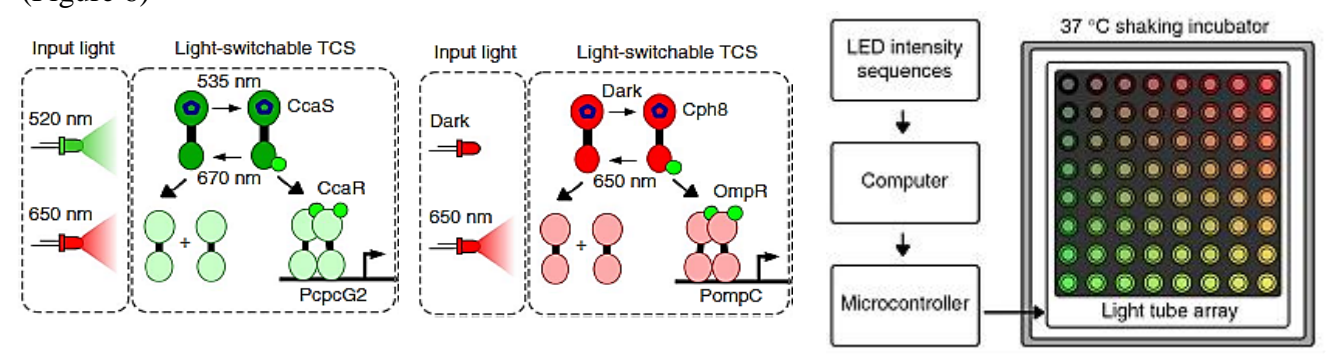


Figure 6 Circuit of green and red sensor systems with activation and deactivation wavelengths of light; Design of Light tube $array^3$

The Array Tube Illuminator built for this project can accommodate 12 test tubes. A design of the device is shown in Figure 7 – part A. Different components used to build the device is shown in part B. The microcontroller, LEDs and test-tube array can be seen. Part C shows the device after all the parts were assembled. Proper calibration of the intensity of each LED was done with respect to the current supplied to the device. This is described in Appendix II-4. Part D shows the Array Tube Illuminator kept at 37 °C shaking incubator at 170 rpm.

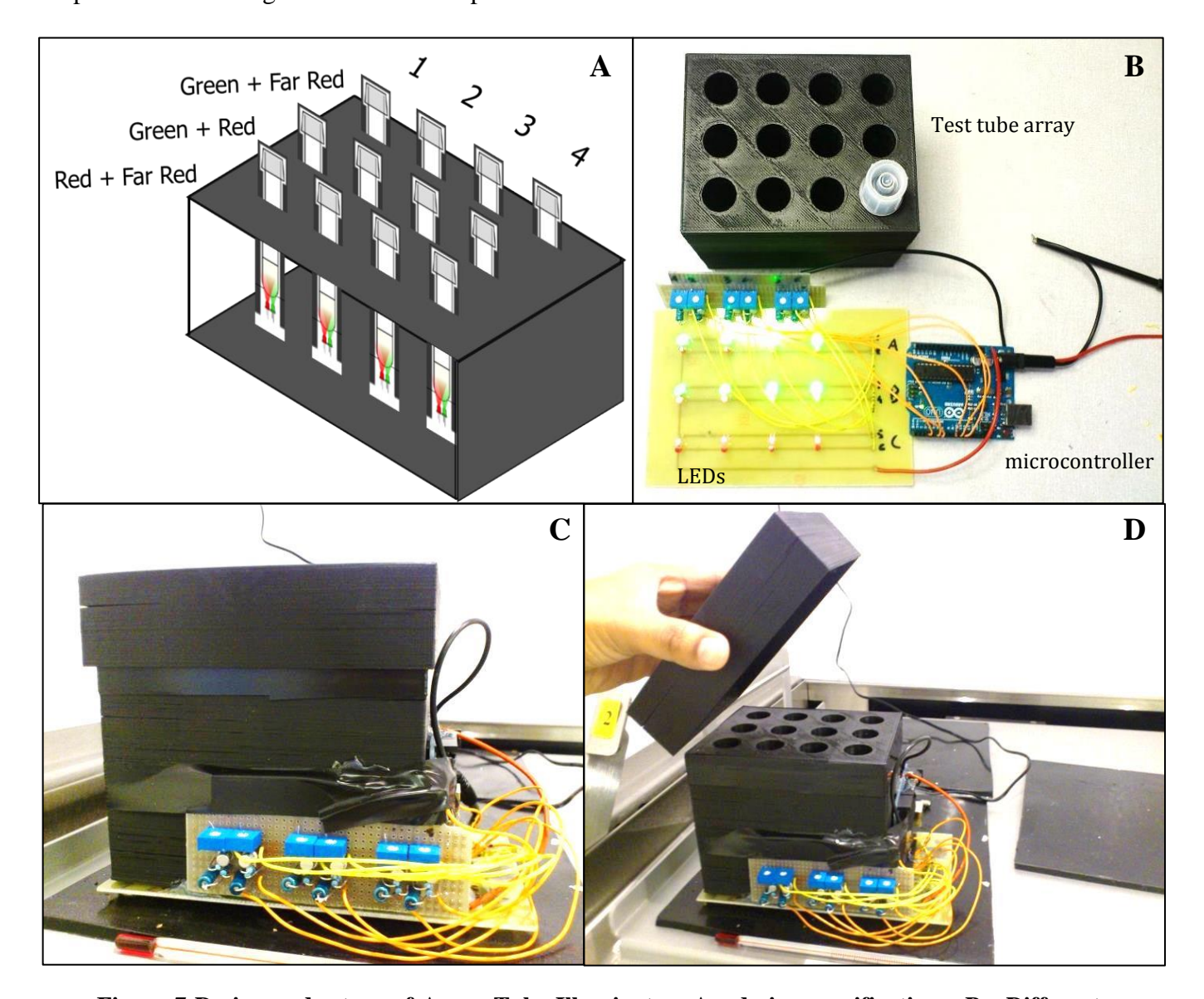


Figure 7 Design and set-up of Array Tube Illuminator; A - design specifications; B - Different components of Array Tube Illuminator; C - set-up after assembling; D - Array Tube Illuminator kept inside 37 $^{\circ}$ C shaking incubator.

Cells containing the sensor systems were grown overnight in dark with appropriate antibiotics in LB medium. After measuring the OD_{600} , a dilution of OD_{600} upto 0.005 was done in Azure Medium (+ 0.2% glucose). These tubes were placed in the Array Tube Illuminator to allow for light induction. Samples from the tubes were taken until ~8-9 hours of light induction and Miller assay was carried out on each sample to quantify the output LacZ. Experiments with varying intensity of lights were done for all sensor systems. Results are shown in Section 3.4.

2.3.2. Quantifying signal intensity using Miller assay

Precise quantification of the output LacZ or β -galactosidase can be made by Miller assay, a colorimetric assay of β -galactosidase. It is a simple and reliable assay which uses a colourless substrate o-nitrophenyl- β -D-galactoside (ONPG) to give galactose and o-nitrophenol (ONP) in the presence of β -galactosidase²⁸.



Figure 8 Chemical reaction of Miller assay

The product o-nitrophenol (ONP) is yellow in colour. The production of ONP per unit time is proportional to the concentration of enzyme β -galactosidase. Therefore, quantification of yellow color is proportional to the enzyme concentration.

The sample activity of the enzyme present in a sample is a rate or velocity of reaction, which is how much yellow colour is produced after incubation for some specific time. The units for sample activity is ΔA_{420} min⁻¹.

But in order to calculate the enzyme activity with respect to the cell biomass, specific activity is calculated. First a standardized volume and standard sample activity is calculated. The units for standard sample activity will be ΔA_{420} min⁻¹ mL⁻¹. Then the OD₆₀₀ of the culture will be the standard cell biomass. Therefore the specific activity units are ΔA_{420} min⁻¹ mL⁻¹ OD₆₀₀⁻¹.

$$\beta$$
 – galactosidase activity = $\frac{1000 * A_{420}}{t * V * OD_{660}}$

Where, t = time (in minutes) of incubation

V = volume of cells (mL) used in the assay

A₄₂₀ = absorbance of the yellow o-nitrophenol (ONP) product at 420 nm

 OD_{600} = cell density at 600 nm

This is called the Miller Unit. Miller unit gives the best quantification of LacZ output and the protocol is described in Appendix I-4. The assay was also calibrated for each sensor system and is shown in Appendix III-6.

2.4. Fine tuning the sensor system

Pattern creation on the bacterial plates resulted by activation of light sensitive sensors proves that the sensor system is sensitive to light induction. However, it can be observed from the results shown in Section 3.3 that the background output, i.e, the output of the sensors under dark areas, in all the pattern developments was quite high. The output LacZ quantified in Section 3.4 shows light induction of sensors compared to under dark but clearly an output signal under dark was observed. Therefore, at this stage, the sensor systems cannot be directly used in the production of nacre. There is a requirement to fine-tune the existing system especially the red sensor system, to reduce its output under dark.

Strategies to improve the circuit can be achieved by mutation in the sensor domains to increase their efficiency in responding to light. Promoter mutation can also improve the circuit output but its complex binding makes it difficult to mutate the correct base pairs in order to get desired phenotypes. Mutations of the sensor protein are also highly complicated and requires in-depth knowledge of the protein structures and light switch mechanism.

Strategy to improvise the circuit downstream of the sensor parts can be a rather simpler approach and within the scope of this project. Tuning the strength of RBSs present in the circuit is a fairly possible option to improve the output of the circuit. The plasmids pJT106b/b3 show possibilities of a RBS library generation and which could lead to suitable fine-tuning of the system. This is explained more in Section 2.4.1.

2.4.1. RBS library generation

The reason for output signal under dark is because the range of activity of the input promoter does not match the range required for proper behaviour of the circuit. Such gene circuits have been studied before and an attempt to improve the circuit design was done using error prone PCR²⁹. Mutation of the rbs region by rational substitutions or random mutagenesis has also been reported to improve the circuit efficiency^{29,30}. This project aims to fine-tune the existing circuit of red sensor by creating a random RBS library using site-directed mutagenesis that allows change of specific base pair in a cloned DNA sequence. Since this attempt was never made on the circuit of the red sensor, it would be interesting to observe the outcomes.

To tune the range of P_{ompC} in pJT106b/b3 (Figure 9), a mutagenic library of three positions in the RBS upstream of cI was designed. This could help control the cI- P_{cI} repressor switch which regulates the expression of lacZ.

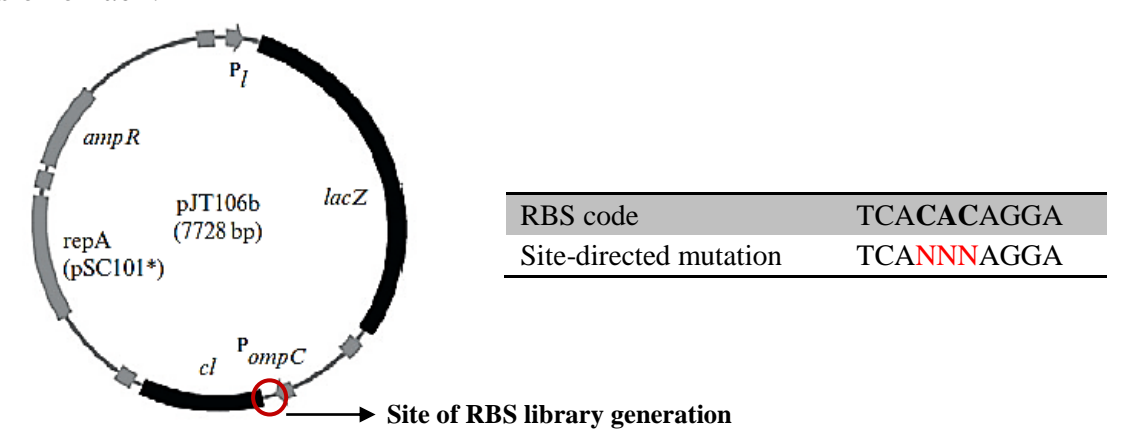


Figure 9 Plasmid map of pJT106b indicating the site of RBS library generation

Results for RBS library creation and screening are shown in Section 3.5.

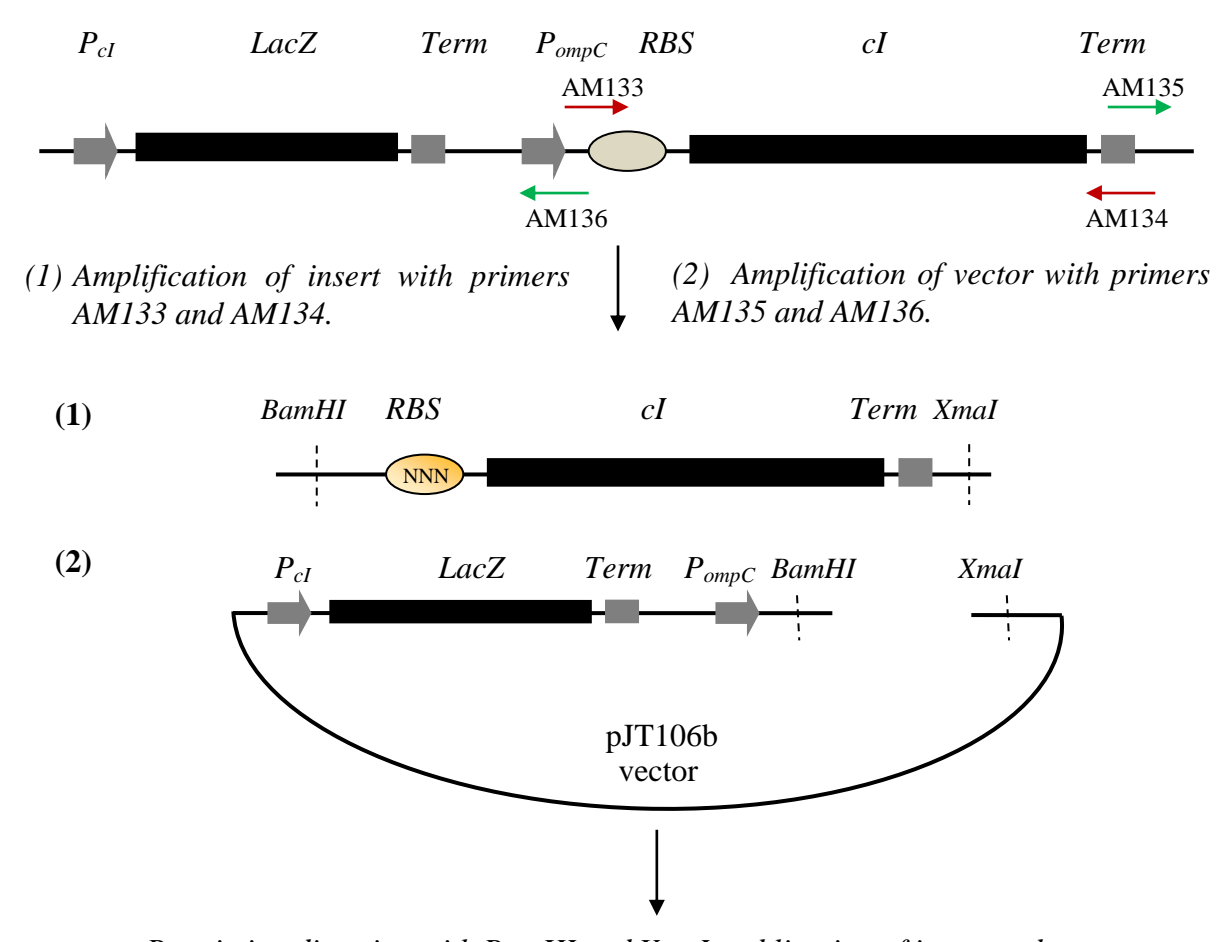
Three types of approaches to engineer the RBS library were applied:

I. Method using site-directed mutagenesis by randomized primers:

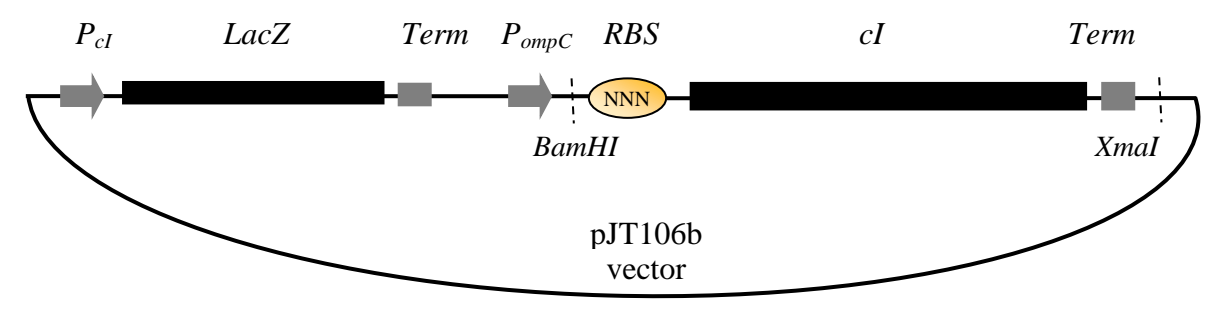
Primers were designed containing random base pairs to create a library of variants in the RBS code upstream of *cI*. 5'- ATATGGATCCTACTAGAGTCANNNAGGACGGCCGGATGAGCACAA-3' (AM133) and 5'- ATATCCCGGGGCAGGGTGGTGACACCTTGC – 3' (AM134) were used to introduce the random basepairs and restriction sites BmaHI and XmaI in plasmid pJT106b/b3 and to PCR out the insert.

Similarly, primers 5'- ATATACCCGGGTTTTTCTTTAAAACCGAAAA – 3' (AM135) and 5'- ATATGGATCCAGTCCATTCTCCCCAAAA – 3' (AM136) were used to introduce restriction sites BmaHI and XmaI and to PCR out the vector. Restriction digestion and ligation of insert and vector was followed by transformation into *E. coli* strains.

A diagrammatic view for the approach is shown below:



Restriction digestion with BmaHI and XmaI and ligation of insert and vector



RBS library created at rbs site infront of cI gene.

Figure 10 Diagrammatic view of RBS library creation using method I

II. Method using Error Prone PCR coupled with site-directed mutagenesis:

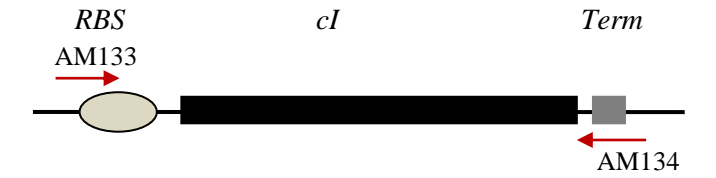


Figure 11 Insert containing RBS and cI for error prone PCR

Method I was upgraded using error prone PCR on the insert region to create more mutations. Mutations on the *RBS-cI-TT* (insert) gene was introduced by error prone PCR amplification using the primers AM133 and AM134 (from Method I). A detailed protocol is given in Appendix I-2. Using low annealing temperatures and MnCl₂ during the PCR can create errors in DNA replication to create more variation in RBS library³¹.

Implications in Method I and Method II:

The method I and II may develop few mutant colonies for the RBS library, since there may be preference towards the native RBS sequence 'TCACACAGGA'³².

III. Method using synthetically designed oligonucleotide with random base pairs:

This approach uses a synthetically designed oligonucleotide containing 'NNN' random base pairs in the region of RBS upstream of cI to create the library. Simple primers were used for PCR amplification. Restriction sites were not introduced and Gibson assembly was used to ligate the strands (Appendix I-3). This method gave a wider range of RBS library as the 'native' RBS sequence was deleted. This allowed for better randomization of the RBS sequence.

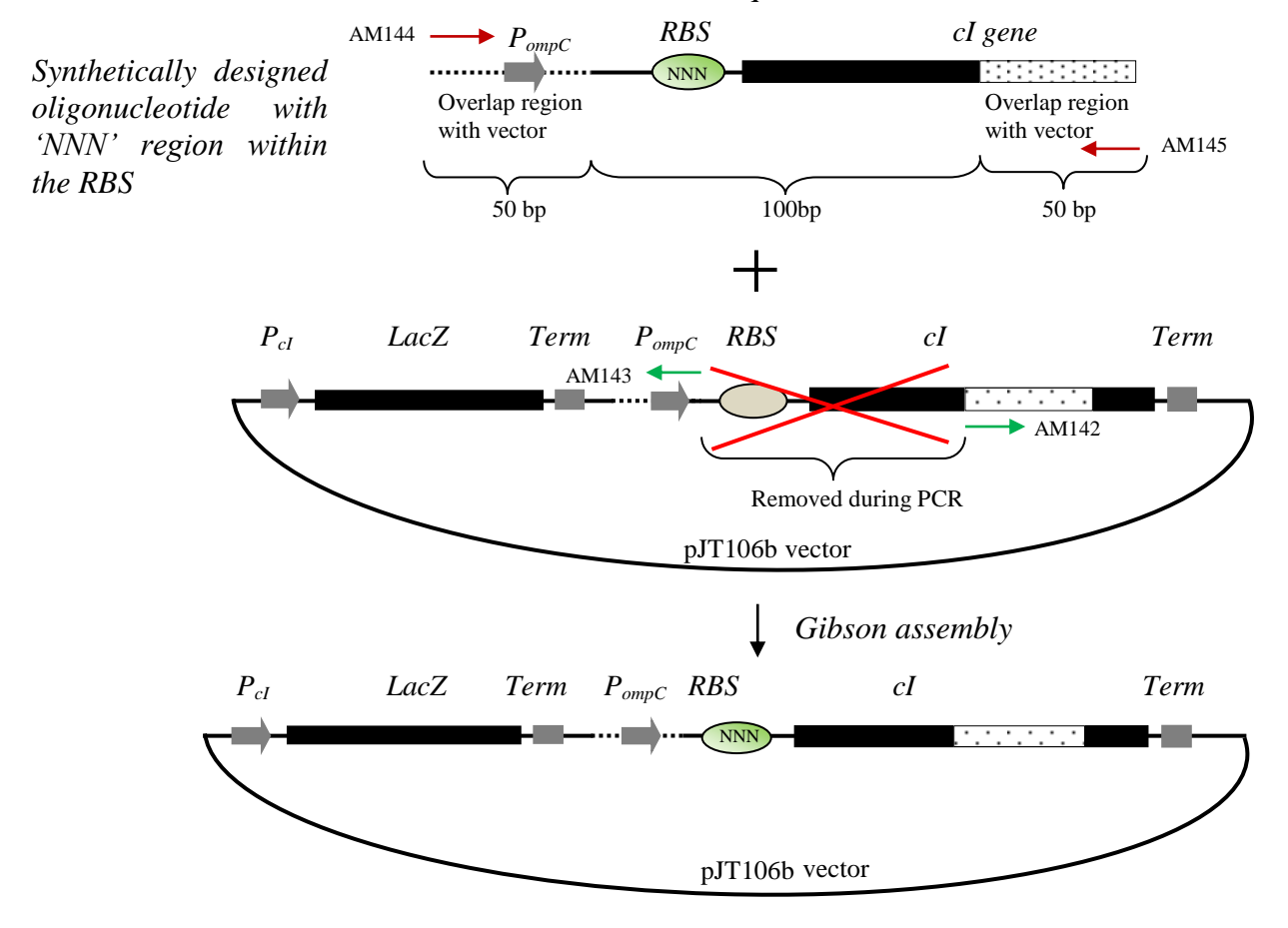


Figure 12 Diagrammatic view of RBS library creation using method III

Results

3.1. Overview

An overview of the results is tabulated in this section. The objectives, experimental details and results obtained are summarized to give the reader over-all gist of the project's conclusions. Experimental results, graphs and images for each experiment are shown in Section 3.2, 3.3, 3.4 and 3.4.

Table 3 Overview of results

Objective	Experiment details	Results/Observations	
Preliminary experiments Section 3.2	To check red, green, green-red sensors under dark, red, green and green + far-red light induction.	All sensors gave black output under dark as well as under light induction. (Figure 14)	
Characterize sensors by pattern creation Section 3.3 Light induction device (LID) was built and used for this experiment. (Figure 4)	Pattern creation: To create patterns using mask on red, green and green-red sensors by inducing with red, green and green + far-red light.	 Red sensor created patterns under red light of intensity 0.02 W/m². Also, under green and green + far-red light (0.2 W/m²) the red sensor developed faint patterns. Both, green and green-red sensors showed pattern developments under green and green + far-red light (0.2 W/m²), but no patterns were seen under red light (0.026 W/m²) (Figure 16) 	
	Scope of pattern creation: To understand the scope of pattern creation	• Patterns of TU Delft logo and self-image were created. After ~12-15 hours, sensor gave crisp patterns. (Figure 17) (Figure 18)	
	Comparison of sensors: To compare all sensors using pattern creation under red, green and green + far-red light. To quantify the output by ImageJ software.	 Red sensor gave patterns with green and red light. But under, green + far-red light, there was no pattern formed. Green and Green-red sensors did not give patterns under red light. But formed patterns under green, green + far-red light induction. (Figure 19) ImageJ analysis showed very less difference between light induced and dark areas. Far-red light may be deactivating the sensor systems. (Figure 20) 	
	Gradient experiment: To apply a gradient of light intensities using pattern mask on a petri dish containing only one sensor (green or red sensor) To analyse output signal by ImageJ software.	 Output signal increases with increasing light intensity for green sensor systems. (Figure 21) Under far-red light, green sensor may be induced more. Although the induction under light compared to dark is not very high, it may be significant (Figure 23) Red sensor shows induction under light, which is not very high, but may be significant. (Figure 24) 	

Characterize sensors by quantification of LacZ

Section 3.4

Array tube illuminator was built and used for this experiment. (Figure 7) To characterize red, green and greenred sensors using Miller assay under different intensities of:

- · red light
- · green light
- · combinations of red and green light

Light intensities used		
Green	$0, 2, 4, 6 \text{ W/m}^2$	
Red	0, 2, 4, 6 W/m ²	
Green Red	0 W/m ² 0 W/m ²	
Green Red	4 W/m ² 1 W/m ²	
Green Red	2 W/m ² 2 W/m ²	
Green Red	$\begin{array}{cc} 2 & \text{W/m}^2 \\ 0.1 & \text{W/m}^2 \end{array}$	

- Red sensor showed exponential trend with red, green and green + red light. However, output under red light was much more than under green light. (Figure 25)
- Green sensor may be deactivated under red light. Increasing intensities of green light activated the green sensor. Combination of green + red light also induced the sensor, though red light does not have a direct effect on green sensor. (Figure 26)
- Green-red sensor showed less output under higher red light intensity $2W/m^2$. Under increasing intensities of green light, a stepwise increase in output was observed. Under combinations of green + red light, increase in output of the sensor was noticed as intensity of green light increases. (Figure 27)
- Green-red sensor under dark overlaps with the lowest intensity of light applied to it. This may be due to presence of two sensor systems. (Figure 27)

Comparing all three sensors (Figure 28)

- Red sensor compared to green and green-red sensor gave high Miller unit output under all combinations of light.
- Green-red sensor had higher Miller unit output with all combinations of light as compared to green sensor. Compared to red sensor, the green-red sensor had less output and was less sensitive towards red light.
- Background output during dark was seen under all sensors, but was highest for red sensor.

Fine tuning the sensor system

Section 3.5

RBS library generation on the RBS upstream of *cI* to reduce background output of red sensor.

<u>Aim</u>: To decrease the background output of red sensor under dark by mutating output plasmid pJT106b/b3.

Method I

Primers with random base pairs were used to mutate the RBS site. Standard PCR was carried out.

- Sequencing results showed the native RBS sequence to be dominant, thus unable to create a RBS library.
- · Visual screening did not give desired phenotype. (Figure 29)

Method II

Random primers of method I were used along with error prone PCR to introduce mutations in the insert region (*RBS-cI-TT*).

- Sequencing showed the native RBS code to be present even though error-prone PCR introduced mutations in *cI* region of the insert.
- Some desired phenotype seen in the visual screening. But sequencing showed no mutation in the RBS code. (Figure 30)

Method III

Synthetic oligonucleotide insert containing random site in the RBS code was used instead of the native insert region from the plasmid pJT106b/b3.

Standard primers were used to amplify the insert and vector, then ligated by Gibson assembly.

- RBS mutated colonies were confirmed by sequencing. Successful in creating RBS library.
- Miller assay was carried out on the mutant colonies.
 However, none of the mutant colonies showed desired phenotype. Most colonies had Miller unit output higher or similar to the positive control pJT106b3. (Figure 31) (Figure 32)

3.2. Preliminary results

The first experiment in this project was to test the engineered strains containing red, green and green-red sensor systems under green, red and far-red wavelengths of light. The fundamental question to answer through this experiment was whether these sensor systems are sensitive to different wavelengths of light when engineered into *E. coli?* And whether there is a scope of using these strains for the production of biomaterials?

The set-up described in Section 2.1 was first implemented at room temperature and later on a heat block at 37 °C. The exact temperature in the petri-dish was measured using a digital thermometer. The sensor tip of digital thermometer Omega HH12 with a thermocouple type K was kept under the petri dish which gave the exact measure of temperature.

Experiments on red, green and green-red sensors along with control (without sensors) were carried out.

Observations made

1) 37 °C is important for green sensor to become active

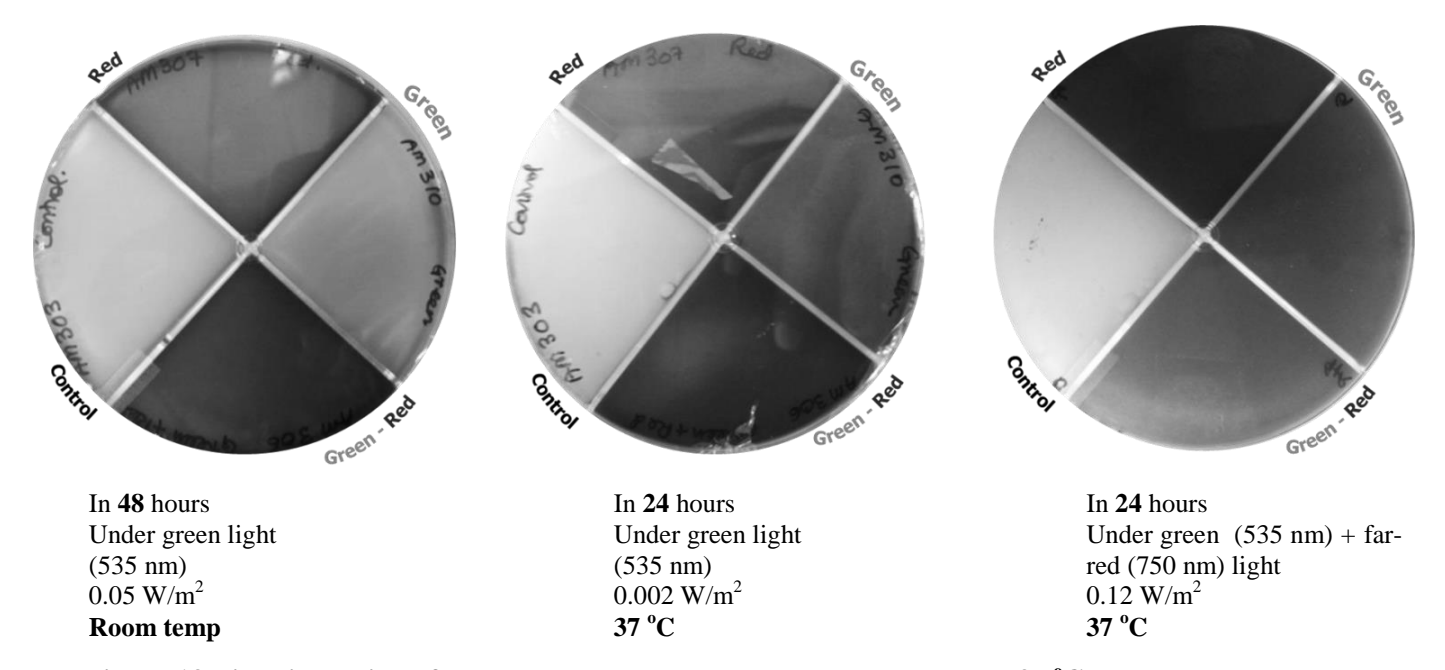


Figure 13 Light induction of all sensors and control under room temp and 37 °C

Quad-petri plates containing all the three sensors (red, green and green-red) and control strain (cells with no sensor system) were induced by green light (535 nm) and green light with far-red (750 nm) light. The first plate was kept in room temperature and other two at 37 °C. This experiment showed that temperature was essential for the activation of sensors and growth of cells, especially the green sensor. Since the green sensor took long hours to give black output until the temperature was raised to 37 °C. This can conclude that optimum temperature is important for the expression of output LacZ.

2) All sensors under dark, red, green and green + far-red light

In order to understand the characteristics of each sensor system, they were kept under dark, red (0.06 W/m^2) , green (0.2 W/m^2) and green + far-red (0.2 W/m^2) light.

Results of the petri-dish after 12 hours and 24 hours are shown below:

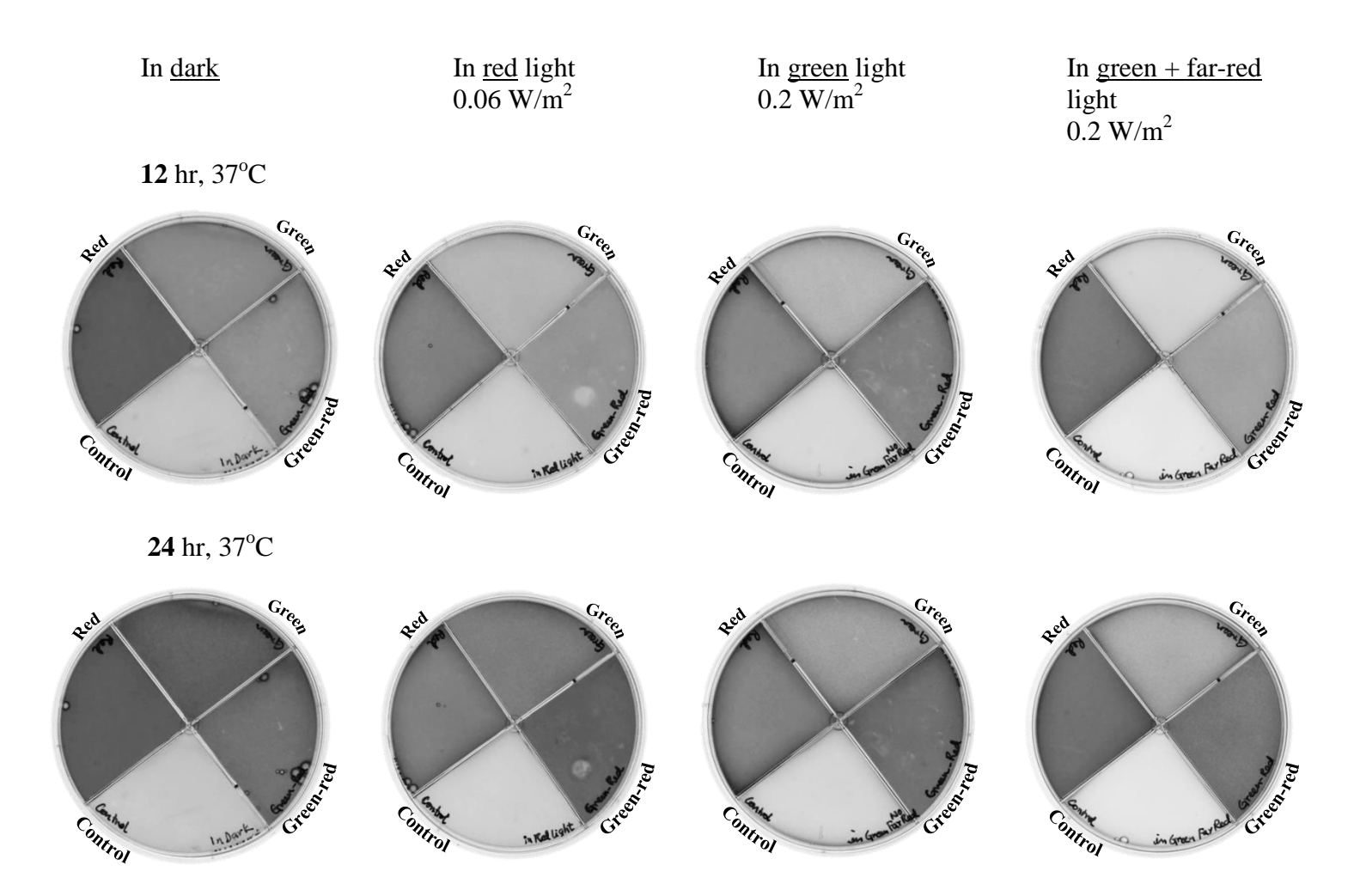


Figure 14 All sensors and control under dark, red, green and green + far-red light - 12 hr and 24 hr (edited images) Appendix III-1 shows the original plates.

From the above experiment it can be noticed that the sensors - red, green and green-red turned 'on' under dark as well as under red, green and green + far-red light. There is a distinct black output noticed in all sensors after 12 and 24 hours of incubation. It is not clear, at this stage, if light does activate the sensor systems present in bacteria or the system is always 'on'.

3) Note on plasmid pPL-PCB, glycerol stock and media

PCB producing plasmid when transformed last was more stable in the sensor system and better for light induction.

The glycerol stock of the sensor systems should be made at mid log phase of the culture to avoid instability²³.

LB Media containing S-gal and ferric ions should be used within a week as it turns black in colour as time passes. Storing the media under dark can help avoid any unwanted reactions by light. Crystal formation of the ferric ions can also be seen, as ferric ions are insoluble in water.

3.3. Characterization of sensors by pattern creation

As the results in Section 3.2, did not show significant activation of sensors using light, in this section we tried to characterize the sensor systems by creating patterns using the *Light Induction Device (LID)* Set-Up. The set-up specifications of LID are described in Section 2.2.1. Pattern creation can be helpful to analyse if we can create layers of output using these sensor systems. A comparison between all the three sensors was done using pattern creation. In order to analyse the variation in output signal under a gradient of input light intensity, the gradient experiment was carried out.

All the sensors were tested under different wavelengths of light. Agarose plates were prepared using the protocol mentioned in Appendix I-1. Example of the patterns used are shown in Figure 15.

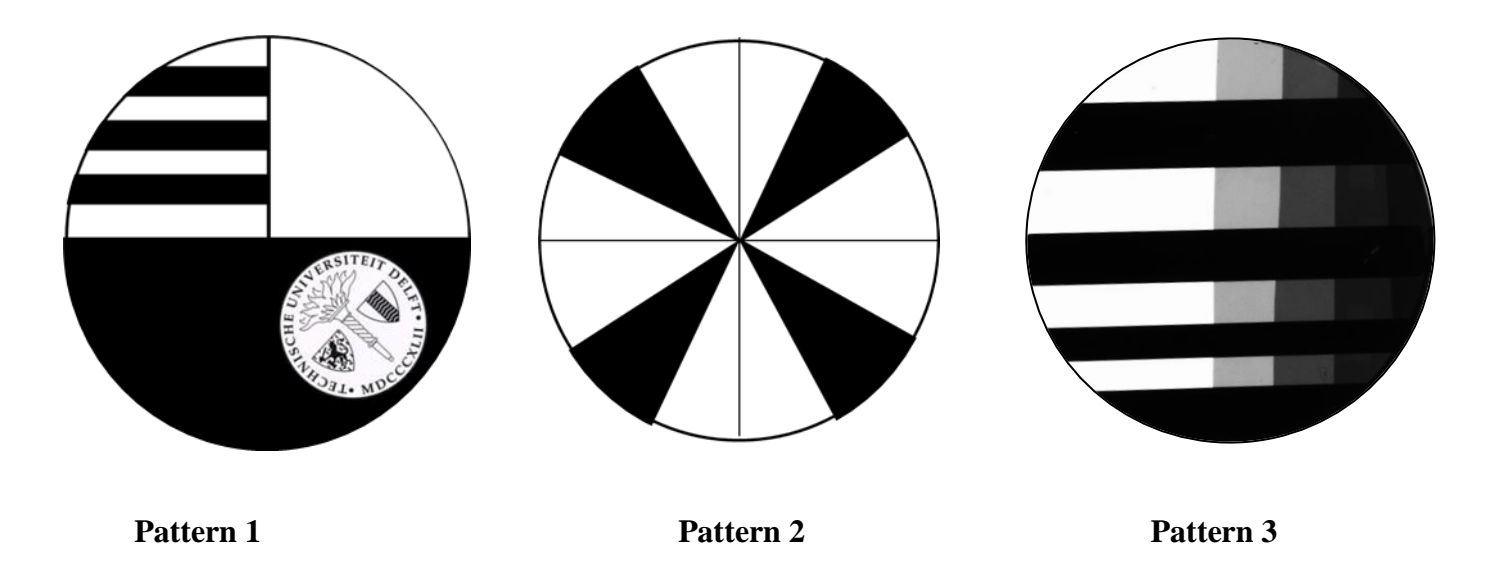


Figure 15 Different pattern examples used for analysis

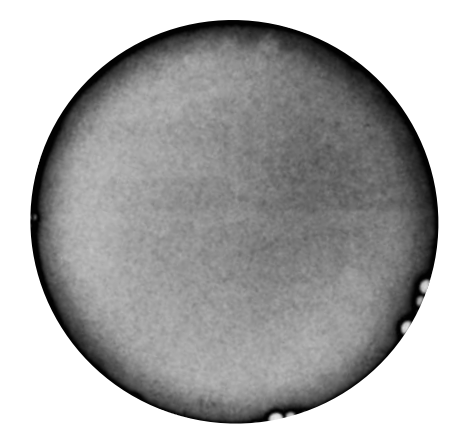
3.3.1. Pattern creation

Experiments with pattern 1 using red, green and green-red sensors are shown in Figure 16. The intensity of red light used was $0.026~\text{W/m}^2$ and green and green + far-red light was $0.2~\text{W/m}^2$. These were the highest intensities for red and green light which could be achieved in the LID set-up.

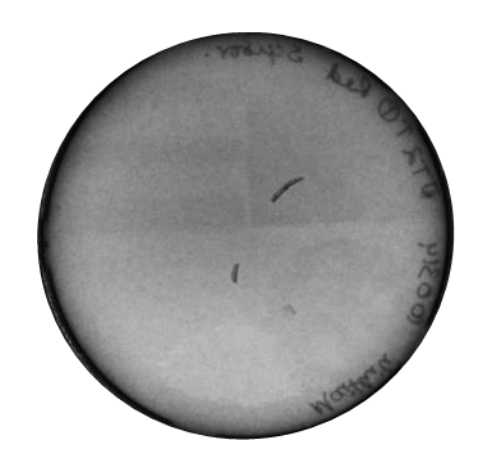
It can be noted that the red sensor gets activated by red light and gave a very clear pattern. However, under green and green + far-red light, one can observe faint pattern developments. The green sensor gave patterns with green and green + far-red light in 24 hours. The pattern created under green + far-red light was more crisp than the pattern developed under only green light. Green-red sensor does not develop any pattern under red light. Green-red sensor was expected to give patterns with both the wavelengths of light. But patterns were noticed only in the green and green + far-red light. The reason for no pattern development by green-red sensor under red light can be due to the low intensity of red light 0.026 W/m². Another factor, could be the output plasmid pJT106b3 in green-red sensor, which has a weak RBS upstream of *lacZ*, may lead to slow expression of LacZ and no pattern development for green-red sensor.



Red sensor Under red light (650 nm) 0.026 W/m², 24 hours



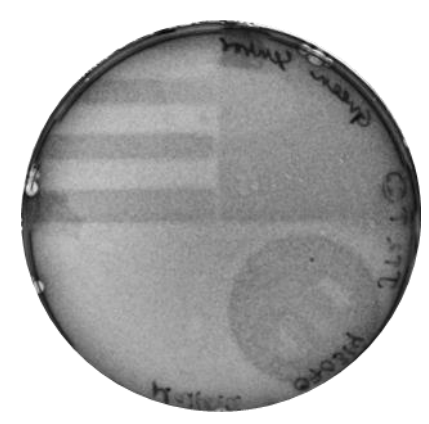
Red sensor Under green (535 nm) + far-red (750 nm) light 0.2 W/m², 24 hours



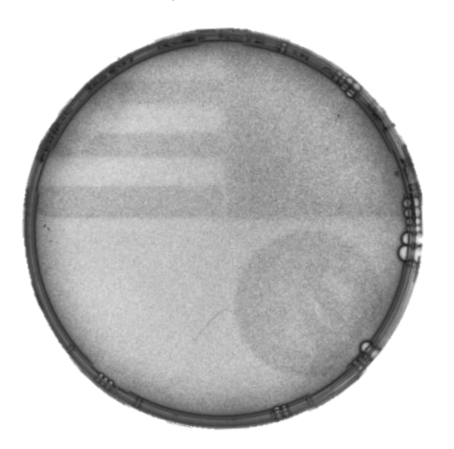
Red sensor Under green light (535 nm) 0.2 W/m², 24 hours



Green sensor Under red light (650 nm) 0.026 W/m², 24 hours



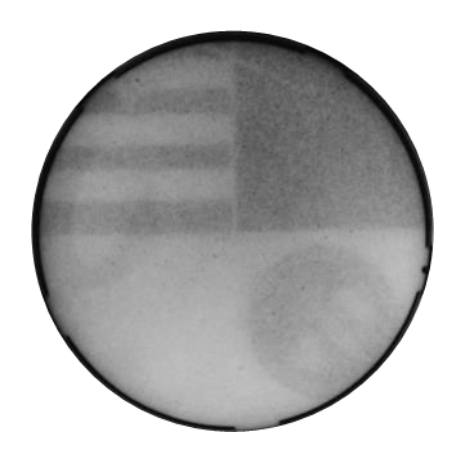
Green sensor Under green (535 nm) + far-red (750 nm) light 0.2 W/m², 24 hours



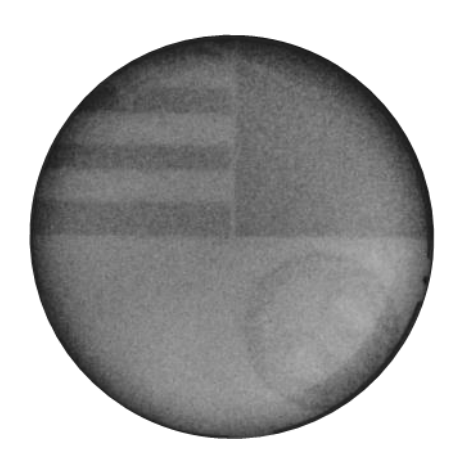
Green sensor Under green light (535 nm) 0.2 W/m², 24 hours



Green-Red sensor Under red light (650 nm) 0.026 W/m², 24 hours



Green-Red sensor Under green (535 nm) + far-red (750 nm) light 0.2 W/m², 24 hours



Green-Red sensor Under green light (535 nm) 0.2 W/m², 24 hours

Figure 16 Pattern creation on petri dish containing red, green and green-red sensor by red, green and green + far-red light (edited images) Appendix III-1 show original images.

3.3.2. Scope of pattern creation

Pattern developments can be clearly seen after 12-15 hours of incubation for all the sensors. An example of pattern created by red sensor under red light 0.06 W/m² is shown in Figure 17.

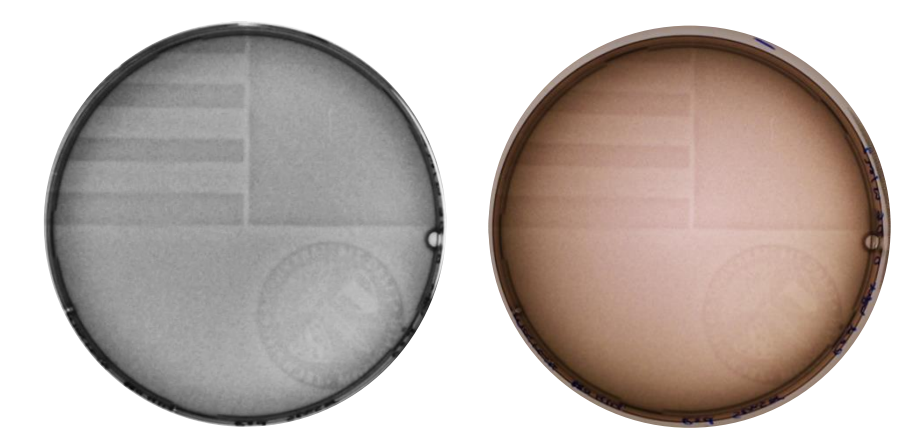


Figure 17 Pattern creation using red sensor under red light 0.06 W/m2 after 12-15 hours (both grey scale (original); coloured version)

Some other pattern examples are shown in Figure 18, representing the scope of pattern creation.

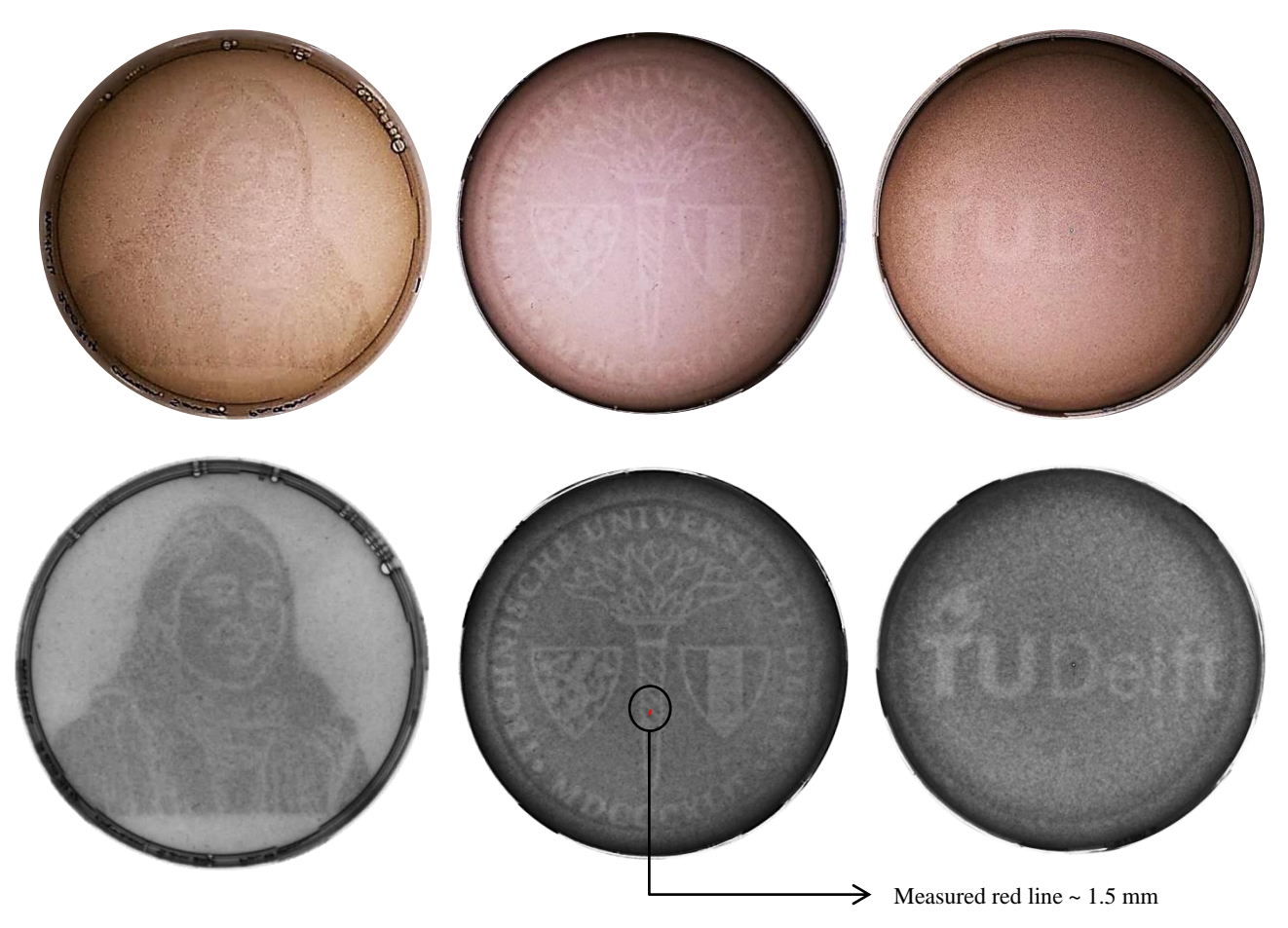


Figure 18 Examples of pattern development using the sensor systems (both grey scale (original) and coloured) - picture image of a person on a petri dish (left); TU Delft logo (middle); TU delft written on petri dish (right); The bacterial image can be clearly distinguished till ~ 1.5 mm, which was measured by a red line on the design on the flame holder in TU Delft logo (middle - bottom plate).

3.3.3. Comparison of sensors

Although the pattern creations using different sensors shown in Figure 16, gave an indication about which wavelengths of light are needed to create patterns on a certain sensor system, it does not allow us to compare and quantify the output from different sensors, as the experiments were conducted on different days and on different plates. The microenvironment conditions and experiment handling are required to be as similar as possible for us to make a comparison between the three sensors.

Therefore, induction using pattern 2 on the three sensor strains and control strain (no sensor system) under red, green and green + far-red light conditions were carried out. Outcome of patterns were recorded after 24 hours.

In 24 hours

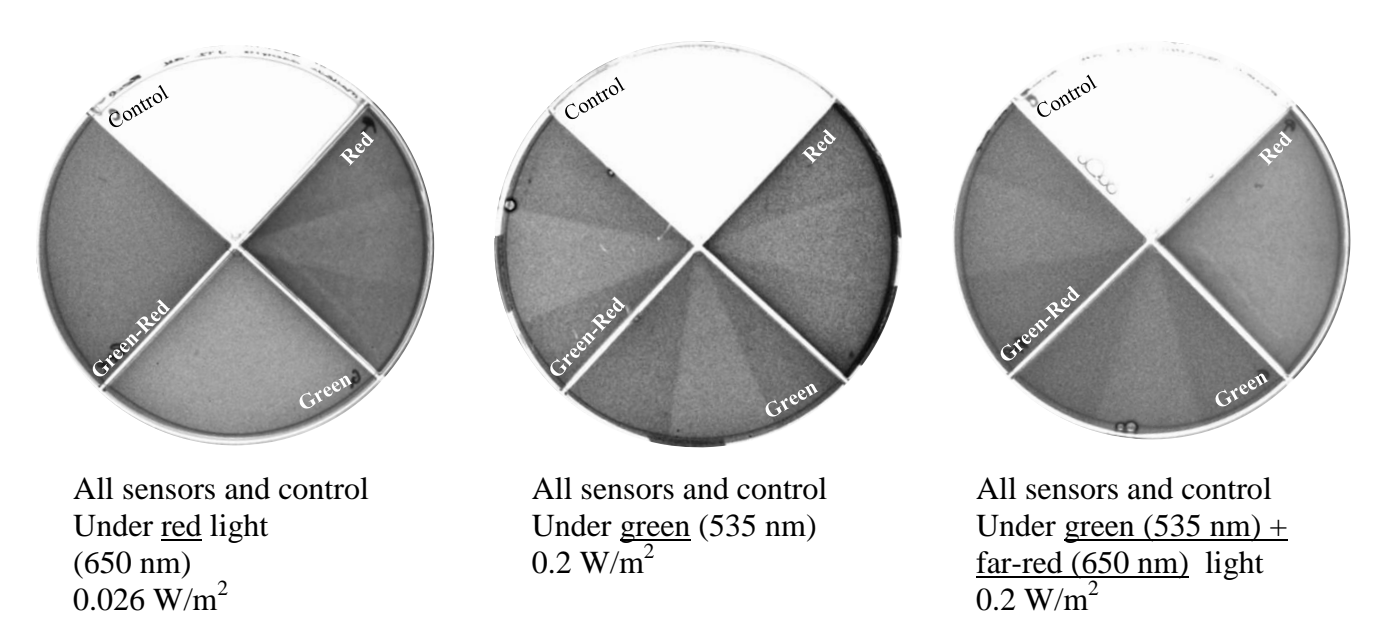
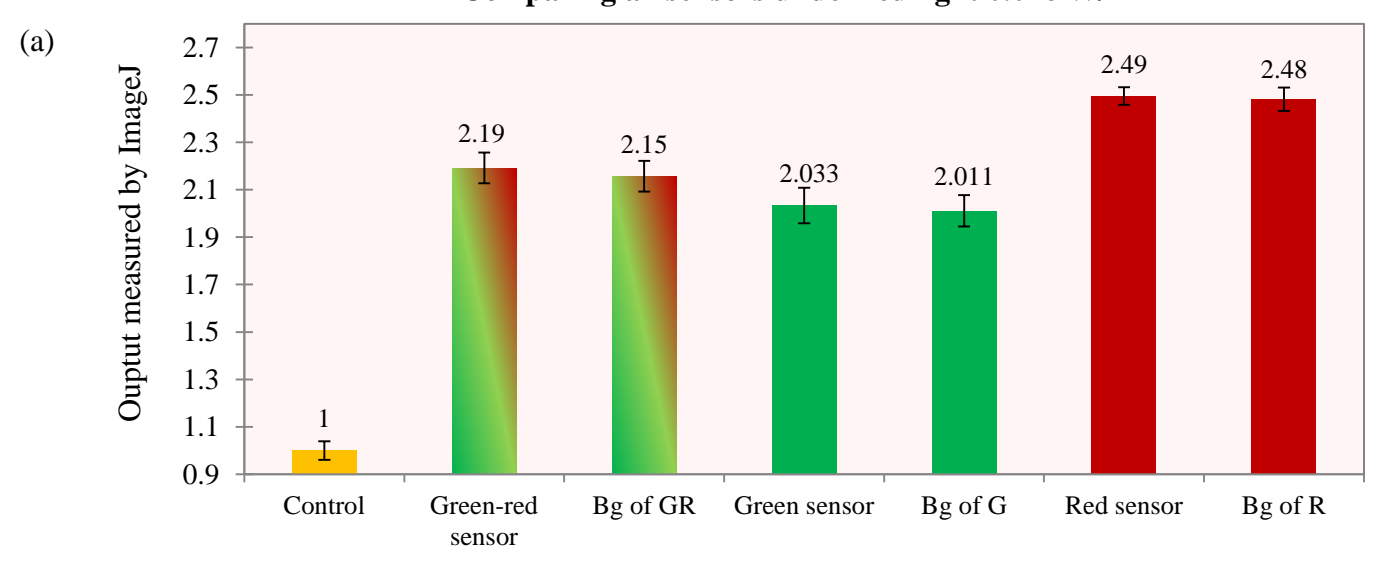


Figure 19 Comparison of all sensor systems and control strain under red, green and green + far-red light with pattern 2 using LID after 24 hours (edited images). Appendix III-1 shows the original image of plates.

Under red light, red sensor forms pattern but the cells containing green and green-red sensor systems do not give any patterns (Figure 19 (left plate)). Pattern formation by all three sensors can be observed (middle plate) under green light by visual screening of plates. But under green + far-red light, only the red sensor did not form any patterns (right plate). The green-red sensor was expected to give a pattern under red light, however it can be noticed that the red light intensity was very low (0.026 W/m²). The green-red sensor system also has in its output plasmid for red sensor, a weaker RBS in front of *lacZ*, which could lead to no pattern development under red light.

For better understanding of the plates, they were analysed using ImageJ to quantify for the output LacZ. Calibration for ImageJ software was done and is shown in Appendix III-7. Analysis using ImageJ software gave intensity values for points across the plates. This was then referred as '1' for the control strain containing no sensor system and the output of other sensors were normalized to it. Red, green and green-red sensors along with control (without sensors) plated on a quad-petri dish were quantified for the output signal. The background output given by the sensor is the output under dark area of the pattern. Basically, the area under dark should not give a black output, but in every pattern there is a background of output under dark area. For reference, this background output of each sensor systems has also been quantified and shown in Figure 20.

Comparing all sensors under red light 0.026 W/m²



Comparing all sensors under green light 0.2 W/m² (b) 2.7 2.41 2.39 Ouptut measured by ImageJ 2.5 2.27 2.28 2.20 2.3 2.1 1.9 1.7 1.5 1.3 1.1 0.9 Control Bg of GR Green sensor Bg of G Red sensor Bg of R Green-red

sensor

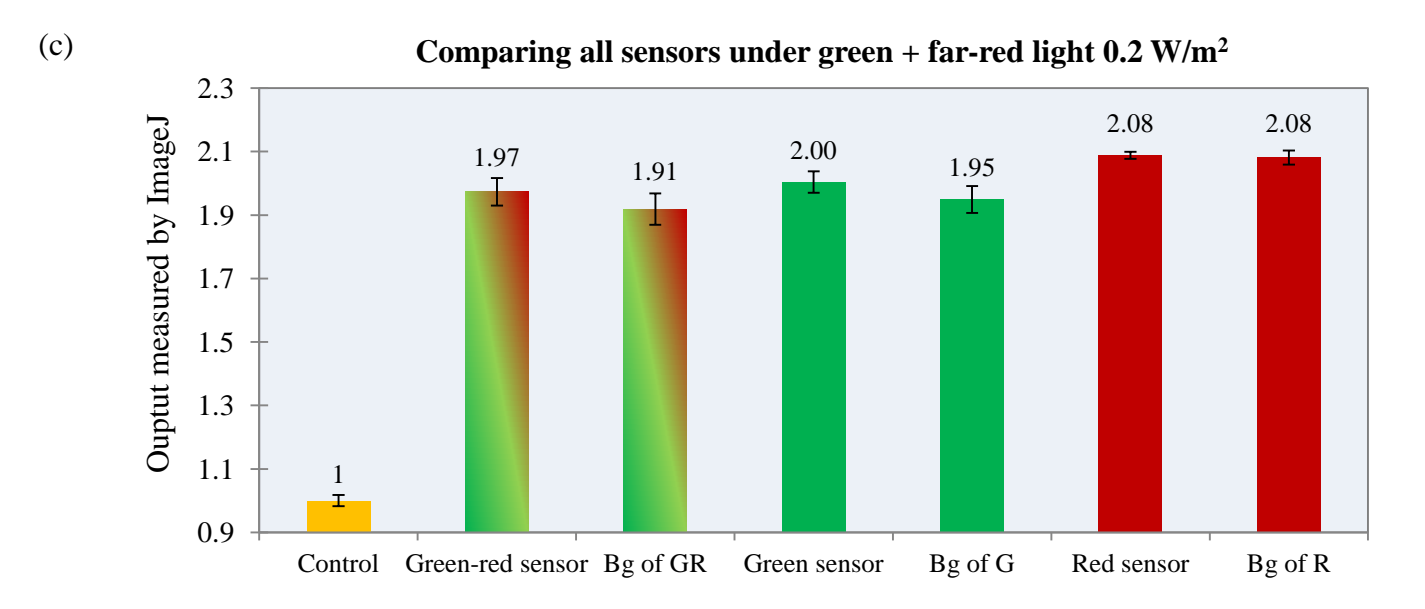


Figure 20 Output signals of different sensor systems under red, green and green + far-red light; Bg: background output of GR (green-red sensor), G(green sensor), R (red sensor).

In Figure 20, the red sensor does not show a considerably high difference in its output signal under all three conditions of light induced area to the area under dark. The background output, i.e, the sensor systems in dark area of the pattern, was significantly high compared the actual light induction of red sensor. However, by visual examination of the plates, one can see a pattern being created under red and green light, stating that the red sensor is indeed induced under light. It is enough to create patterned pictures on a petri-dish containing bacterial sensors systems. Some patterns created using the sensor systems are shown in Figure 18.

Both the sensors green-red and green show slight increase of output signal under green and green + far-red light as compared to under dark. Through ImageJ analysis, this difference does not seem very high but it may be significant, since in the visual examination of plates a clear pattern can be seen.

Under green + far-red light, these two sensors show output similar to the output under green light. The main concept of using far-red light was to analyse its effect on de-activating the sensors. Although, far-red light does not seems like it has a decreasing effect on the green and green-red sensor, it would be irrational to conclude this based on ImageJ analysis (Figure 20 (b)(c)). For the red sensor, the far-red light combination did not form any patterns (Figure 19 (right plate)). Analysis by ImageJ did not show very high difference in output of sensor under light induction as compared to under dark (Figure 20 (c)). This may be due to the deactivation of red sensor by far-red light. Accurate analysis using Miller assay can reflect more upon whether far-red light has a role in the deactivation of sensor systems or not?

On the same note, under red light, the green-red and green sensors did not develop any patterns when checked visually. Even by analysis of ImageJ, the sensors did not show output signals significantly higher than the background output. Although, green sensor was expected not to give pattern under red light, the green-red sensor system was expected to sense red light. The low intensity of red light could be a reason why no patterns were developed by green-red sensor under red light

More analysis using a gradient of light intensity to create patterns and to characterize the output signal with respect to input light for individual sensors was done in Section 3.3.4.

[Please turn over]

3.3.4. Gradient experiment

In order to analyse the variation in output signal under a gradient of input light intensity, pattern 3 was used to create patterns using green and red sensor. Green sensor was induced with a gradient of both green light and green + far-red light. Red sensor was induced with different intensity gradient of red light. Results can be seen in Figure 21.

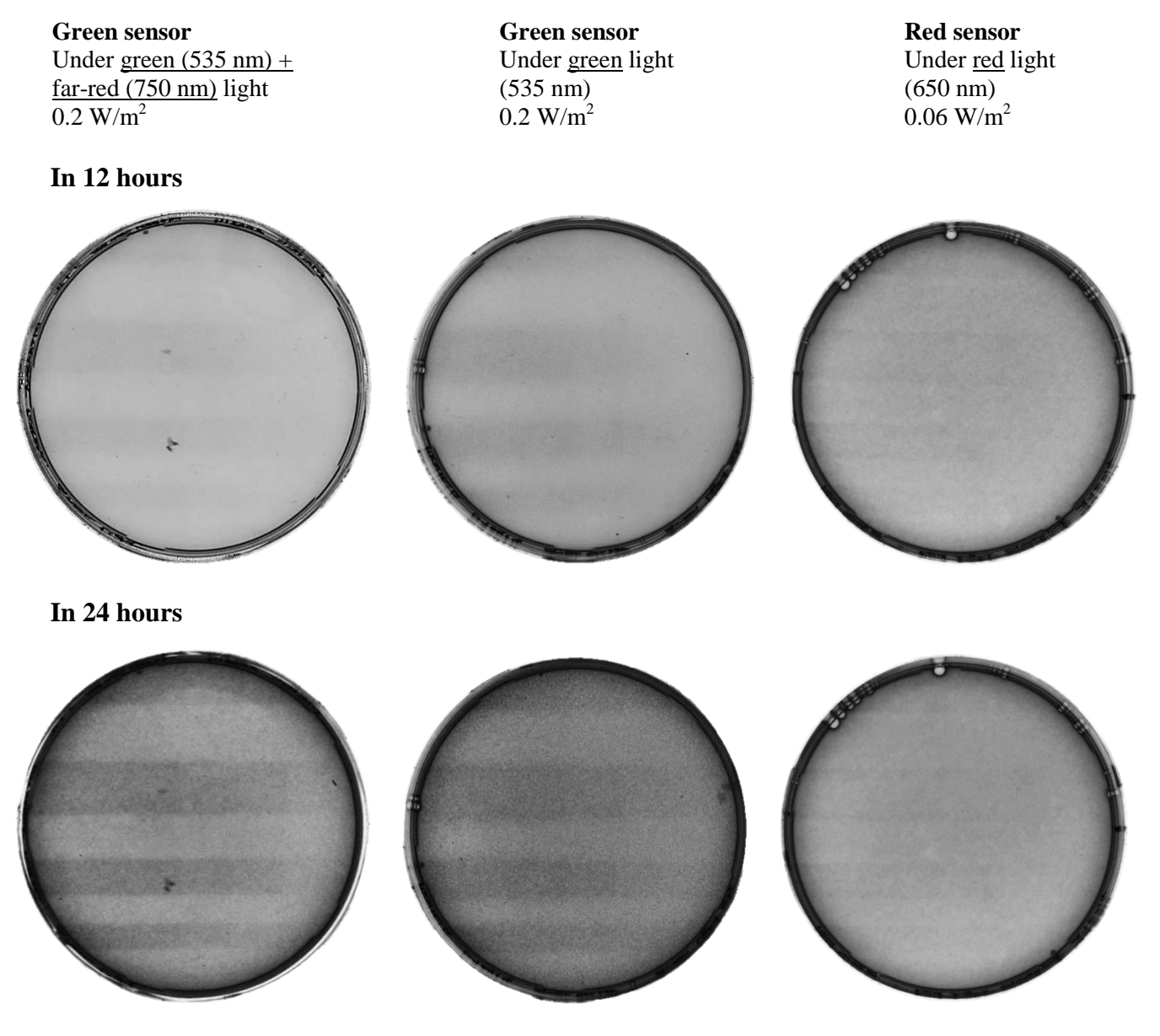


Figure 21 Gradient of green, green + far-red and red light intensity on green and red sensors (original)

The intensity of black output in the patterns decreased gradually in both green and red sensors as the light intensity was decreased. The plates were quantified using ImageJ software. Since there was a gradient of light intensity across the plate, quantification of two strips on the plate was done; One strip with light induction and the other under dark (Figure 22). This analysis was done on the plates of 24 hour induction for all three combination of experiments:

- 1) Green sensor under green light
- 2) Green sensor under green + far-red light
- 3) Red sensor under red light

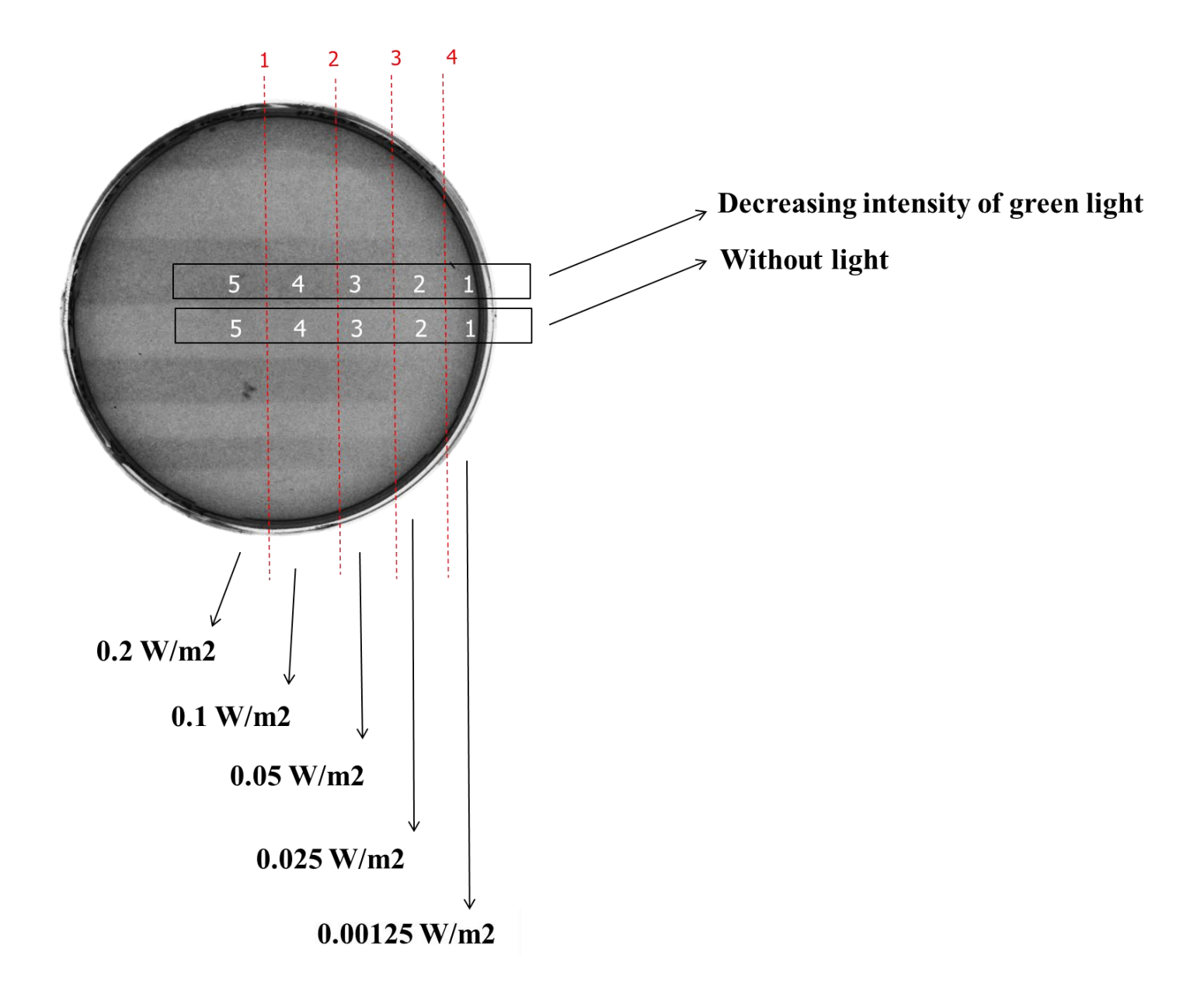


Figure 22 Gradient plate showing different intensities for green light and bands which were quantified using ImageJ software.

Analysis using ImageJ software gave output intensity values for points across the plates. This was then referred as '1' for the 0% light falling on the plate (i.e, under dark) and the other values were normalized to it. Output of green sensor under gradients of green and green + far-red light induction and under dark were plotted.

Green sensor under different intensities of green and green+far-red light

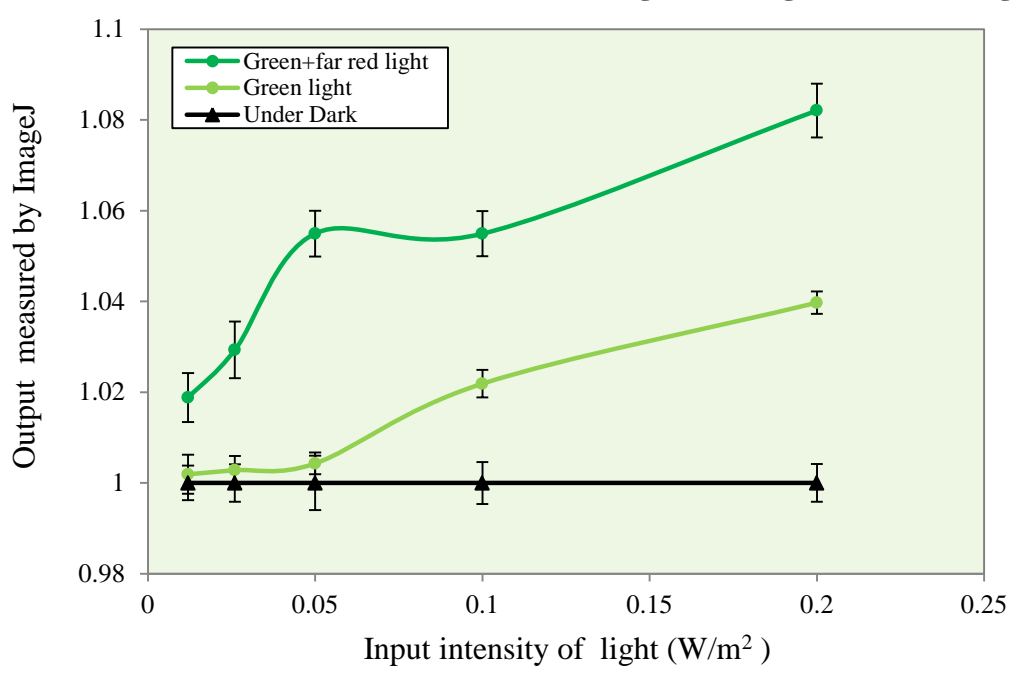


Figure 23 Output signals of green sensor with respect to gradient intensities of green and green + far-red light.

It can be noticed from Figure 23 that the green sensor when induced by green + far-red light gave a higher output as compared to when induced by only green light. The background under dark was much lower than both the light induced areas.

Red sensor under different intensities of red light

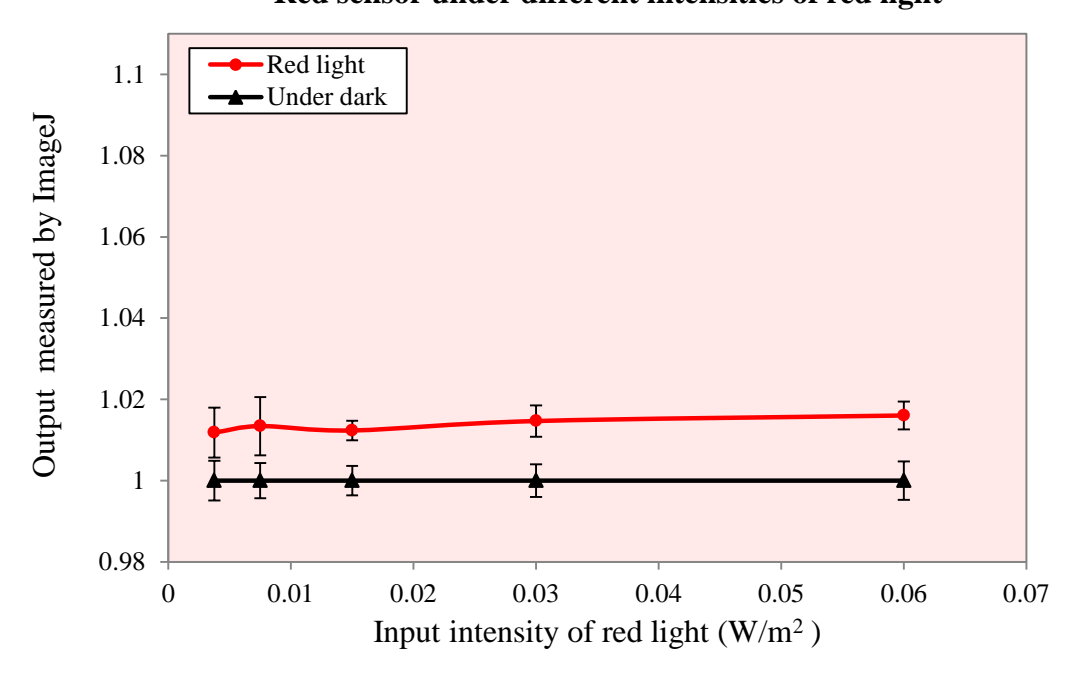


Figure 24 Output signals of red sensor with respect to gradient intensities of red light.

Figure 24 shows output signal of the red sensor under different intensities of red light and under dark. The gradient intensities used for red light were 0.06, 0.03, 0.015, 0.0075, 0.00375 W/m². The output signal under red light induction compared to area under dark, is not very high but it might be significant.

These experiments were only tried out on green and red sensor systems and not on bacteria containing both the sensors. Since having the two sensors together is a complex system leading to unknown variation in the output signal, it was considered to first try and characterize the individual sensors.

Thus, the gradient experiment implies that gradual increase in input intensity leads to higher output signals. Green light activated the green sensor as compared to under dark. Green + far-red light showed slight increase in the output signals of green sensor as compared to when induce only green light. Even at lower intensities of 0.00125, 0.025 W/m², the green + far-red light induced the green sensor more than the induction seen under only green light (Figure 23). The use of far-red light was employed to de-activate the green sensor, as suggested in the literature². Whereas, in this experiment far-red light seems to be inducing the green sensor. However, this analysis using ImageJ gave a very rough quantification of output from the plates, which were induced on different days and on different plates. It would be irrational to conclude through these results about the behaviour of green sensor towards far-red light. More precise analysis of the output using Miller assay can give accurate sensor characterization to comment better on the activity of the sensors under far-red light.

The red sensor also showed induction under all intensities of red light, however, they do not seem to increase more than 2%. Since the highest intensity of red light used was 0.06 W/m^2 , quite less from the intensity 0.15 W/m^2 mentioned in literature, it would be interesting to try higher values of red light intensities for better characterization of the red sensor.

[Please turn over]

3.4. Characterization of sensors by quantification of LacZ

In order to have an accurate quantification of the output signal LacZ with respect to input signal, different intensities of light were used to induce the sensor, and then quantify by Miller assay, thus enabling in better characterization of the sensor systems. Miller assay is a colorimetric assay, which was done to quantify the output LacZ. *LacZ* encodes for an enzyme called β -galactosidase, which reacts to a colourless substrate o-nitrophenyl- β -D-galactoside (ONPG) to give galactose and o-nitrophenol (ONP)²⁸. ONP can be measured for its intensity of yellow colour, which is proportional to the quantity of LacZ in the sample (Section 2.3.2). The sensors red, green and green-red were calibrated for Miller assay and is shown in Appendix III - 6.

Different experiments carried out using Array Tube Illuminator set up (Section 2.3.1)were:

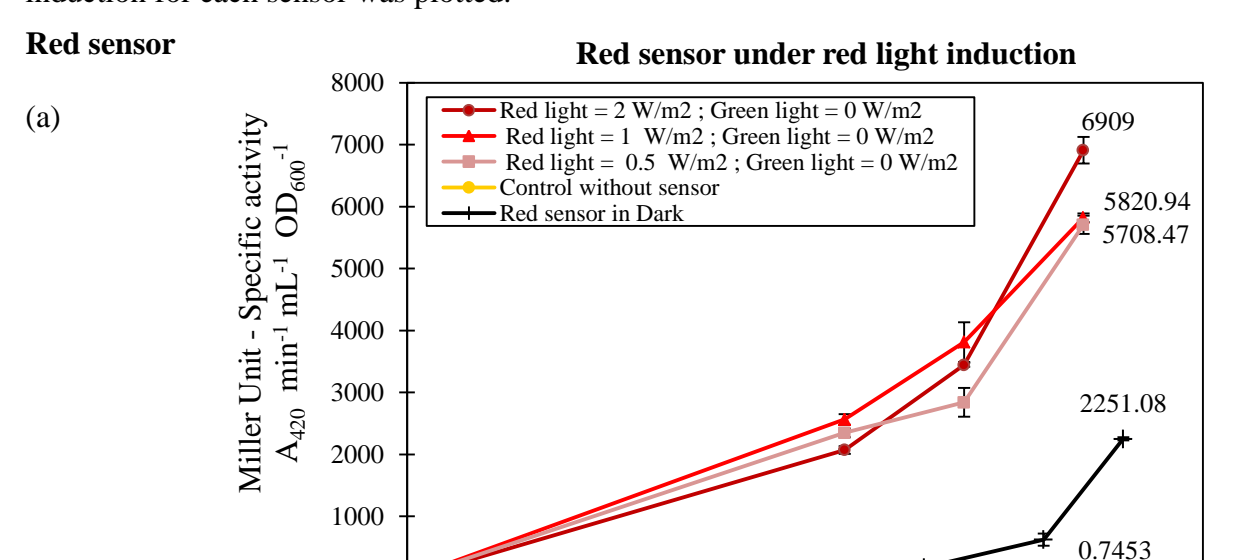
Table 4 List of experiments carried out on Array Tube Illuminator

Experiment No. Green light intensity. Red light intensity.

Experiment No.	Green light intensity	Red light intensity
1	0 W/m ²	2 W/m ²
2	0 W/m ²	1 W/m ²
3	0 W/m ²	0.5 W/m ²
4	6 W/m ²	0 W/m ²
5	4 W/m ²	0 W/m^2
6	2 W/m ²	0 W/m ²
7	4 W/m ²	1 W/m ²
8	2 W/m ²	2 W/m ²
9	2 W/m ²	0.1 W/m ²

For characterization of the sensor systems, different intensities of red light 2, 1, 0.5 W/m² and green light 6, 4, 2 W/m² were used to activate it. Literature suggests red light could be used to deactivated the green sensor³, therefore, different combinations of green and red light were used in this experiment to analyse if it is possible to deactivate the green sensor. Far-red light was also build in the device, but due to very low intensity of LEDs and in-consistency of the LEDs used in the device, it was decided not to use far-red light in these experiments. Miller assay was carried out in triplicates and output signal vs. time of induction for each sensor was plotted:

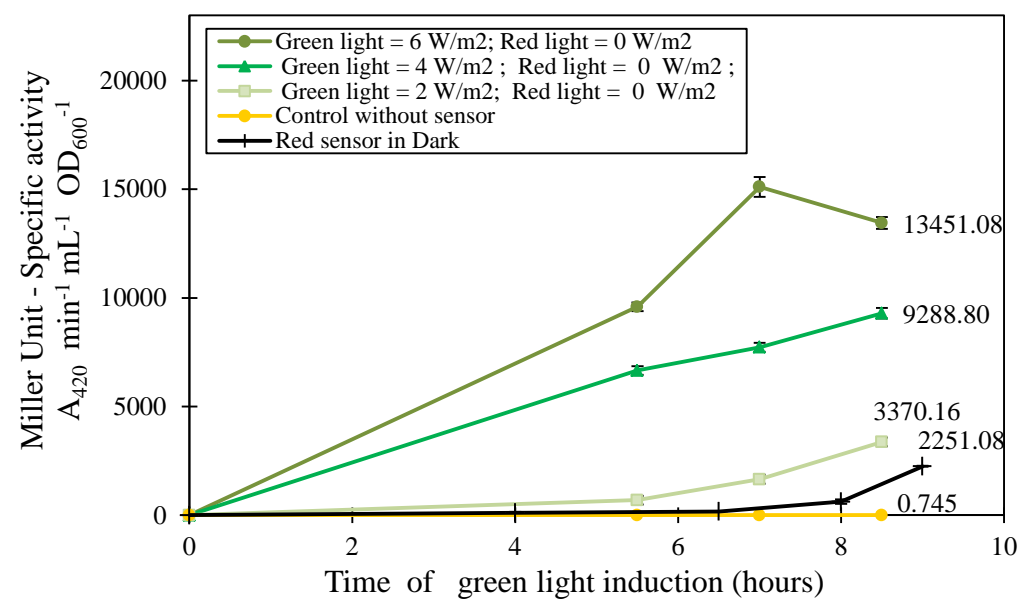
Time of red light induction (hours)



0 +

10





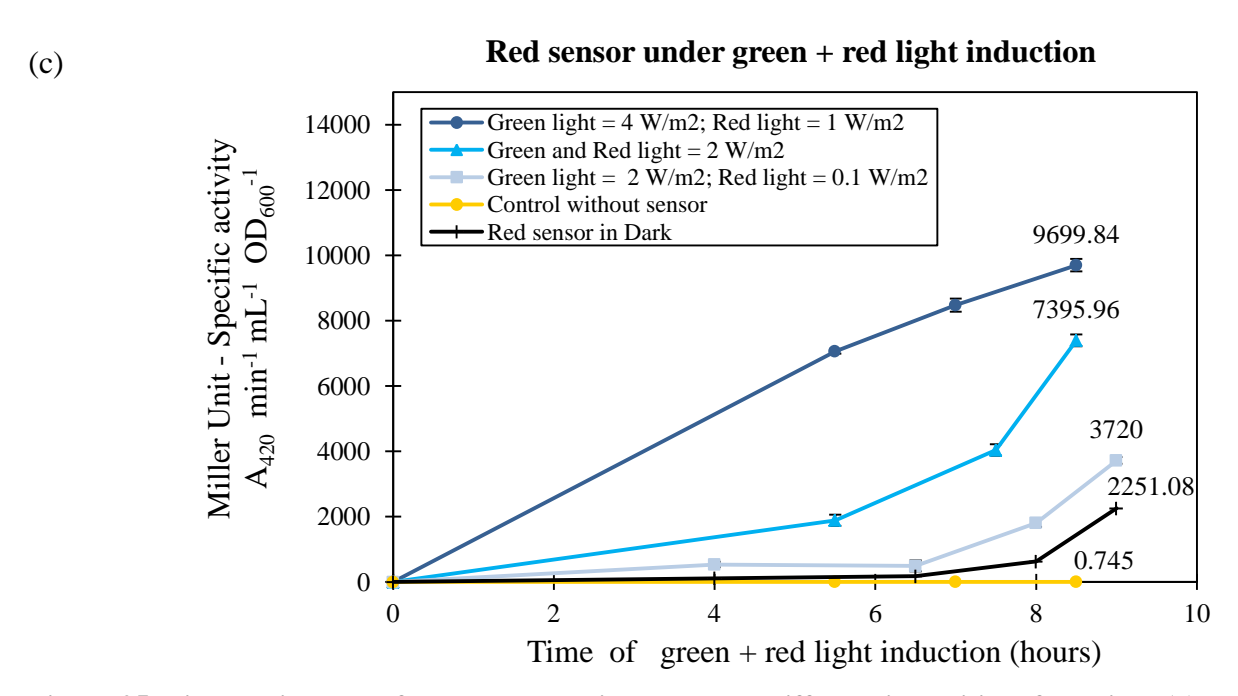


Figure 25 Miller Unit output for red sensor with respect to different intensities of red light (a), green light (b) and green + red light (c) induction over time.

The above graphs in Figure 25, shows red sensor induced with red, green and green + red light for a time period of 8-9 hours. Three samples were taken from the tubes and Miller assay was carried out on the samples. In Figure 25(a), the Miller unit of red sensor induced at red light intensity of 2 W/m^2 was higher compared to 1 W/m^2 and 0.5 W/m^2 . However, there was almost no difference in the Miller units for red sensor under 1 W/m^2 and 0.5 W/m^2 of red light.

The experiment carried out under green light intensities of 6,4 and 2 W/m², shows the red sensor to be highly sensitive to green light and gave Miller unit measurements ~15000. There was a stepwise increase in the Miller unit output as the intensity of green light was increased. (Figure 25(b))

A combination of green light with red light was also used to induce the red sensor shown in Figure 25(c). Miller unit output \sim 9700, under a combination of green light 4 W/m² and red light 1 W/m² can be noticed.

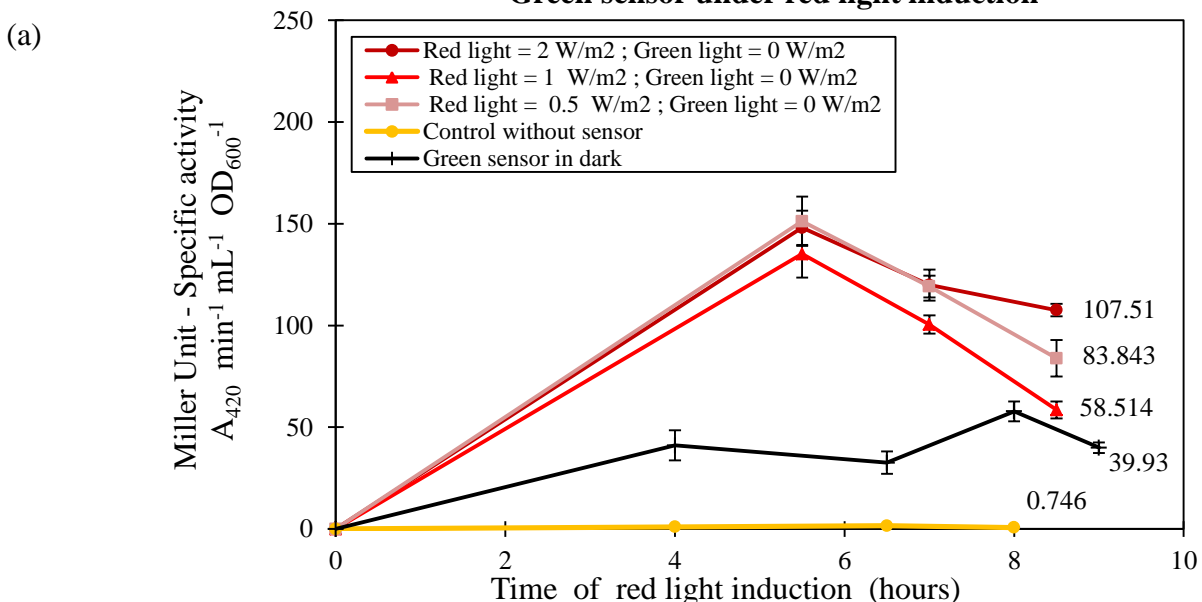
The combination of green and red light at $2~W/m^2$ gives ~7400 Miller units which was double the Miller units under green light $2~W/m^2$ and red light $0.1~W/m^2$ (~3700). Similarly, Miller unit output of red sensor under green light of $2~W/m^2$ was ~3370 (in (b)) which was less than Miller units 6909 under red light of $2~W/m^2$ (in (a)). Therefore it can be concluded that green light does have an effect on the red sensor system but not as much as the red light.

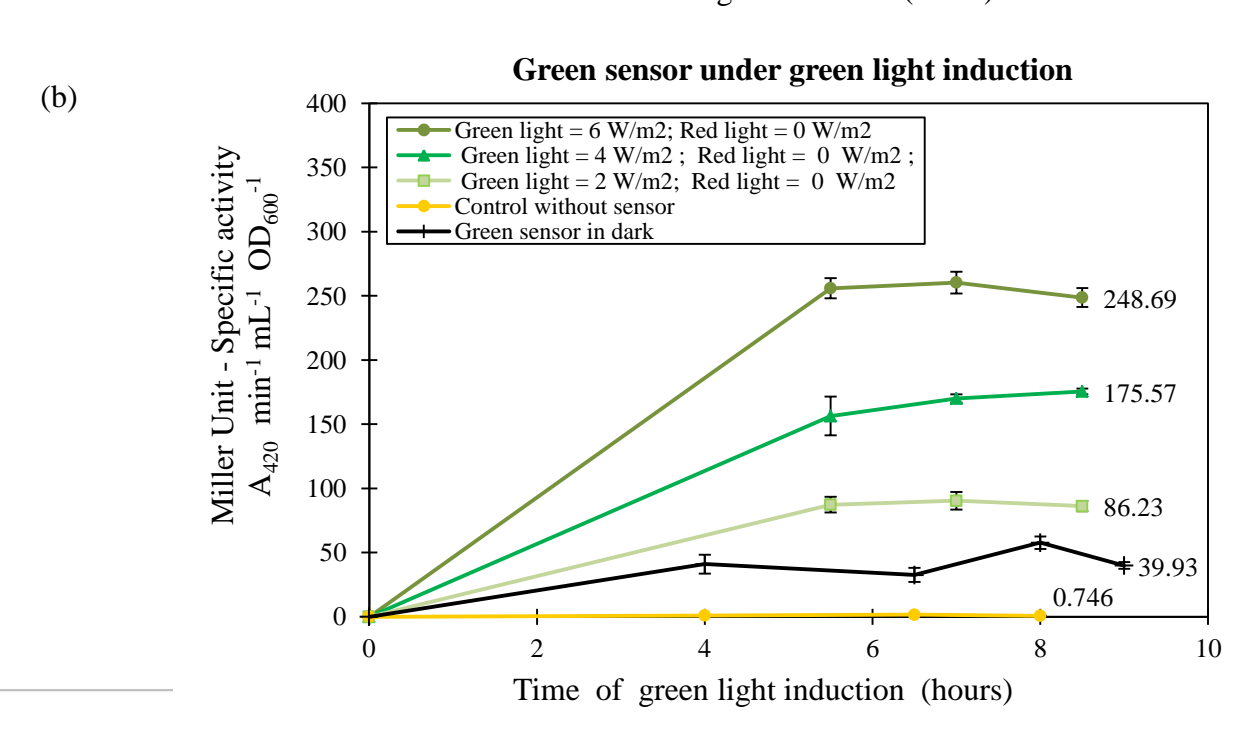
When comparing the (b) and (c), it can be noted that combination of green light 2 W/m^2 with and without red light of 2 W/m^2 has Miller units ~7400 and ~3400. This is a high difference to observe. Again, concluding that the red light has more effect on the red sensor.

Therefore, an overall conclusion can be made about the red sensor, to be sensitive towards both red and green light. However, a little more sensitive towards red light than green light. Increase in the light intensity leads to an increase in the output signal, however with increase in time of exposure we can notice that the output signal also increases. This can be due to the growth of cells over time leading to more output signal when exposed to light.

Green Sensor

Green sensor under red light induction





Green sensor under green + red light induction

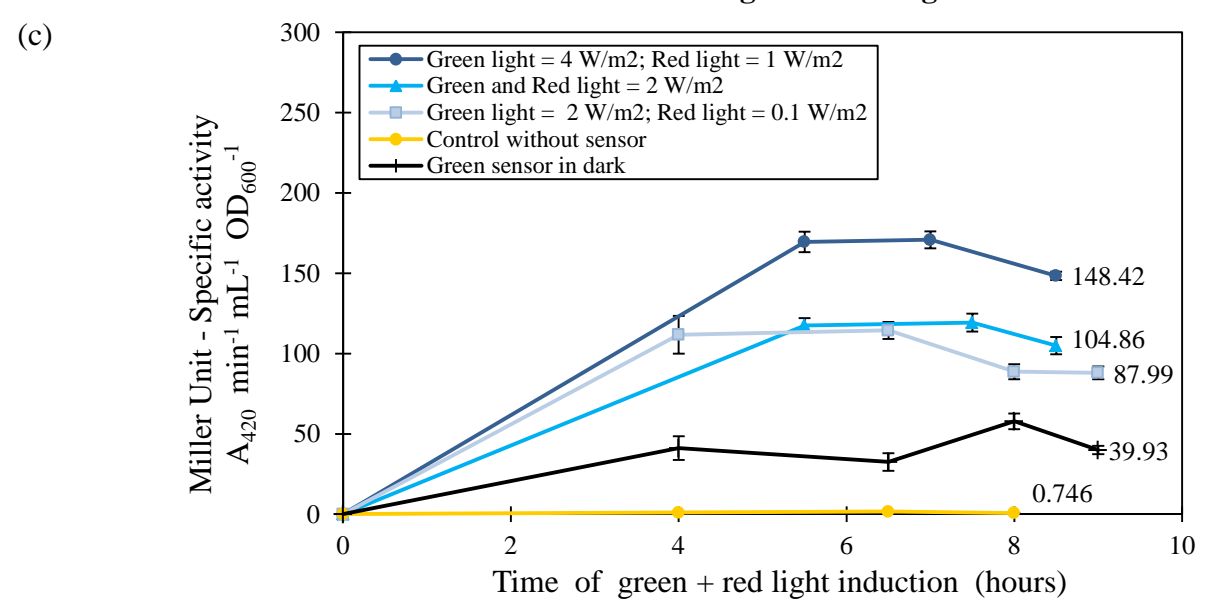
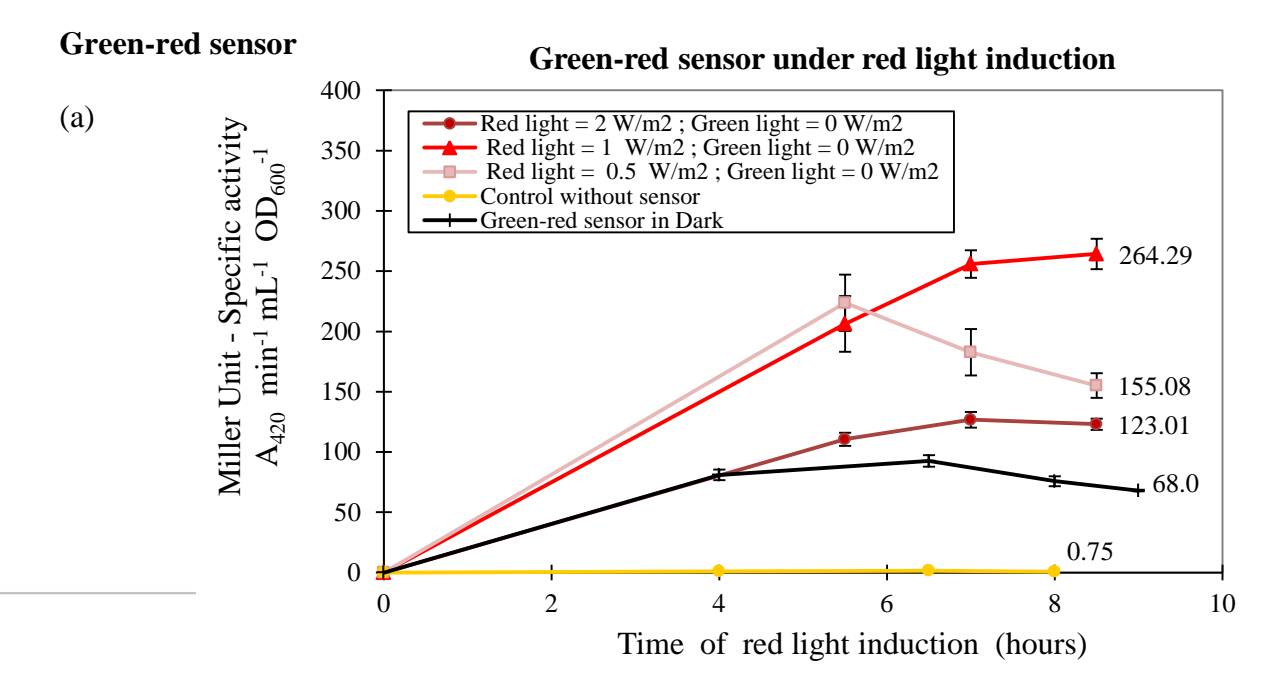


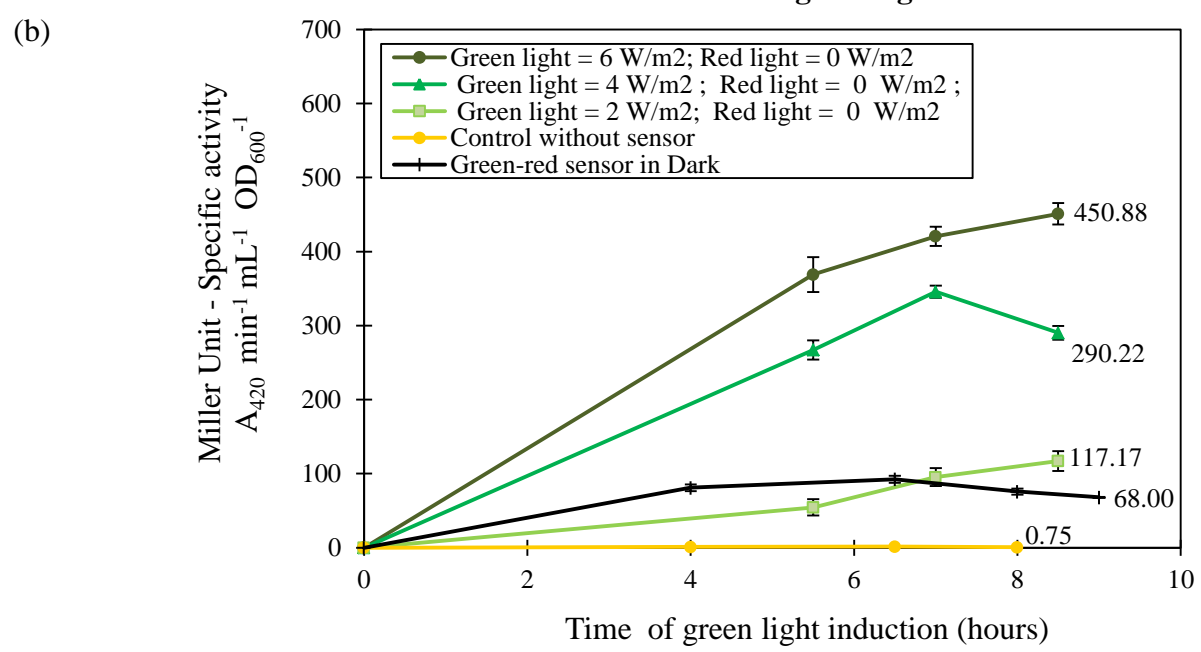
Figure 26 Miller Unit output for green sensor with respect to different intensities of red light (a), green light (b) and green + red light (c) induction over time.

Green sensor under different light intensities are shown in Figure 26. In (a), the green sensor appears to be repressed due to the red light. It can be noticed that the Miller units for green sensor was ~120 Miller unit, whereas the red sensor reaches upto 6000-7000 Miller units Figure 25(a). Shown in (b) is green sensor under green light intensities. There was a stepwise increase in output noticed with increase in green light intensity. The output signals reached a plateau after ~6 hours of light induction. Under combinations of green and red light, the green sensor appears to reach a saturation as seen under the green light induction. However in (c), combination of green and red light at 2 W/m² gave similar output as combination of green light at 2 W/m² and red light at 0.1 W/m². This can infer that although red light was 2 W/m² (much higher than 0.1 W/m²), it did not activate the green sensor.

When comparing (b) and (c), Miller units for green sensor reaches ~175 under green light 4 W/m², whereas under combination of green light 4 W/m² with red light 1 W/m² gives output ~150 after 7 hours of light induction. Similarly, in (c) under combination green and red light at 2 W/m², the Miller unit reached after 7 hours was ~100, similar to output under only green light of 2 W/m² (Miller unit ~90). This can conclude that green sensor may not be activated under red light intensities or could be deactivated by it



Green-red sensor under green light induction



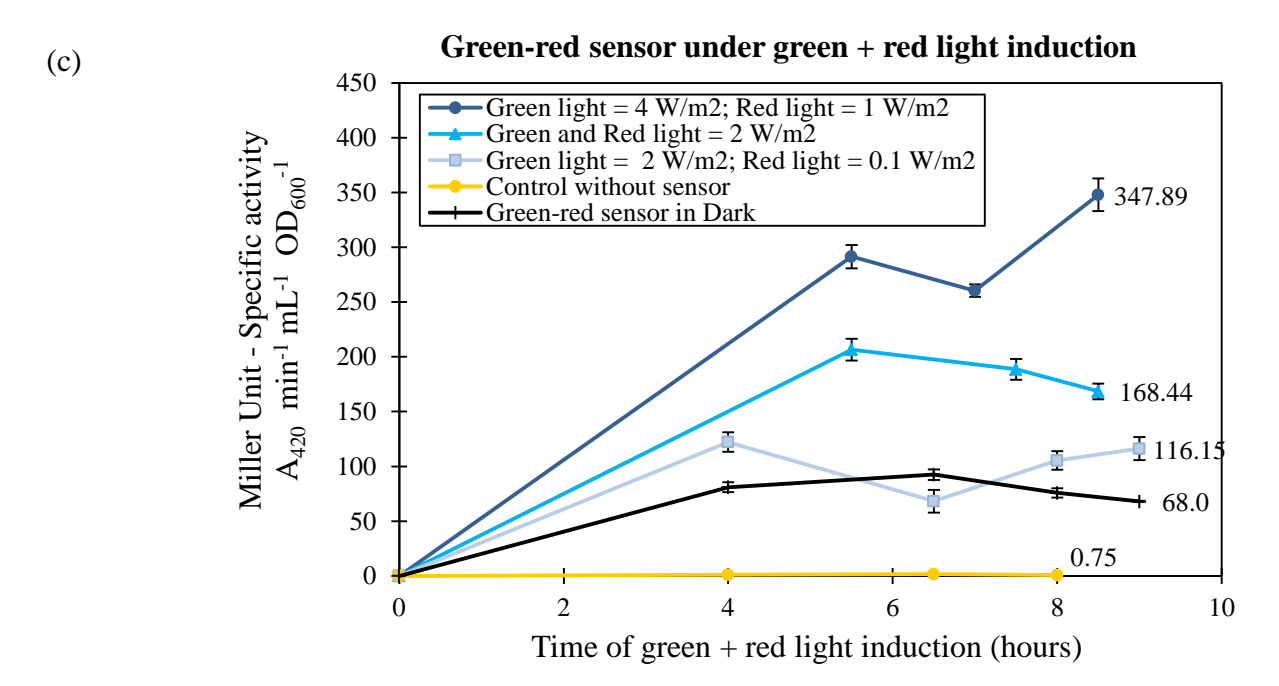


Figure 27 Miller Unit output for green - red sensor with respect to different intensities of red light (a), green light (b) and green + red light (c) induction over time.

For green-red sensor seen in Figure 27(a), red light intensity of 1 W/m² induces Miller unit output ~270, but at 2 W/m² the Miller unit output was ~130. In the green-red sensor there may be a repression of the green sensor due the red light intensity at 2 W/m², but at 1 W/m² the red sensor may be activated leading to some increase in the Miller unit. Whereas, red light at 0.5 W/m² may not be enough to induce continuous activation of red sensor present in green-red sensor. However, this is not a very conclusive observation.

There was a step-wise increase in Miller unit output of green-red sensor with increase of green light intensities (b). In (c), increasing intensities of green + red light express higher Miller unit output under each combination. However the output under dark was quite high and overlaps with the lowest light intensity in (a) (b) and (c). Integrated Miller assay graphs for red, green and green-red sensors are shown in Appendix III-4.

Comparing Miller unit outputs for all sensors

Green-red sensor with green sensor:

Green-red sensor under green light (Figure 27(b)) reaches ~450 Miller units, much more than green sensor in Figure 26(b). This can be due the sensitive red sensor system present in green-red sensor which is getting activated by the green light.

Similarly, comparing Figure 27(c) and Figure 26(c), the green and red light combination on the green-red sensor induces a similar effect like in the green sensor. Under green light 4 W/m² and red light 1 W/m², Miller unit value reached \sim 340 for green-red sensor and for green sensor it was \sim 170. This showed that the green-red sensor system was more sensitive to the light induction. This may be due to the presence of two sensor systems.

Red sensor with green-red sensor:

The red sensor gave Miller unit output in the range of ~4000 to ~10000 compared to green-red sensor and was very sensitive to all intensities of light (Figure 25). This can be due to the output plasmid pJT106b present in the red sensor circuit, having a strong RBS in front of *lacZ*, whereas in the green-red sensor system, the plasmid pJT106b3 present in the red sensor circuit contains a weaker RBS upstream of *lacZ*. This could be a reason why green-red sensor did not give as high Miller output as compared to red sensor.

Red sensor with green sensor:

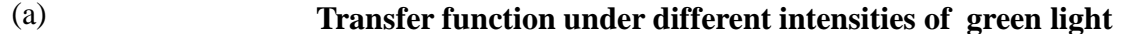
The red sensor gave higher values of Miller units output ~15000 under green light (Figure 25(b)), while the green sensor gave ~250 Miller units output (Figure 26(b)). This shows that red sensor highly sensitive to green light compared to the green sensor.

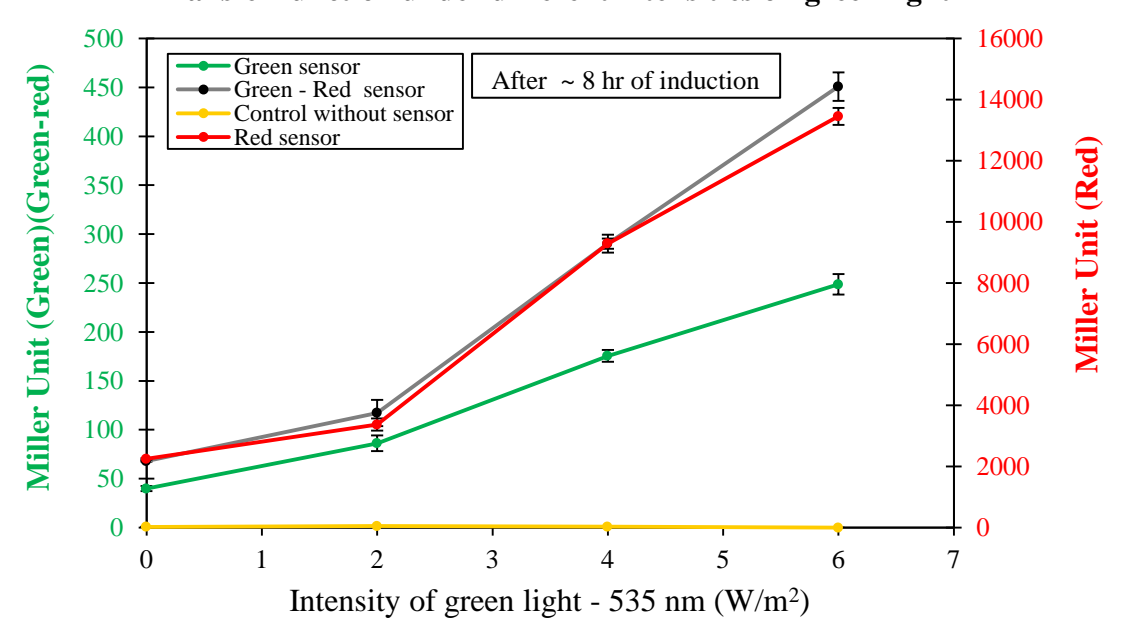
In dark - comparing all sensors:

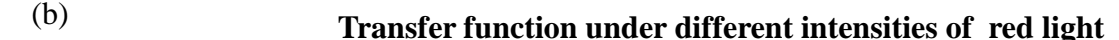
Under dark, the three sensor systems show a minimum output or background output signal. Comparing this for the three sensors, showed that the red sensor had the highest background output of ~2250. Green sensor had ~40 Miller Units output and green-red sensor had ~70 Miller units output under dark.

Cumulative Transfer functions

To illustrate the variation in the control of transcription, light intensity transfer function of strains carrying red, green and green-red sensor under red light of intensity 0, 0.5, 1 and 2 W/m² and green light of intensity 0, 2, 4 and 6 W/m² are shown in Figure 28.







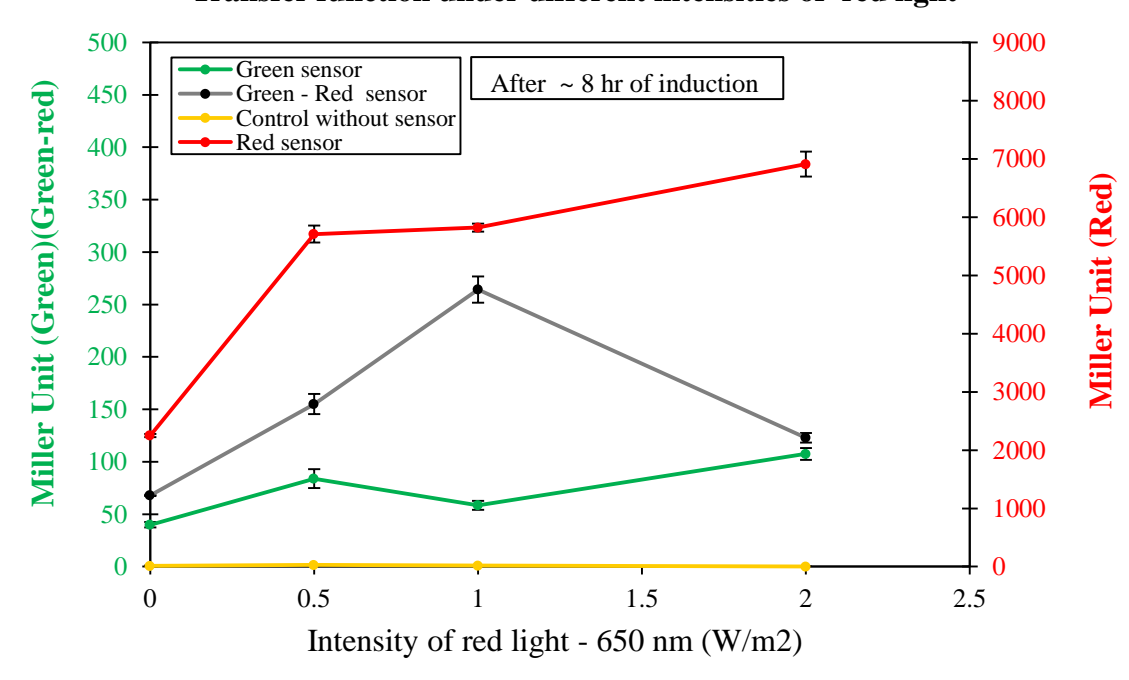


Figure 28 Light controlled gene expression in $E.\ coli$, (a) Under different intensities of green light -0, 2, 4 and 6 W/m²; (b) Under different intensities of red light -0, 0.5, 1 and 2 W/m² after ~8 hours of induction; Green and green-red sensors correspond to the left axis, red sensor corresponds to the right axis.

The control of gene expression in *E. coli* using light of wavelength 535 nm (green) and 650 nm (red) showed that red sensor was highly sensitive to red light and reached ~13400 Miller units as seen in Figure 28(a). The green-red sensor reached ~450 Miller units compared to the green sensor at ~240 Miller Units. However, the trend of increasing input light intensity, exponentially increases the output signal.

In (b), the red sensor reached a saturation level between ~7000 to 6000 with all intensities of red light. The green sensor was observed to be suppressed under red light and does not increase more than 110 Miller units under all red light intensities.

Green-red sensor had a linear relationship till red light 1 W/m², but at 2 W/m² the Miller unit output decreased. This can lead to an inference about the presence of green sensor in green-red sensor, being repressed by red light intensity at 2 W/m². However, low intensities of red light, does not repress or effect the green sensor present in green-red sensor system. This may make the red sensor more active or available to the red light, hence leading to higher Miller unit output of green-red sensor at 0.5 and 1 W/m² of red light. However, this is still an observation noticed with only three intensities of red light. More accurate conclusion can be made if other intensities of red light were also applied on the green-red sensor.

Under dark, the red sensor gave high Miller unit output as compared to other sensors. This can be due to the strong rbs present upstream of *lacZ*. Green-red sensor had more background output under dark than green sensor, which could be due to the presence of two sensors in one system. Green sensor has a simple light input to output circuit, therefore it showed the least background output under dark.

3.5. Fine tuning the sensor system

Results shown in Section 3.3 and 3.4 show an increase in the output signal by light induction of sensors. But, we also observe under dark some amount of output signal. In this section, an attempt to fine tune the current circuit was made. Mutation of plasmid containing the output gene by site-directed mutagenesis to create random library of RBS region was carried out.

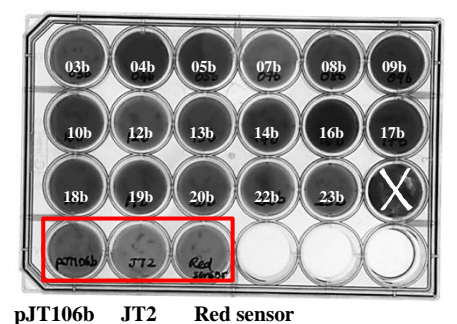
Different strategies were used to create a RBS library for the rbs upstream of *cI* in the plasmid pJT106b/b3 (Section 2.4.1). This library was then visually screened for colonies giving the least output under dark, in order to improve the pattern development. Selected mutants were then quantified for output using Miller assay.

3.5.1. Using site-directed mutagenesis by randomised primers (method I)

Randomized primers were designed containing 'NNN' base pairs. Standard PCR protocol was followed to generate the RBS library. This method uses plasmid pJT106b as template on which the random primers bind to create mutation in the RBS site upstream of *cI*. Section 2.4.1 - I describes the method in detail.

23 colonies were formed after transformation. Colony PCR was done on all colonies to check for presence of the insert region and successful transformation. 17 colonies were positive and visual screening of these colonies were done using 24-well plate along with pJT106b, *E. coli* JT2 and red sensor as controls (in red box). Time zero and plates after 6 hours under dark at 37 °C are shown in Figure 29.





In dark 37 °C 0 hr 6 hr

Figure 29 Screening of RBS library colonies created from Method I.

Most of the colonies turned as black as the positive controls pJT106b and red sensor (in red box). This means that the output signal under dark was high in the mutant colonies, whereas the aim was to create a mutant with weaker output under dark. Also, the sequencing results of all colonies revealed the presence of native 'CAC' sequence in the RBS code except for colony 17b.

787 1 1	_	a •	14	•		•	41 1 T
Inhia	•	Sequencing	racilite	Λŧ	COLONIAG	ın	mothod I
Lanc	J	Sequencing	Louis	VI.	COLOTHES		mcmou i

Colony No.	Sequence of RBS	Colony No.	Sequence of RBS
03 b	TCA <u>CAC</u> AGGA	14 b	TCA <u>CAC</u> AGGA
04 b	TCA <u>CAC</u> AGGA	16 b	TCA <u>CAC</u> AGGA
05 b	TCA <u>CAC</u> AGGA	17 b	TCA <u>TTG</u> AGGA
07 b	TCA <u>CAC</u> AGGA	18 b	TCA <u>CAC</u> AGGA
08 b	TCA <u>CAC</u> AGGA	19 b	TCA <u>CAC</u> AGGA
09 b	TCA <u>CAC</u> AGGA	20 b	TCA <u>CAC</u> AGGA
10 b	TCA <u>CAC</u> AGGA	22 b	TCA <u>CAC</u> AGGA

12 b	TCA <u>CAC</u> AGGA	23 b	TCA <u>CAC</u> AGGA
13 b	TCA <u>CAC</u> AGGA		

Although, we can noticed colony 17 (highlighted in green) with changed rbs code to 'TTG', the visual screening did not have a desired phenotype. Therefore, no library of RBS's was created. This method may not be the most efficient way to create RBS library as the primers which bind to native DNA sequence favours those primers with 'CAC' sequence to bind every time, thus making it impossible for mutations to occur. In addition to this, *E. coli* has methyl-directed mismatch repair system which favours the repair of non-methylated DNA and leads to low yield of mutants³².

3.5.2. Using error prone PCR coupled with randomized primers (method II)

The method I was further upgraded by combining it with error-prone PCR instead of the standard PCR. Adding $MnCl_2$ in the PCR mix adds error in the insert sequence (RBS - cI - TT) and can lead to a mutant with less background output under dark. Section 2.4.1 - II describes the method in detail.

22 colonies were formed with this method. They were plated on 24-well plates for visual screening, but many colonies were much darker than the positive control pJT106b.

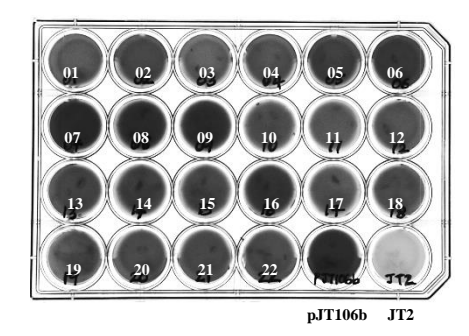


Figure 30 Screening of RBS library colonies created from Method II.

Selected colonies from the plate, colony 4, 7, 8, 10, 11, 12, 13, 14, 18 and 20 were sent for sequencing.

		-	9	•	14	•		•	41 1 TT
Tah		h	•	ոռուորուոր	racilite	Λt	COLONIAS	ın	method II
1 av	10	v	v	cuuchchiz	Louis	VI.	COLUMES	111	mumuu H

Colony No.	Sequence of RBS	Colony No.	Sequence of RBS
04	TCA <u>CAC</u> AGGA	12	TCA <u>CAC</u> AGGA
07	TCA <u>CAC</u> AGGA	13	TCA <u>C</u> ACAGGA, mutations in <i>cI</i>
08	TCA <u>CAC</u> AGGA	14	TCA <u>TTG</u> AGGA
10	TCA <u>CAC</u> AGGA	18	TCA <u>CAC</u> AGGA
11	TCA <u>CAC</u> AGGA	20	TCA <u>CAC</u> AGGA

The results for sequencing showed no change in the RBS sequence except colony 14. Again, the native RBS sequence 'CAC' was dominant in most colonies. In colony 13 (highlighted in orange), the *cI* region had some mutations due to error prone PCR, but this colony did not have the desired phenotype during visual screening. Colony 14 (highlighted in green) has mutated rbs code to 'TTG', but does not have the desired phenotype.

3.5.3. Using synthetically designed oligonucleotide with random base pairs (method III)

This method was planned in order to avoid the native insert sequence from the plasmids pJT106b/b3. A synthetic oligonucleotide containing 'NNN' sequence in the rbs upstream of *lacZ* was ordered. Primers were used to amplify this insert and then ligated to the vector using Gibson assembly technique. Section 2.4.1 - III describes the method in detail.

Use of synthetic insert proved to the best way to create a RBS library. 84 colonies were formed by Gibson assembly of the insert and vector pJT106b3. After several trials to bind the primers to vector pJT106b, it was not successful. So this method was carried out only on pJT106b3, which is the output plasmid for red sensor in the green-red sensor system. Out of the 84 colonies, 63 were positive for successful ligation, which was checked by colony PCR. The expected size in colony PCR was ~518 bp using primers AM107 and AM145 shown in Appendix III-3.

These 63 colonies were visually screened for their phenotype along with *E. coli* JT2 strain with no plasmid, plasmid pJT106b3 in JT2 strain and green-red sensor system in JT2 *E. coli* strain. Following are the results:

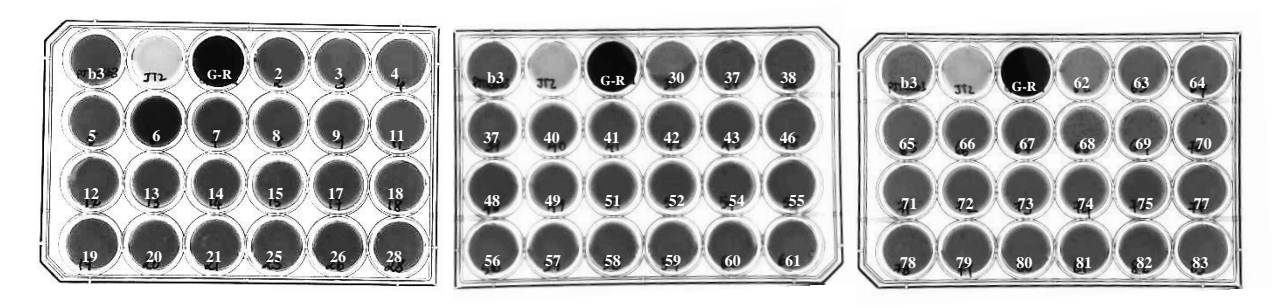


Figure 31 Screening of 63 colonies of RBS library from Method III for less black output generation under dark at 37 °C (b3:pJT106b3 plasmid; JT2: *E. coli* strain; G-R: green-red sensor)

The visual screening of colonies on 24-well plates showed all the colonies with similar background output as the positive control pJT106b3 except for colony 6, which showed higher expression of black pigment and colony 62, which showed slightly less black output compared to control. Sequencing of 16 random colonies showed that the RBS sequence was mutated at site 'NNN' as planned.

The sequencing results in Table 7 showed 6 mutant colonies (highlighted in green):

Table 7 Sequencing results of colonies in method III

Colony No.	Sequence of RBS	Colony No.	Sequence of RBS
06	TCA <u>CAC</u> AGGA	39	TCA <u>CAC</u> AGGA
09	TCA <u>TTT</u> AGGA	46	TCA <u>CAC</u> AGGA
10	TCA <u>CAC</u> AGGA	48	TCA <u>CAC</u> AGGA
19	TCA <u>CAC</u> AGGA	56	TCA <u>CAC</u> AGGA
21	TCA <u>ATG</u> AGGA	62	TCA <u>CAC</u> AGGA
22	TCA <u>CAC</u> AGGA	65	TCA <u>ATC</u> AGGA
26	TCA <u>GTT</u> AGGA	72	TCA <u>CCC</u> AGGA
27	TCA <u>CAC</u> AGGA	79	TCA <u>GTG</u> AGGA

Thus a RBS library was successfully engineered. Colony 6 (highlighted in purple), showed more background output as compared to positive control pJT106b3 by visual screening and the sequencing showed existence of native sequence 'CAC'. A reason for this may be fast growth of cells within the agarose, leading to high black output while visual screening. Colony 62 showed slightly less black output than control pJT106b3 in visual screening. There may be less number of cells present in the agar-well due to longer lag phase during the growth of cells. Even though the cell population belongs to strain JT2, there may some slight variations in behaviour of each colony, which may lead to a longer lag phase. Colony 48 (highlighted in orange) still containing the 'CAC' sequence, was also selected to check for its output through Miller assay.

Colonies 09, 21, 26, 65, 72, 79 and 48 were selected based on their sequencing results for Miller assay. The mutated plasmids were retransformed into fresh JT2 strains of *E. coli* before further analysis by Miller assay. Quantification of LacZ was done after placing for 7 hours under dark on the selected mutant colonies and compared with the control (no sensor), pJT106b3 plasmid and green-red sensor (Figure 32).

As noticed in the above graph, plasmid pJT106b3 containing the RBS code 'TCACACAGGA' gave much lower Miller unit output compared to the green-red sensor, which contains the sensor circuit along with pJT106b3 plasmid. However, it would be rational to compare the mutant colonies only to the control pJT106b3 plasmid since the green-red sensor contains the sensor system due to which it displays a high Miller unit ~120.

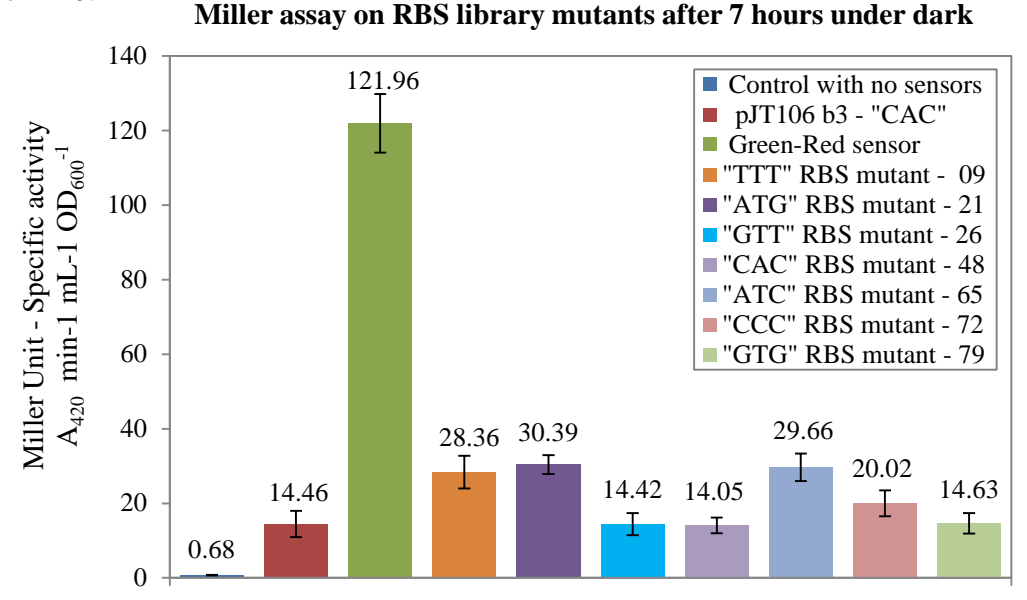


Figure 32 Miller assay on RBS library colonies after 7 hours of under dark

The mutant colonies have changed RBS code at site of "CAC" replaced by "TTT"(colony 9), "ATG" (colony 21), "GTT" (colony 26), "ATC" (colony 65), "CCC" (colony 72) and "GTG" (colony 79). Colony 48 still retains the "CAC" sequence code in its RBS. The mutant colonies 09, 21, 65 and 72 have higher Miller unit output than the pJT106b3. The colonies 26, 48 and 79 have almost similar Miller unit output to pJT106b3.

To conclude, the RBS library created was not successful in engineering a mutant with low background output under dark. Although, RBS sequence was mutated in six strains, they did not show the desired phenotype. The rbs code mutation noticed in this section may not be the best sequence needed for improving the circuit, hence there was no decrease in the background output while screening of these colonies. However, it should be noticed that the library created was very small and had less variation for rbs code. A library with more variation is needed in order to attain the desired phenotype.

Discussion

Recombinant light sensors are an attempt to control gene expression in *E. coli* cells and help understand how environment plays a role in the development of various species. For example, plants use light sensors to regulate seed germination, stem extension, flowering time and many other biological processes²³. The red and green sensor systems, Cph8 and CcaS-CcaR, engineered in *E. coli* provide a gene regulatory system which has different promoters controlled by different wavelengths of light². This project dealt with various strategies to understand these sensor systems for its wide spread application in field of synthetic biology. A brief summary of results is given in Table 3. Discussion for each is as follows.

Preliminary results

In the presence of chromophore phycocyanobilin (PCB), green and red sensor systems give a high Miller unit when compared to in absence of PCB molecules². This clearly suggested that the light sensing PCB molecule is responsible for the increase in output of LacZ². From the preliminary results (Section 3.2), it was observed that in dark and as well as in light induction, an output signal can be seen for all three sensors – red, green and green-red.

Sensor systems under dark were expected to give a certain amount of background output along with output under light induction² (Appendix III-5). However, based on the results in Figure 14, it is not clear if the sensor systems engineered during this project were sensing light or they were always turned 'on', even under dark. A clear distinction between the actual induction by light and the background output under dark can be made only when light is exposed on the same plate having both light and dark conditions together.

Characterization of sensors by pattern creation

Preliminary experiments with sensors on different plates and light conditions were difficult to compare as the microenvironment in these plates may differ with handling conditions for each experiment. Thus, a bacterial plate under the *Light Induction Device* (*LID*) with a mask of pattern above it having both light induced and dark areas was carried out to provide similar environment for the cells to react with and without light.

Using pattern creation on the three sensor systems (red, green and green-red sensors) provided an indication of how they would behave under different light intensities to create layers of output. Under Section 3.3, different experiments were done to judge the effect of different wavelengths of light on pattern creation by the sensor systems and on the effect of gradient of light intensities on the output signal. Quantification of output using ImageJ software provided a rough analysis of how these sensors behave.

The red sensor system is observed to turn ON even during green light induction². Literature shows the red sensor (Cph8) to be sensitive to wavelengths of green (535 nm) as well as red (650 nm) and can be suppressed using far- red light (750 nm)². The green sensor is induced by green light (535 nm) and is repressed when light of 650 nm (red) wavelength is used² (Appendix III-5).

It would be interesting to analyze if far-red light could deactivate the red sensor, present in green-red sensor, while keeping only the green sensor active. This could be a great application in creating layered bio-materials. Influence of far-red light (750 nm) on the red and green sensors were also studied. Patterns were successfully created using green, red and green-red sensor systems (Section 3.3.1)(Figure 16).

Red sensor

The red sensor formed a crisp pattern under red light. It also formed faint patterns under green and combination of green + far-red light (Figure 16). The wide spectra of wavelengths of light which triggers the red sensor could be a reason for pattern developments under green and green + far-red light (Appendix III-5).

Green sensor

Green sensor creates patterns under both green and green + far-red light while having no pattern development under red light. Thus suggesting that red light may not trigger the green sensor system. The far-red light (750 nm) created crisp patterns compared to the patterns under only green light.

Green-red sensor

Green-red sensor was expected to show pattern developments under both green and red light, as it contains both the sensors. However, under red light no patterns were seen. This can be due to the extremely low (0.026 W/m^2) intensity of red light, which may not be enough to trigger the red sensor present in the green-red sensor system. Also, the output plasmid in this sensor system as mentioned in Table 2, contains a weaker RBS upstream of lacZ (pJT106b3), as compared to the red sensor system (pJT106b). This could cause delay in expression of lacZ by green-red sensor system, thus not forming patterns under red light induction. Likewise, in the green sensor system, the RBS in front of lacZ is of medium strength leading to a normal output of black pigment. Also, the green sensor system does not contain the invertor switch $cI-P_{cI}$ in its circuit like in the red sensor, making it a rather simple input to output circuit. But since red light may be deactivating the green sensor present in green-red sensor, there may be no pattern formation.

Comparison of sensors

Comparison of all three sensors plated in a quad-petri dish was done using pattern creation. Analysis of each sensor and its background output was done using Image J. Red sensor did not give pattern with green + far-red light, but formed patterns under green and red light. The deactivating effects of far-red light on the red sensor may be a reason why no patterns were developed, however, analysis by ImageJ did not show very high differences (Figure 20(c)). Green and green-red sensor gave patterns under green and green + far-red light but not under red light. Although, green-red sensor was expected to form patterns under red light, it did not form patterns (Figure 19). This may be due to the presence of green sensor in green-red sensor which gets deactivated by red light and a very low intensity of red light (0.026 W/m²) does not trigger red sensor for pattern formation. Analysis of output signal by light induction seen through this experiment was not very high. But the visual screening of plates showed pattern creation, which may be significant. (Figure 19)(Figure 20)

Gradient experiment

Gradients of light intensities were also applied on individual sensor systems and output was analyzed using ImageJ. With increase in light intensity, the output signal also increases for green sensor (Figure 23). Far-red light may be triggering the induction of green sensors, but we do not know if this is conclusive effect. Red sensor does not show any increase with increase in red light input (Figure 24). This may be because the maximum red light intensity applied on red sensor was very low (0.06 W/m²).

Effect of far-red light

The effect of far-red light on sensors was analyzed using ImageJ. However it is not clear if far-red light deactivates the sensors, since there was no significant difference seen between plates with and without far-red light. Although, the plates under far-red light gave much crisper patterns, ImageJ analysis did not conclude the deactivation of sensors. Far-red light was applied by Tabor et al., 2014, on the same sensor systems of green and red, and they showed no difference in output between far-red light and dark. The LEDs for far-red light used in Array tube illuminator were of very low power. Therefore, the proposed far-red light exposure in the Array tube illuminator was not done. It would interesting to find more conclusive literature about the effects of far-red light and then experimentally proved it, before concluding its role in the deactivation of sensors.

Characterization of sensors by quantification of output

Furthermore, quantification of output using Miller assay for each sensor system was done to characterize their transfer function with respect to duration and intensity of light. Section 3.4, shows the quantification of output LacZ using the *Array Tube Illuminator* described in Section 2.3.1.

Red sensor under different intensities of light:

The red sensor was highly sensitive to most intensities of green and red light. There was an exponential trend observed in output signal of red sensor as the intensity of light increased (Figure 25). This sensitivity of red sensor towards light can be due to the presence of a strong rbs upstream of *lacZ* (pJT106b), which gave more output than the other sensor systems. However, over time, the output signal for red sensor increased. Along with the sensitivity of red sensor towards light, the cells were also growing over time, to add to this increased output. The red sensor was activated under green light and gave Miller unit ~15000 (green light 6 W/m²). The sensitivity of red sensor towards red light was more than towards green light, since under red light of intensity 2 W/m², output reached was ~7400, whereas under green light of 2 W/m², the output reached was ~3700. This shows the activation of red sensor domain by a wider spectra of wavelength of light containing green and red light (also see Appendix III-5).

Green sensor under different intensities of light:

The output signal of green sensor seemed to decrease under red light induction, concluding that red light deactivates the green sensor (Figure 26(a)). The behaviour to notice is that the green sensor is induced by green light (535 nm) and is repressed when light of 650 nm (red) wavelength is used² (also see Appendix III-5). This could occur due wavelength of red light dephosphorylating CcaR, regulator of green sensor system.

The green sensor attained a saturation level in output after \sim 6 hours of light induction. Under increasing intensities of green light, the green sensors showed a stepwise increase. However, in combination of green and red light (green - 2 W/m², red - 2 W/m²) and green light 2 W/m², red light 0.1 W/m², we noticed similar Miller unit of outputs of \sim 100 and \sim 90 respectively (Figure 26 (c)). Here, the red light intensity differed for both cases, yet the Miller unit outputs were almost similar. This could conclude that red light may be having no effect or decreasing effect over green sensor as mentioned in literature².

Green-red sensor under different intensities of light:

Similarly, the green-red sensor had less output signal under red light at 2 W/m² compared to red light at 0.5 and 1 W/m² (Figure 27(a)). This led to a reasoning that the green sensor in the green-red sensor gets supressed at higher intensities of red light - 2 W/m², but at lower intensities of red light (0.5 W/m²), the green sensor was not supressed, but red sensor was activated. Thus leading to a higher Miller unit output by green-red sensor under influence of red light of 0.5 and 1 W/m². Presence of green sensor, could also make the red sensor compete for PCB molecules and get activated to generate more output signal². Under different intensities of green light and combinations of green + red light, the green-red sensor showed a step-wise increase in output signal as the input signal was increased (Figure 27(b)(c)). The background output under dark was quite high for green-red sensor and overlapped with the minimum green and red light intensities applied. This may be due to presence of two sensor systems leading to cellular complexity and more leakiness in the output signal.

Comparing green-red sensor with green sensor:

The overall Miller units for green-red sensor was higher than green sensor under all intensities of light (Figure 26)(Figure 27). The presence of red sensor in green-red sensor could be a reason for this increased output. The red sensor domain has a wide range of action spectra of wavelengths of light (Appendix III-5), which would activate it under green light as well, thus leading to higher output when compared to green sensor. The red sensor could also compete with green sensor for PCB molecules and generate more output in green-red sensor².

Comparing red sensor with green sensor:

Red sensor gave high output signals under green light intensities as compared to green sensor (Figure 25(b)) and (Figure 26 (b)). Red sensor is stronger than green sensor, may be due to the presence of cI - pcI repressor circuit before lacZ (Figure 1 - red sensor). This could bring about unwanted leakiness in the output signal, which was seen as high background output for the red sensor. Undesired signal transductions due to the presence of such complex circuits may also cause the red sensor to be more sensitive under light. The sensor domain of Cph8 (red sensor system) and PCB molecule which makes the core unit for absorption of light could also get activated under a wide spectra of wavelengths of light, hence leading to a stronger output signal by the red sensor compared to the green sensor.

Comparing red sensor with green-red sensor:

In Figure 27(c), the difference between combination of green light with red light at 2 W/m2 and 0.1 W/m^2 reached was ~50 Miller units, whereas for red sensor (alone) the difference was 3000 Miller units (Figure 25(c)). Slow activation of the green-red sensor under red light can be observed. This can be due to the presence of green sensor which could be deactivated by the red light, or due to the red sensor (in green-red sensor system) not being as sensitive as the red sensor (alone), due to the weaker rbs infront of lacZ. Similarly, under other light intensities also the red sensor shows higher Miller unit output as compared to green-red sensor. The output plasmid (pJT106b) for red sensor (alone) contains a stronger rbs upstream of lacZ, which may lead to more output signal. Thus, making the red sensor stronger than the green-red sensor.

Comparing transfer functions under red and green light:

When comparing all the three sensors under different intensities of green and red light, the red sensor showed the highest output signal. This is shown in Figure 28. It can be noticed that the transfer function of green and red sensor does not add up to the value of transfer function of green-red sensor. Though it may be logical to expect a cell containing two sensors to give double the output signal. However, that is not the case. The major reason could be the difference of rbs strengths in red sensor output plasmid (pJT106b and pJT106b3) for red and green-red sensors. Other reasons like direct or indirect interactions occurring in the cell, could lead to this non-additivity. For example, the presence of green sensor under red light causes the output to reduce, even though the red sensor is present in the same cell². Non-specific effects like protein degradation or competition for ribosome binding has also been reported to affect the circuit^{2,33}. The red sensor domain could also compete for PCB chromophore molecules, while decreasing the presence of green sensor when both sensors are present in one cell².

Miller assay quantification compared to ImageJ quantification:

Using Miller assay to characterize the sensors reflected upon interesting insights about the sensors as compared to analysis by ImageJ software. Although a rough analysis to characterize the sensors was done using ImageJ, the behaviour or sensors were not very conclusive. Quantification of LacZ using Miller assay and the use of Array Tube illuminator on the other hand, proved very accurate in comparing the output signals of sensors in liquid culture growing over time. Very high intensities of light (green light 6 W/m^2 and red light 2 W/m^2) could also be applied on the sensor systems using the Array tube illuminator, which was not possible through LID used for pattern creation.

Sensors under dark:

Characterization of sensors using Miller assay indicates great potential for these sensors in the production of biomaterials. However, the results from pattern creations indicated that under dark there is an expression of LacZ, leading to a background darkening of the regions under dark area. The Miller assay also resulted in high output under dark for red sensor as compared to green and green-red sensor

(Figure 28). The difference in background output for each sensor is due to the difference in their sensor circuits. However, every sensor has a background output. Since, it is a biological light switch and has complexities at cellular levels, which are yet not clearly understood, it may be very difficult to develop a switch which is completely turned 'off' under dark.

For the production of nacre, this may not be advantageous and should be avoided. Since the future goal is to create layers of protein with a light control of gene expression, leakiness of the system does not make it readily applicable at this stage. As the background output for red sensor was quite high, an attempt to fine tune the red sensor system was made (Section 2.4).

Fine tuning the sensor system

Improving the current circuit can be done by mutation of sensor parts, however, it requires high level of expertise about the structure of sensor domains. Mutation of the rbs region by rational substitutions or random mutagenesis has been reported to improve the circuit efficiency^{29,30}. Therefore, an attempt was made to fine tune the circuit upstream of lacZ, leading to better output signal. Different gene manipulation strategies were used to create a RBS library of the rbs region in front of cI in plasmids pJT106b/b3. This is the plasmid containing the output lacZ for the red sensor system.

In view of that, goal was to reduce the background output (black pigment) under dark by mutating three random base pairs in the RBS region, thus altering the strength of RBS (Figure 9). The initial creation of RBS library by site-directed mutagenesis and error prone PCR using randomized primers was not as successful as planned. Method I and II (Section 3.5) led to development of some colonies after transformation, however, the sequencing results showed the native RBS code to be dominant in most colonies. Literature states that site-directed mutagenesis with synthetic oligonucleotide primers can lead to low frequency with which mutated clones arise, compared with wild-type clones³². This is due to the repair system present in *E. coli*. The mismatch repair system, in theory, is believed to yield equal numbers of mutant and non-mutant progeny, but in practice the mutants are counter selected³². The methyl-directed mismatch repair system of *E. coli* favours the repair of non-methylated DNA and is the major reason for this low yield of mutant progeny³².

Method III using synthetically designed insert containing three random base pairs at the site of rbs was carried out (Section 2.4.1). This was done to avoid the problem mentioned above and was successful in creating many colonies with a changed RBS code. Thus creating a RBS library as planned. However, the visual screening results for these colonies did not show any changed effect on the output signal when compared to the positive control pJT106b3 (Figure 31). Miller assay was carried out on the six mutant colonies to accurately quantify the output and compare with control strains (Figure 32). Most mutants had either higher or similar Miller units as compared to plasmid pJT106b3, indicating that the mutants from the existing RBS library did not have less background output under dark, which was the desired phenotype. The rbs code mutations developed under Method III may not be the best improved RBS sequence needed for fine tuning the circuit. Therefore, we did not notice any decrease in the background output while screening of these colonies. Engineering more variants for the RBS library should be done, since only 6 mutants were obtained during this project. Replacing the existing RBS with a RBS of known strength could also help in fine tuning the circuit. RBS calculators could be used to predict the strength of new RBS codes or the existing RBSs to help develop new mutants with improved output circuit.

5 Outlook

Through this project, an attempt to control gene expression of *lacZ* in *E. coli* was successfully done. However, research never ends. Proposed are a few suggestions which can be done further to this project.

Light sensors sensitive to red and green wavelengths of light offer a stable mechanism to switch between different input signals and generate different outputs. Characterization of the green sensor has shown induction and deactivation of the sensor. If this is combined to fluorescent reporter genes, then a real-time control of expression within a population of cells can be observed². For creating bio layers of nacre, this can be very helpful.

The attempt to improve the red sensor system during this project by creating RBS library using site-directed random mutagenesis did not lead to creation of RBS library and was always dominant by wild type sequence (Method I and II). Since, *E. coli* has methyl directed mismatch repair system, the non-methylated mutant DNA sequence are repaired leading to dominant wild type colonies^{32,35}. Using strains carrying the *mut L*, *mut S*, or *mut H* mutations can prevent the methyl-directed repair of mismatches and can prevent the dominance of wild type colonies³².

Strategy using synthetically designed insert containing three random base pairs (Method III) was successful in creating a RBS library, but created only 6 mutants. However, did not lead to the development of any mutant which has less background output LacZ under dark. This strategy can further be repeated to generate more diverse library for all combinations of RBS code, which can increase the probability of creating a desired variant. Changing the RBS code to a RBS of known strength by calculating through RBS calculators could help bring a directed mutation in the circuit³⁴.

For improving the red sensor performance, the light-sensing domains can also be mutated into a much effective sensor. Study of the structure of sensor proteins and domains reveal that PAS-GAF domain of the Cph1 sensory module completely closes the binding pocket, thus isolating the chromophore phycocyanocobilin (PCB)²³. New structural confirmation ZZZssa has also been predicted for the Cph1 from *Synechocystis* 6803^{23} . The D-ring of PCB photo-flips from $Z \rightarrow E$ isomerisation within picoseconds and brings about confirmation changes in the sensor²³. Mutations like Y176H in the D-ring of PCB molecule failed to photo convert and lost its excitation energy by fluorescence. Replacing D207A mutants bleached in red light and R472A mutants had very little effect of absorbance²³. Hypothesis stating the protonation of the bilin as an important factor in optimizing the absorbance has also been made²³. However, since there is no obvious proton channel detected yet and as the proton exchange occurs in milliseconds, conformational changes of the PCB are more likely to play a vital role in the mechanism of interconversion by red and far-red light²³. The structure of Cph1 is very complicated and has not been fully studied yet²³. Attempts to regulate the red sensor systems can be done by mutating the domains of Cph1 for improved efficiency. While, mutation is the best option in fine-tuning the sensor proteins, the structure to function characterization for these sensors is not very well understood. The complexity of the signalling molecules which trigger these systems limit our in-depth understanding of the sensors and hence random mutation in sensor domains could lead to a decrease efficiency in the existing sensor. Therefore, careful considerations should be made before mutation of sensor domains is carried out.

The action spectra of the red sensor can be seen in almost all wavelengths of light². Mutations of the binding pocket of the chromophore to alter the absorbance spectrum has been implemented earlier². However, mutating critical amino acids in the conserved domains, or applying domain shuffling on the structure gene of the phytochrome can be implemented. This may lead to development of new photoreceptors with more narrow spectral sensitivity.

The conformational changes in the PCB molecules takes picoseconds, and the transcription takes minutes to start however, it takes almost 1 hour to reach a steady state^{2,36}. This means the time to switch between on and off states of a sensor is in order of hours. If the transcription of gene has to be stopped then the light induction should be for hours before the deactivation of sensors can take place. An interesting aspect would be to study the effect of deactivation of sensor and characterize the suppressing transcription rate.

The recombinant red sensor Cph8 is a combination of Cph1 and EnvZ linked by a peptide linker¹⁷. The length and composition of this linker that joins the photoreceptor to the response regulator, effects the signal transduction¹⁷. A number of chimeras with different linker lengths can be created to test for an efficient chimera with improved quality.

Apart from the sensor parts, the circuit itself can also be tuned further to make it more efficient. Bistable genetic switch^{2,37} placed between the light sensor and output can help decrease the response of the sensors after a certain threshold of input is attained. This can also help narrow down the wide action spectra of wavelengths of light, which activates the red sensor.

Despite these issues of sensitivity of sensor systems to different wavelengths of light, the characterization using Miller assay has shown that having both sensors in a single cell may not be an ideal way to control gene expression. Since green-red sensor is induced by both green and red light, but the red sensor is trigger by green light. And the far-red light does not have significant effect to reduce or suppress the expression of the red sensor. Though the red light activates red sensor while deactivating the green sensor, the green-red sensor has more complexity at the molecular level. A more ideal approach can be to have the red and green sensors system behave separately in different strains and inducing them with desired wavelengths of light for different output signals. Miller assay characterization of red and green sensors done during this project is a good starting point. This can be feasible in creating layers of biomaterials such as nacre, while controlling the output via two different wavelengths of light. The exact intensity of light to be applied over these sensors should be studied more.

While characterization using Miller assay gave a brief notion for how each sensor may behave like, inducing with more intensities of light should be done. This may lead to a certain range of light which could trigger or de-activate specifically the red sensor, thus enabling us to solve the excessive triggering of red sensor by green light. Also, selected mutation on the sensor domain of the red sensor and PCB molecule which make the core unit for sensing light, in a way that it can sense only wavelength of red light (650 nm) can enable us to control the sensor better.

However, red and green sensor systems are very effective in controlling of gene expression to create patterns on a lawn of bacterial cells. These two sensor systems hold promising effects in control of gene expression at two – dimensional state if they are fine-tuned accordingly in a single bacterium. So far, only the output protein analysis has been done for these two sensors, interesting insights will be provided if the mRNA expression analysis for the output *lacZ* could be analysed. Specific tags for *lacZ* can be incorporated during real-time PCR to quantify the mRNA levels particular to the output of the sensor system.

To conclude, we hope to thrive towards production and control of biomaterials using light as an input. Thus, enabling bacterial application controlled by light input in the field of synthetic biology and fundamental research. The two sensor systems characterised in this project have great potential in applications for producing layers of different outputs while controlling it by varying inputs of light. Increasing the input signals for an increased output of a certain product is possible through the conclusions made in this project. Alternate layers of different outputs can also be created since the two sensors systems – green and red can be used to produce different outputs when one is controlled by green light and the other by red light. Although, the application of both sensors in one cell to produce biomaterial may be challenging at this stage due to the overlap of light wavelengths which trigger the two sensors, it will be possible to use the two sensors as two separate strains.

Bibliography

- 1. Drepper, T., Krauss, U., Meyer zu Berstenhorst, S., Pietruszka, J. & Jaeger, K.-E. Lights on and action! Controlling microbial gene expression by light. *Applied microbiology and biotechnology* **90**, 23–40 (2011).
- 2. Tabor, J. J., Levskaya, A. & Voigt, C. a Multichromatic control of gene expression in Escherichia coli. *Journal of molecular biology* **405**, 315–24 (2011).
- 3. Olson, E. J., Hartsough, L. a, Landry, B. P., Shroff, R. & Tabor, J. J. Characterizing bacterial gene circuit dynamics with optically programmed gene expression signals. *Nature methods* **11**, (2014).
- 4. Kaplan JH, Forbush B III, H. J. Rapid photolytic release of adenosine 5'-triphosphate from a protected analog: utilization by the sodium:potassium pump of human red blood cell ghosts. *Biochemistry* **17**, 1929–1935 (1978).
- 5. Young DD, D. A. Photochemical activation of protein expression in bacterial cells. *Angew Chem Int Ed* 46:4290–4292
- 6. Van der Horst MA, H. K. Photoreceptor proteins, star actors of modern times: a review of the functional dynamics in the structure of representative members of six different photoreceptor families. *Acc Chem Res* **37**, 13–20 (2004).
- 7. Giraud E, Fardoux J, Fourrier N, Hannibal L, Genty B, B. P. & Dreyfus B, V. A. Bacteriophytochrome controls photosystem synthesis in anoxygenic bacteria. *Nature* **417**, 202–205 (2002).
- 8. Losi, A. Flavin-based Blue-Light photosensors: a photobiophysics update. *Photochemistry and photobiology* **83**, 1283–300 (2007).
- 9. Rajagopal S, Key JM, Purcell EB, Boerema DJ, M. K. Purification and initial characterization of a putative blue lightregulated phosphodiesterase from Escherichia coli. *Photochem Photobiol* **80**, 542–547 (2004).
- 10. Kehoe DM, G. A. Similarity of a chromatic adaptation sensor to phytochrome and ethylene receptors. *Science* **273**, 1409–1412 (1996).
- 11. Terauchi K, Montgomery BL, Grossman AR, Lagarias JC, K. D. RcaE is a complementary chromatic adaptation photoreceptor required for green and red light responsiveness. *Mol Microbiol* **51**, 567–577 (2004).
- 12. Kehoe DM, G. A. New classes of mutants in complementary chromatic adaptation provide evidence for a novel four-step phosphorelay system. *J Bacteriol* **179**, 3914–3921 (1997).
- 13. Hirose Y, Shimada T, Narikawa R, Katayama M, I. M. Cyanobacteriochrome CcaS is the green light receptor that induces the expression of phycobilisome linker protein. *Proc Natl Acad Sci* **105**, 9528–9533 (2008).
- 14. Schirmer T, J. U. Structural and mechanistic determinants of c-di-GMP signalling. *Nat Rev Microbiol* **7**, 724–735 (2009).
- 15. Won HS, Lee YS, Lee SH, L. B. Structural overview on the allosteric activation of cyclic AMP receptor protein. *Biochim Biophys Acta* **1794**, 1299–1308 (2009).
- 16. Losi A, G. W. Bacterial bilin- and flavin-binding photoreceptors. *Photochem Photobiol Sci* **7**, 1168–1178 (2008).
- 17. Anselm Levskaya, Aaron A. Chevalier, J. & Tabor, C. A. V. Engineering Escherichia coli to see light. *Nature* **438**, 441–442 (2005).
- 18. Losi A, Polverini E, Quest B, G. W. First evidence for phototropin-related blue-light receptors in prokaryotes. *Biophys J* **82**, 2627–2634 (2002).

- 19. Strickland, D., Moffat, K. & Sosnick, T. R. Light-activated DNA binding in a designed allosteric protein. *Proceedings of the National Academy of Sciences of the United States of America* **105**, 10709–14 (2008).
- 20. Jeeves M, Evans PD, Parslow RA, Jaseja M, H. E. Studies of the Escherichia coli Trp repressor binding to its five operators and to variant operator sequences. *Eur J Biochem* **265**(3), 919–928 (1999).
- 21. Morgan SA, Al-Abdul-Wahid S, W. G. Structure-based design of a photocontrolled DNA binding protein. *J Mol Biol* **399**, 94–112 (2010).
- 22. Tabor, J. J. et al. A synthetic genetic edge detection program. Cell 137, 1272–81 (2009).
- 23. Essen, L.-O., Mailliet, J. & Hughes, J. The structure of a complete phytochrome sensory module in the Pr ground state. *Proceedings of the National Academy of Sciences of the United States of America* **105**, 14709–14 (2008).
- 24. Tabor, J. J. Plate-based assays for light-regulated gene expression systems. Methods in enzymology **497**, 373–91 (Elsevier Inc.: 2011).
- 25. http://en.wikipedia.org/wiki/Nacre.
- 26. Peters, J. E., Thate, T. E., and Craig, N. L. Definition of the Escherichia coli MC4100 genome by use of a DNA array. *J. Bacteriol.* 2017–2021. (2003).
- 27. Baba, T., Ara, T., Hasegawa, M., Takai, Y., Okumura, Y., Baba, M., Datsenko, K. A. & Tomita, M., Wanner, B. L., and Mori, H. Construction of Escherichia coli K-12 inframe, single-gene knockout mutants: The Keio collection. *Mol. Syst. Biol.* **2**, (2006).
- 28. http://openwetware.org/wiki/Beta-Galactosidase_Assay_%28A_better_Miller%29.
- 29. Yokobayashi, Y., Weiss, R. & Arnold, F. H. Directed evolution of a genetic circuit. *Proceedings of the National Academy of Sciences of the United States of America* **99**, 16587–91 (2002).
- 30. Anderson, J. C., Voigt, C. a & Arkin, A. P. Environmental signal integration by a modular AND gate. *Molecular systems biology* **3**, 133 (2007).
- 31. Cadwell, R. C. & Joyce, G. F. Manual Supplement III1 | 11 Mutagenic PCR. 3–8 (1994).
- 32. CHAPTER 8 Changing genes: site-directed mutagenesis and protein engineering. 141–156
- 33. JJ Tabor, TS Bayer, ZB Simpson, M Levy, A. E. Engineering stochasticity in gene expression. *Molecular bioSystems* (2008).
- 34. Mutalik, V. K. *et al.* Precise and reliable gene expression via standard transcription and translation initiation elements. *Nature methods* **10**, 354–60 (2013).
- 35. Kramer, B., Kramer, W. & Fritz, H. J. Different base/base mismatches are corrected with different efficiencies by the methyl-directed DNA mismatch-repair system of E. coli. *Cell* **38**, 879–87 (1984).
- 36. Dasgupta, J., Frontiera, R. R., Taylor, K. C., L. & J. C. & Mathies, R. A. Ultrafast excited-state isomerization in phytochrome revealed by femtosecond stimulated Raman spectroscopy. *Proc. Natl Acad. Sci. USA* **106**, 1784–1789 (2009).
- 37. Kobayashi, H., Kaern, M., Araki, M., Chung, K. & Gardner, T. S., Cantor, C. R. & Collins, J. J. Programmable cells: interfacing natural and engineered gene networks. *Proc. Natl Acad. Sci. USA* **101**, 8414–8419 (2004).

I. Protocols

1. Plate Based Assay

- 1) To start the plate based assay, use the glycerol stock to inoculate 5mL LB with appropriate antibiotics using a sterile inoculating loop.
- 2) Shake at 37 °C, 250 rpm overnight ($OD_{600} \sim 3-4$).
- 3) Prepare LB agarose for the assay by adding 50 mg ammonium iron (III) sulphate dodecahydrate (221260 Sigma-Aldrich), 30 mg S-gal (S7313 Sigma) and 1g low melt agarose to 100 mL LB²⁴. Autoclave this LB agarose and store at 60 °C. Before adding the antibiotics allow the molten agarose to cool to 42 °C.
- 4) Add 30 μ L of the overnight bacterial culture to 15 μ L of LB agarose. Immediately pour the mixture into a sterile petri dish and let the agarose solidify on the bench top. Try to minimize the exposure to light while preparing the plate.
- 5) Place a mask of desired pattern on the petri dish and place under desired wavelength of light and required intensity. Cut small slits in the pattern to avoid the formation of moisture.
- 6) After 12 or 24 hours, a clear pattern can be seen. Capture the image on Molecular Imager® Gel-DocTM (http://www.bio-rad.com/en-us/product/gel-doc-xr-system)
- 7) Analysis of this grey-scale image can be done using ImageJ software.

2. Error – prone PCR

This protocol has been taken from R C Cadwell and G F Joyce, 1994, Mutagenic PCR. Standard PCR conditions uses 1.5 mM KCl, 10 mM Tris (pH 8.3 at 25° C), 0.2 mM each dNTP, 0.3 μ M each primer and 2.5 units of Taq polymerase in a 100 μ L volume, incubated for 30 cycles of 94 °C for 1 min, 45 °C for 1 min and 72 °C for 1 min in a conventional thermal cycler³¹. In order to introduce mutations the following changes were done:

- 1) The concentration of MgCl₂ is increased to 7 mM to stabilize noncomplementary pairs.
- 2) 0.5 mM MnCl₂ is added to diminish the template specificity to the polymerase.
- 3) Annealing temperature for the primers was set at a low temperature (45 °C).
- 4) The error prone PCR was done on the insert region, which was PCRed out of the plasmid. Confirmation was done on gel for the insert size and then the PCR product was purified.

Use of Taq polymerase brings about high error rates upto ~ 10^{-3} per nucleotide. Taq polymerase has heavy bias towards $A \cdot T \rightarrow G \cdot C$ changes³¹.

3. Gibson Assembly

1) Prepare ISO Buffer to make the Gibson assembly master mix. In a 15mL falcon tube add the following (adapted from Gibson 2009):

3 mL	1M Tris-HCl pH 7.5
+ 150 μL	2M MgCl ₂
+ 240 μL	100 mM dNTP mix
	(25 mM each: dGTP,dCTP,dATP,dTTP)
+ 300 μL	1 M DTT
+ 1.5 g	PEG-8000
+ 300 μL	100 mM NAD
	dH ₂ O to
+ 6 mL	

Store at -20 °C in 320 µL aliquots.

2) Prepare 1.2 mL of Gibson assembly master mix as follows:

320 μL	5 X ISO Buffer
+ 0.64 μL	10 U/ μL T5 exonuclease (optimized for 20-150 bp sequence homology overlaps)
+ 20 μL	2 U/ μL Phusion polymerase
+ 160 μL	40 U/ μL Taq ligase
	dH ₂ O to
+ 1.2 mL	

Store at -20 °C in 15 µL aliquots.

- 3) Thaw a 15 µL aliquot of the Gibson assembly master mix, and keep on ice until use.
- 4) Measure the DNA concentration (ng/μL) of each assembly piece.
- 5) Add 100 ng of the linearized vector backbone and equimolar amounts of the other assembly pieces to the thawed 15 μL master mix in a 20 μL total volume assembly reaction mixture as follows:

	Linearized vector backbone (100 ng)
+	Each additional assembly piece
	(to equimolar with backbone)
+ 15 μL	Gibson assembly master mix
	dH ₂ O to
+ 20 μL	

- 6) Incubate the assembly reaction at 50 °C for 60 minutes and then place on ice.
- 7) Transform 5 μ L of the assembly reaction into 100 μ L of competent *E. coli*.

4. Miller Assay

Miller assay was carried out using Yeast β-Galactosidase Assay Kit from thermo scientific (Product #75768). The kit contains Y-PERTM Yeast Protein Extraction Reagent, 2X β-Galactosidase Assay Buffer and β-Galactosidase Assay Stop Solution. Cells were grown overnight in LB medium in dark, then diluted to 1:1000 in 6 mL Azure medium + 0.2% glucose and allowed to grow under light induction.

Every time 1mL from the culture is extracted, then the exact OD_{660} of each sample is recorded. An aliquot of 350µL of each samples is made into three microcentrifuge tubes for conducting the Miller assay.

Protocol for Miller assay in a microcentrifuge tube:

- 1. Take 350 μ L of cell cultures in a microcentrifuge tube.
- 2. Thaw 2X β-Galactosidase Assay Buffer on ice.
- 3. Add a volume of assay buffer to an equal volume of the Y-PER Reagent to make the working solution (WS). Each assay will require $350\mu L$ of the WS.
- 4. Prepare a blank tube containing $350\mu L$ of culture medium (no cells), $350\mu L$ of the WS and $300\mu L$ of the β -Galactosidase Assay Stop Solution.
- 5. Use a timer to monitor the reaction. Apply 350μL of the working reagent to each test culture and start timer.
- 6. Incubate the reaction tube at room temperature or 37 °C (optimal) until a colour change is observed.
- 7. Note: The solution will become yellow within minutes depending on the amount of β -galactosidase in the sample.
- 8. When the yellow colour appears, add $300\mu L$ of β -Galactosidase Assay Stop Solution to the reaction tube and vortex for 15 seconds. Stop the timer and record the total reaction time.
- 9. Remove cell debris from the reaction tube by centrifuging at $13,000 \times g$ for 30 seconds.
- 10. Transfer supernatant to a cuvette and measure the absorbance at 420nm against the blank tube.

Note: The reaction time will vary depending on the level of β -galactosidase expression in the test culture.

Absorbance values between 0.02-1.0 are within the linear range of the assay.

$$\beta - galactosidase \ activity = \frac{1000 * A_{420}}{t * V * OD_{660}}$$

Where, t = time (in minutes) of incubation

V = volume of cells (mL) used in the assay

 A_{420} = absorbance of the yellow o-nitrophenol (ONP) product at 420 nm

 OD_{600} = cell density at 600 nm

II. Device specifications

To induce the samples at controlled wavelengths, initially some tests were done using a slide projector with colour filters. But, due to difficulties in obtaining two narrow spectra of emission, the light-emitting diodes (LEDs) were chosen. Their low price and large choice of spectra make them an interesting light source. Different devices have been designed and built using LEDs for each wavelength of light and application:

1) Using diffused light for preliminary tests – Section 2.1

2) Using collimated beam to be able to make patterns – Section 2.2.1

3) Using LED's to light array of test tubes – Section 2.3.1

Four different LEDs have been used: green, red, far-red 731 and far-red 700. The supplier is Farnell. The spectra of green, red and far-red 731 have been checked with a spectrometer Ocean Optics QE65 Pro (Figure 33). The measured and manufacturer furnished spectra are similar. The far-red 700 has been used only for the Array Tube Illuminator. The powers of emission has been measured with a power meter Coherent Filedmate with a sensor OP-2 VIS.

Specifications

Green LED

Manufacturer: CREEOrder Code: 1855511

o Manufacturer Part No: C503B-GAS-CB0F0791

Luminous Intensity: 34cd
 Forward Current If: 20mA
 Forward Voltage: 3.2V

• Peak emission measured: 526nm

Red LED

Manufacturer: VISHAYOrder Code: 1045472

Manufacturer Part No: TLDR4900
 Luminous Intensity: 200mcd
 Forward Current If: 20mA
 Forward Voltage: 1.8V

Peak emission measured: 634nm

Far-red 731 LED

o Manufacturer: EVERLIGHT

o Order Code: 1859318

Manufacturer Part No: ELSH-Q61F1-0LPNM-JF3F8

Luminous Intensity: 1W
 Forward Current If: 400mA
 Forward Voltage: 3.85V
 Peak emission measured: 731nm

• Far-red 700 LED

o Manufacturer: KINGBRIGHT

o Order Code: 1142499

Manufacturer Part No: L-424HDT
 Luminous Intensity: 3.2mcd
 Forward Current If: 20mA
 Forward Voltage: 2.25V

o Wavelength Typ.: 700nm

1. Spectrum of LEDs

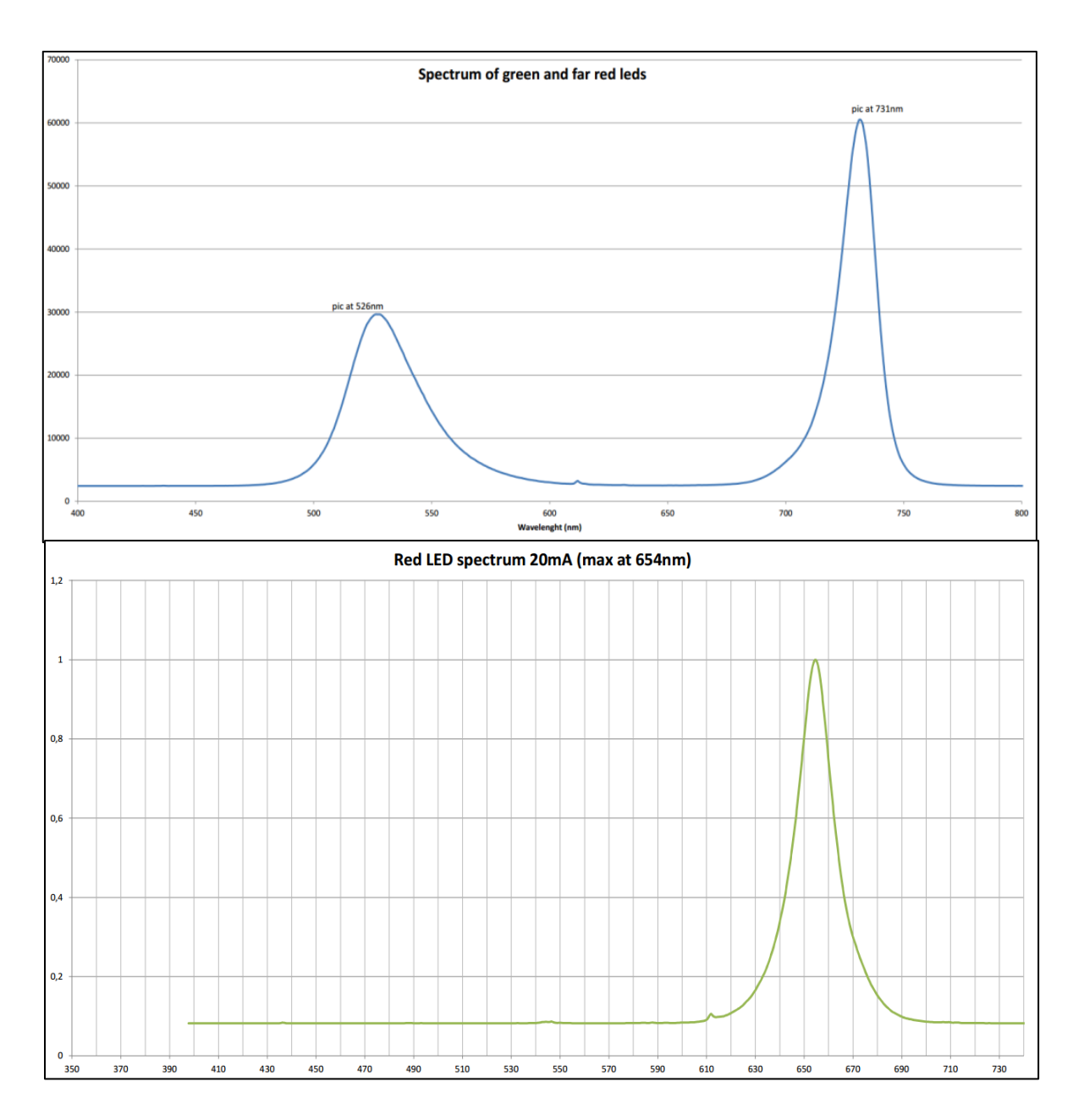


Figure 33 Spectrum of green and far-red 731 LEDs, the supply intensity of each LED has been adjusted for same power intensity.

2. Design of light holder

A series of light holder for embedding the light source have been built. One holder can have one or two LEDs. The intensity of current to supply the LED is controlled by a trimmer resistor in series. The resistor is adjusted to reach the intensity of light emission wanted.

Neutral density filter can be used to reduce the intensity, enable by a cap using magnets (Figure 34). A diffusing filter can be used to obtain a homogenous light on the sample. These holders were made with a 3d-printer with PLA plastic. The holders and PVC tube, used for the body of the lighter, were painted in black.

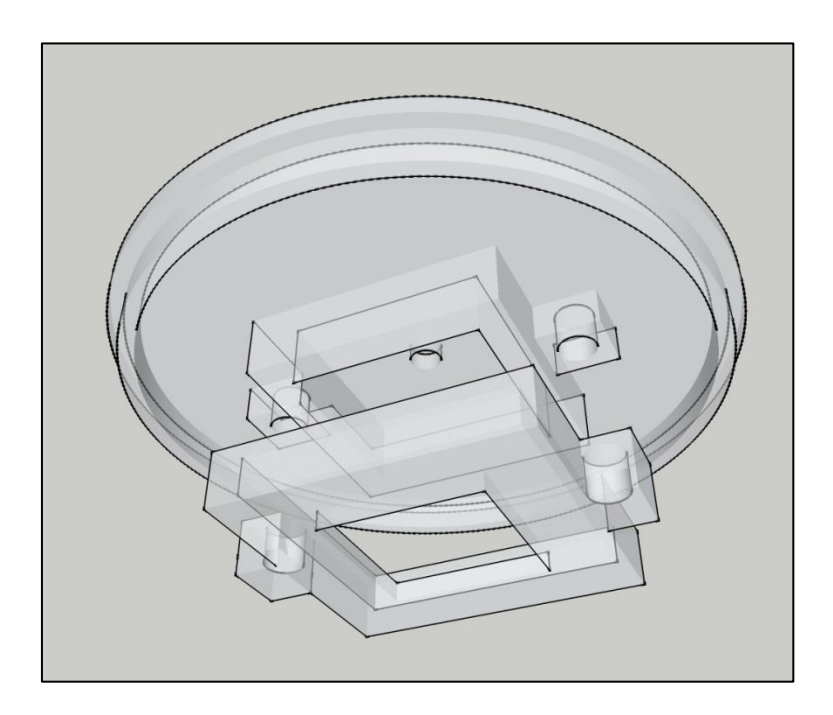


Figure 34 Holder for LED and filters which fit on PVC tube of 95mm inner diameter

Devices with small length cylindrical tube were built for the preliminary set-up. However, the light here is very diffused and is not favorable in creating patterns. A second version of light source with a lens has been designed to obtain a collimated light, enabling the use of a mask to create patterns as shown in Section 2.2.1. The LED has been placed at the focus point of the lens.

Design for Array Tube Illuminator

To have more power of light and to allow for experiments using liquid culture, an array of LEDs are used to light a series of test-tubes. This light array has three lines, each comprising four spots with similar intensity and spectrum (Figure 35). The lines are composed of :

First line: Green and far-red 700

Second line: Green and red

Third line: Red and far-red 700

The test- tube holder and the compartmented cap has been printed with a 3D printer with PLA and painted in black (Figure 35)

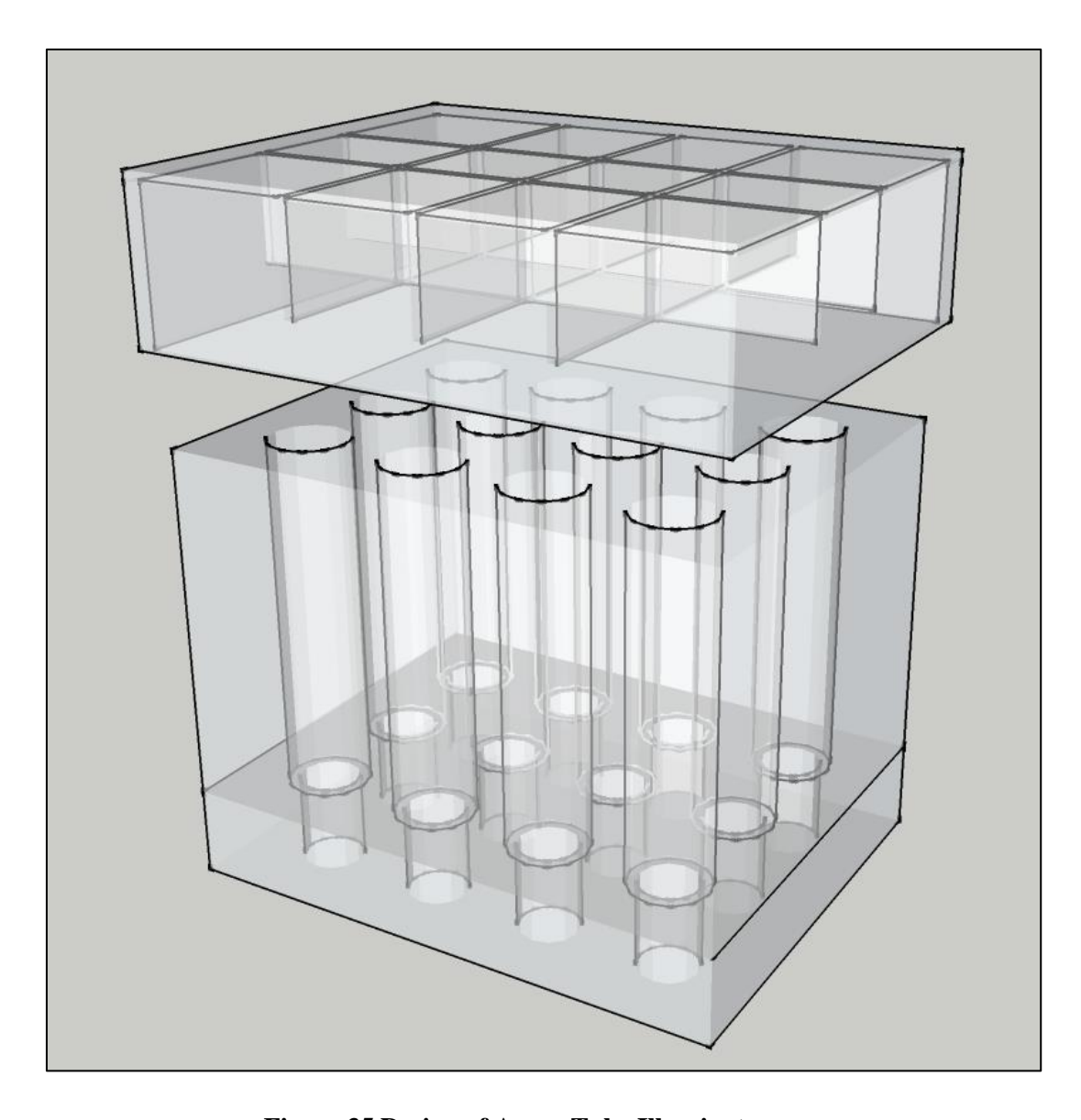


Figure 35 Design of Array Tube Illuminator

To control the intensity of each line, Arduino software (http://arduino.cc/en/Main/Software) was used to generate pulse-width modulation signal (PWM). Six channels of PWM control the six different colours.

The platform Arduino generates the PWM signals, it is a standard signal to control a variable power supply. The pulsed signals (PWM) cannot be used unchanged, a low pass RC filter made by R1 and C1 smooth the signal and prevent a blinking of the LEDs. (Figure 36)

An ideal current generator, build around a NPN transistor 2N2222, is driven by the tension furnished by the filter. An external power supply of 12V is necessary to supply all the LED of the branch. The trimmer resistor R3 enables to adjust the intensity of this branch. The intensity of the green LEDs has been fixed at 5mA and 20mA for other LEDs. The software LTspiceIV was used to make simulations of the circuit to find optimal values of components (Figure 37)

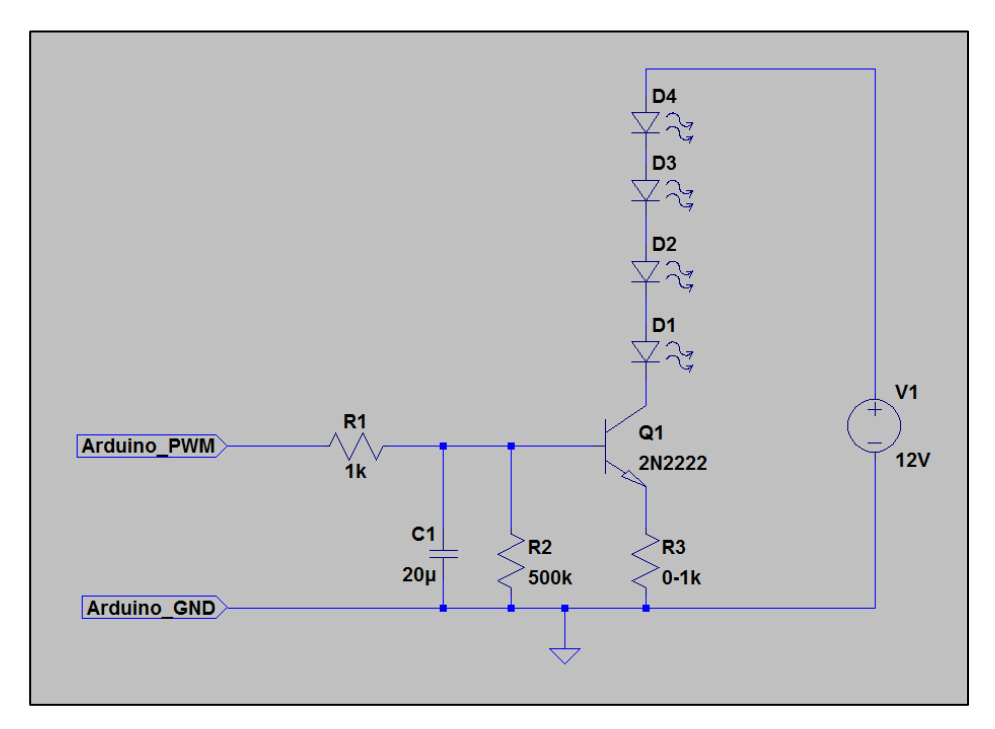


Figure 36 Electronic driver for one line of LED

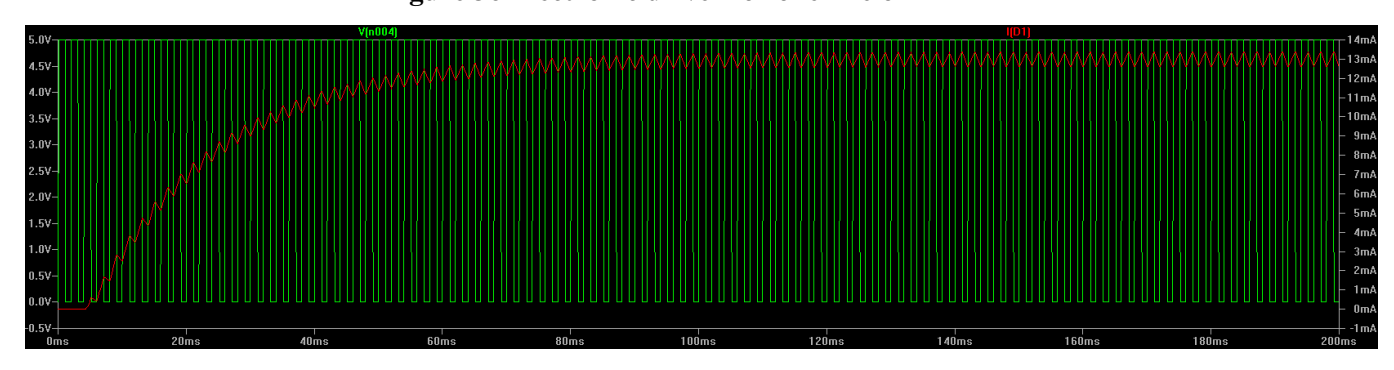


Figure 37 Transient regime simulation of circuit; green line represents a PWM signal at 50% duty cycle from Arduino; red line represents the current in the LED branch.

A custom-made software enables to program the Arduino and to change the duty cycle of PWM signal and allows to control the intensity of the LEDs. Calibration was done with the powermeter. The powermeter sensor was placed inside a tube, 1cm from the bottom. Once the Arduino is programmed, it is autonomous and the device can be placed in an incubator under 37 °C.

4. Calibration of LEDs in Array Tube Illuminator

The Array Tube Illuminator contains 6 lines of LEDs green, red and far-red in combination. Certain mAmp of current is applied to each LED, which corresponds to a certain intensity of light. A software program was written to control the microcontroller, where one can assign values to control the current input, thus controlling the output light intensity. The device was calibrated for this co-relation between the value input in the program and output light intensity. Each line has 4 LEDs and an average of the four LEDs were taken to make the following graphs shown in Figure 38. Green LED intensity in line 1 and line 3 are linear between value 30 to 65. Far-red LED intensity in line 2 and line 6 is not linear but corresponding values give the corresponding light intensity. Red LED intensity in line 4 and line 5 is linear with respect to the values input in Arduino program. Corresponding equations for the value of input in program is determined using linear trend-line for line 4 and line 5. It is much simple to calculate the value input for the red intensity using these equations.

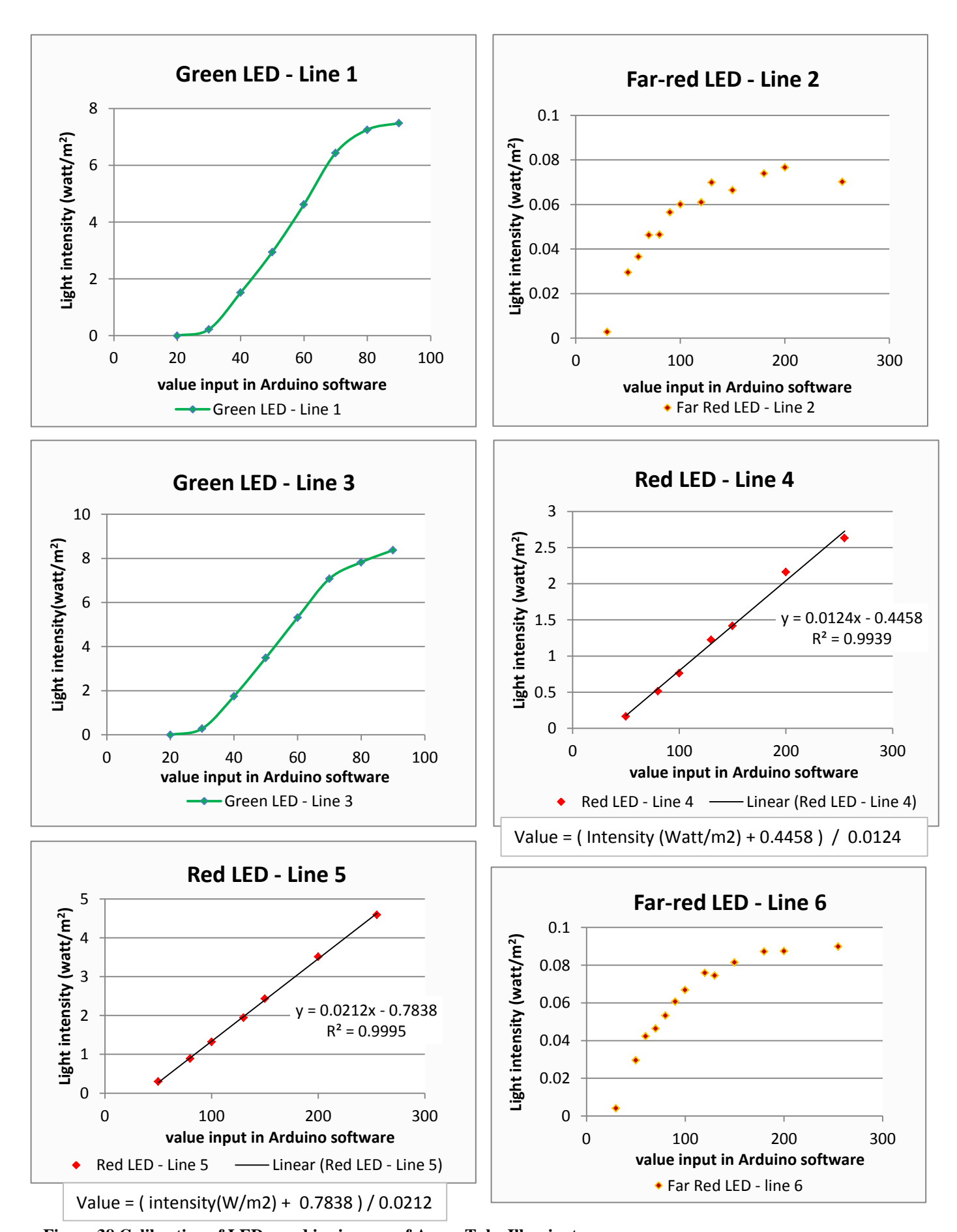
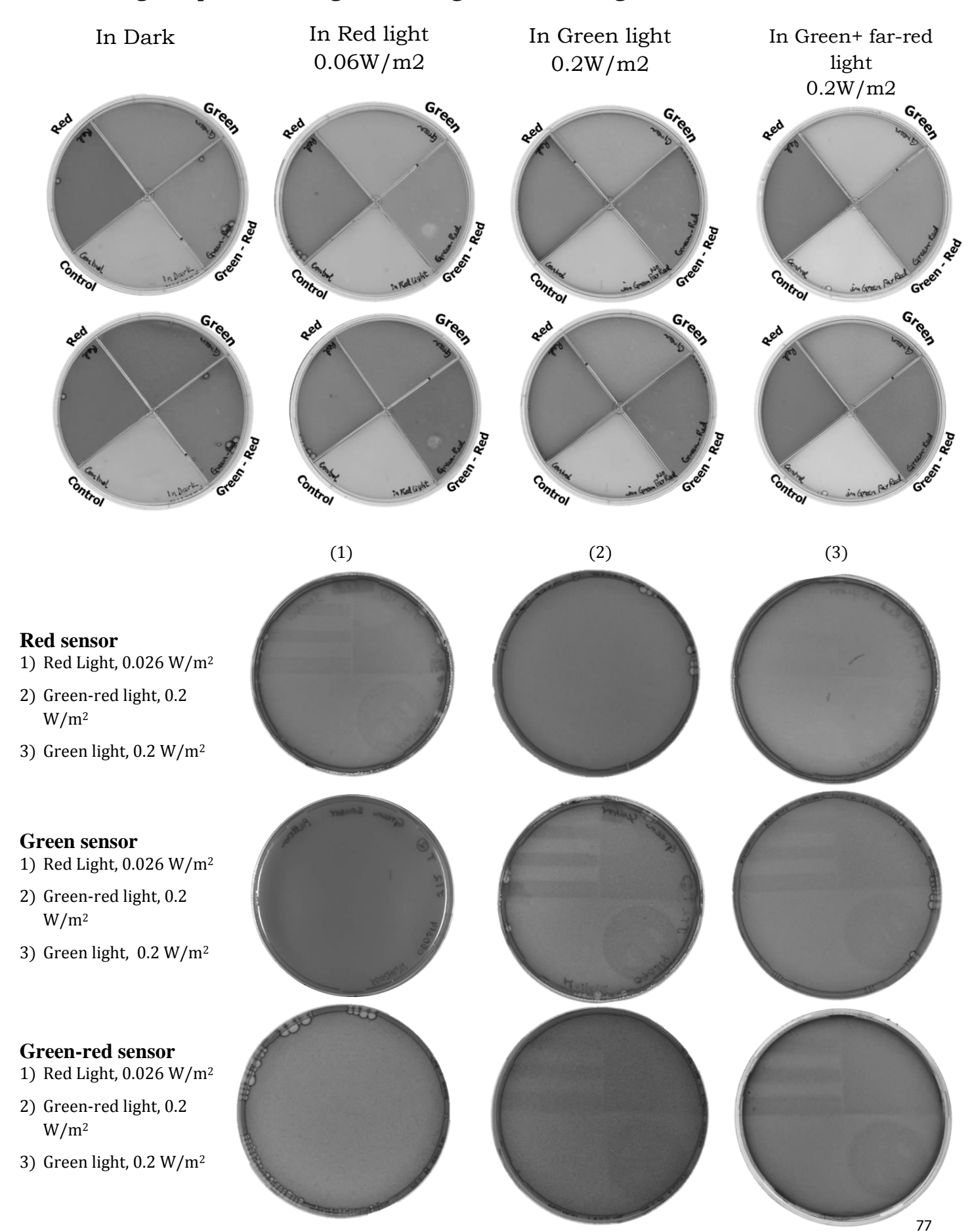
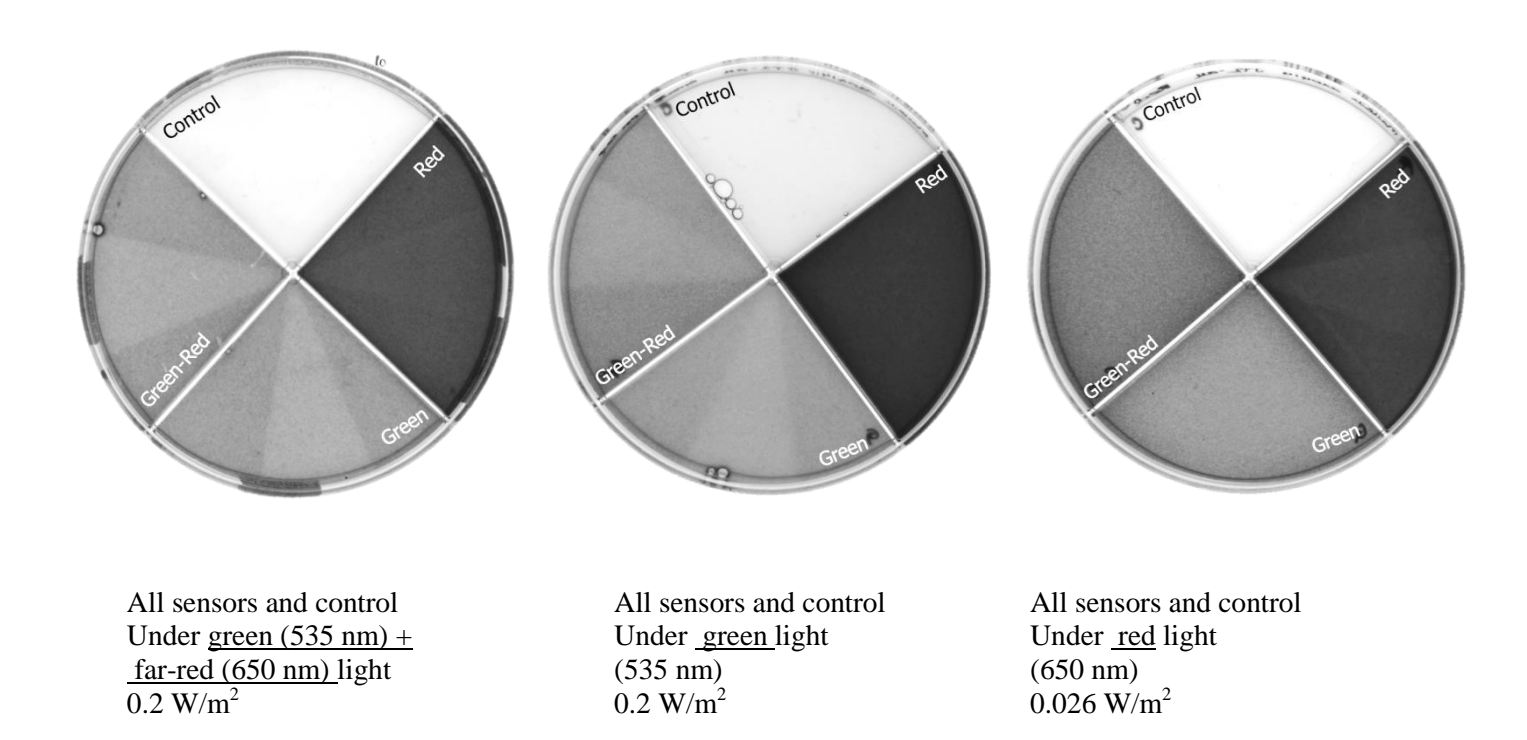


Figure 38 Calibration of LEDs used in six rows of Array Tube Illuminator

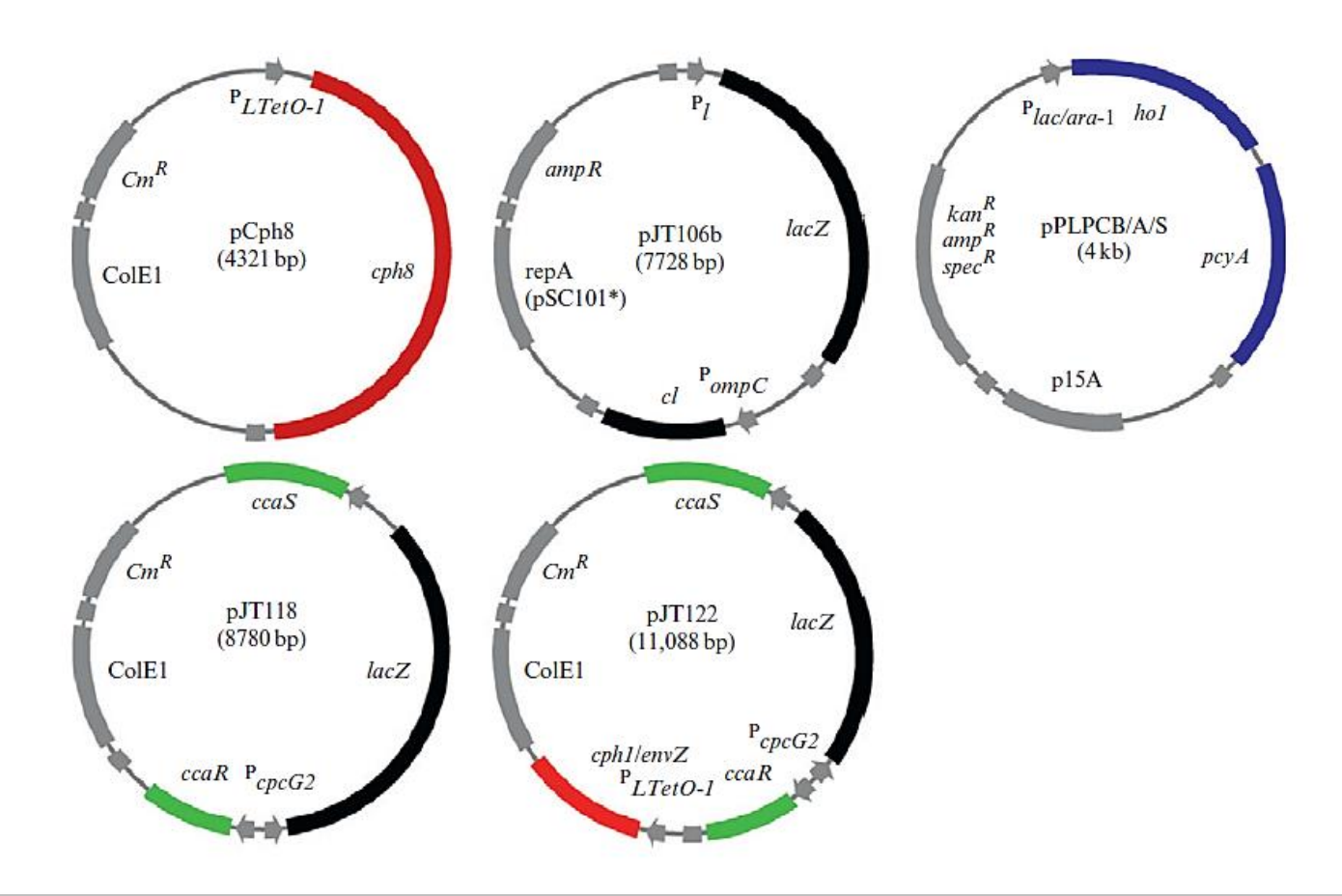
III. Others

1. Original plates for Figure 14, Figure 16 and Figure 19



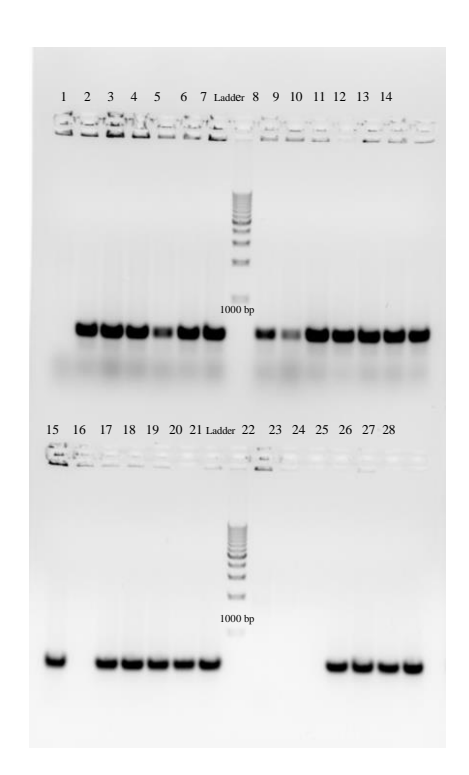


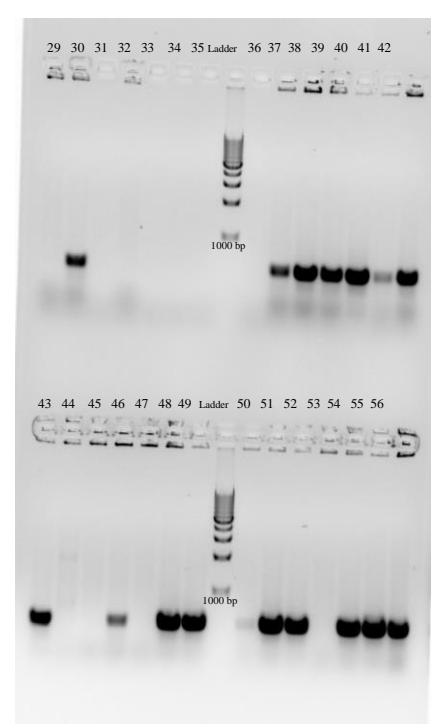
2. Plasmid maps: pCph8, pJT106b, pPL-PCB, pJT118, pJT122 as shown in Tabor et al., 2010.

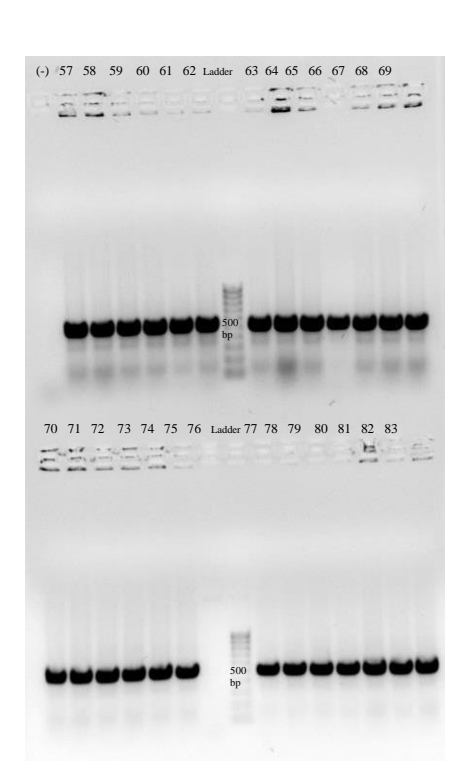


3. Colony PCR on 83 colonies of RBS library by Gibson method (III).

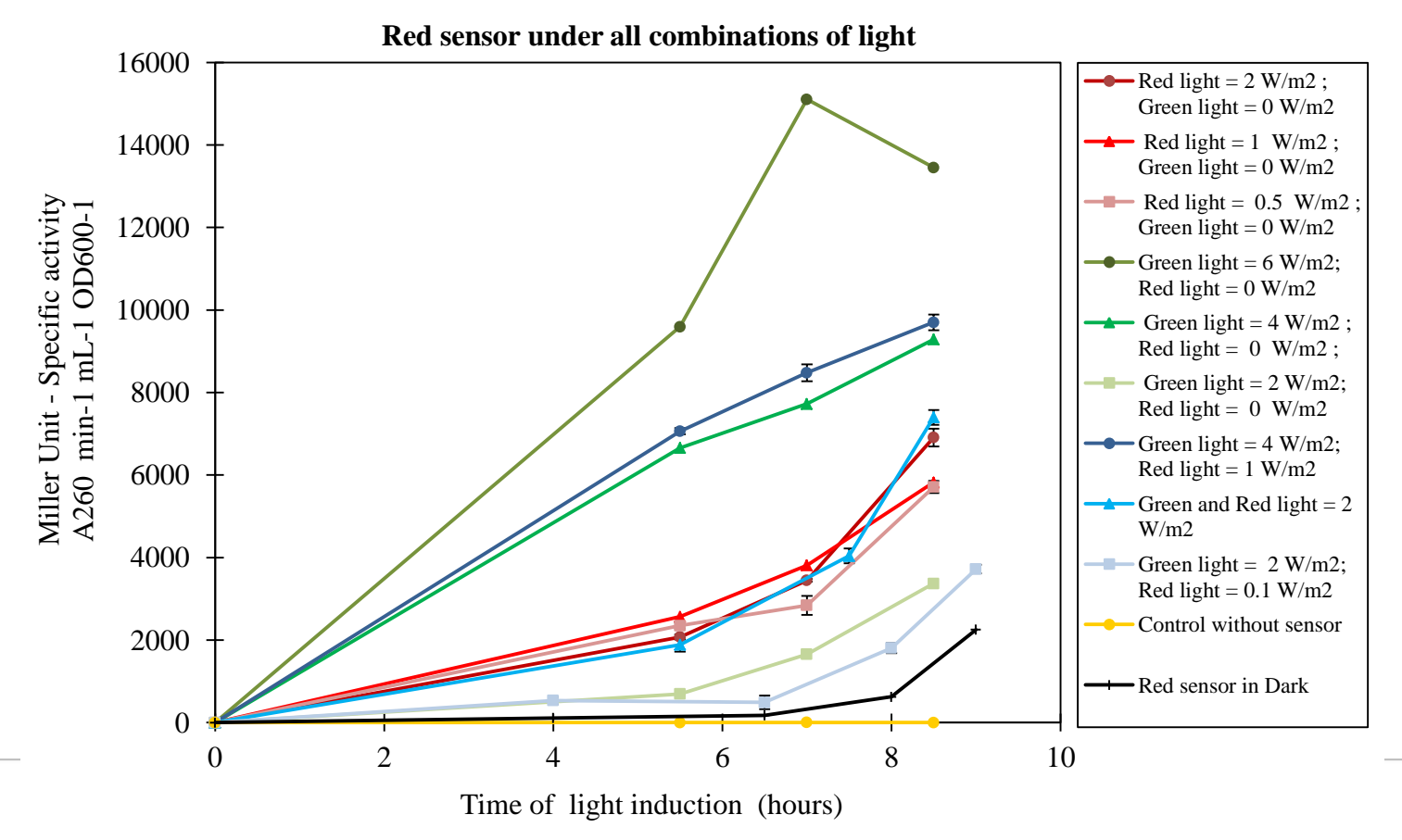
Primers used in colony PCR - AM107: 5' - GGGATTGGTGGCGACGACTC - 3'
AM145: 5' - CCCCATCTTGTCTGCGACAG - 3'

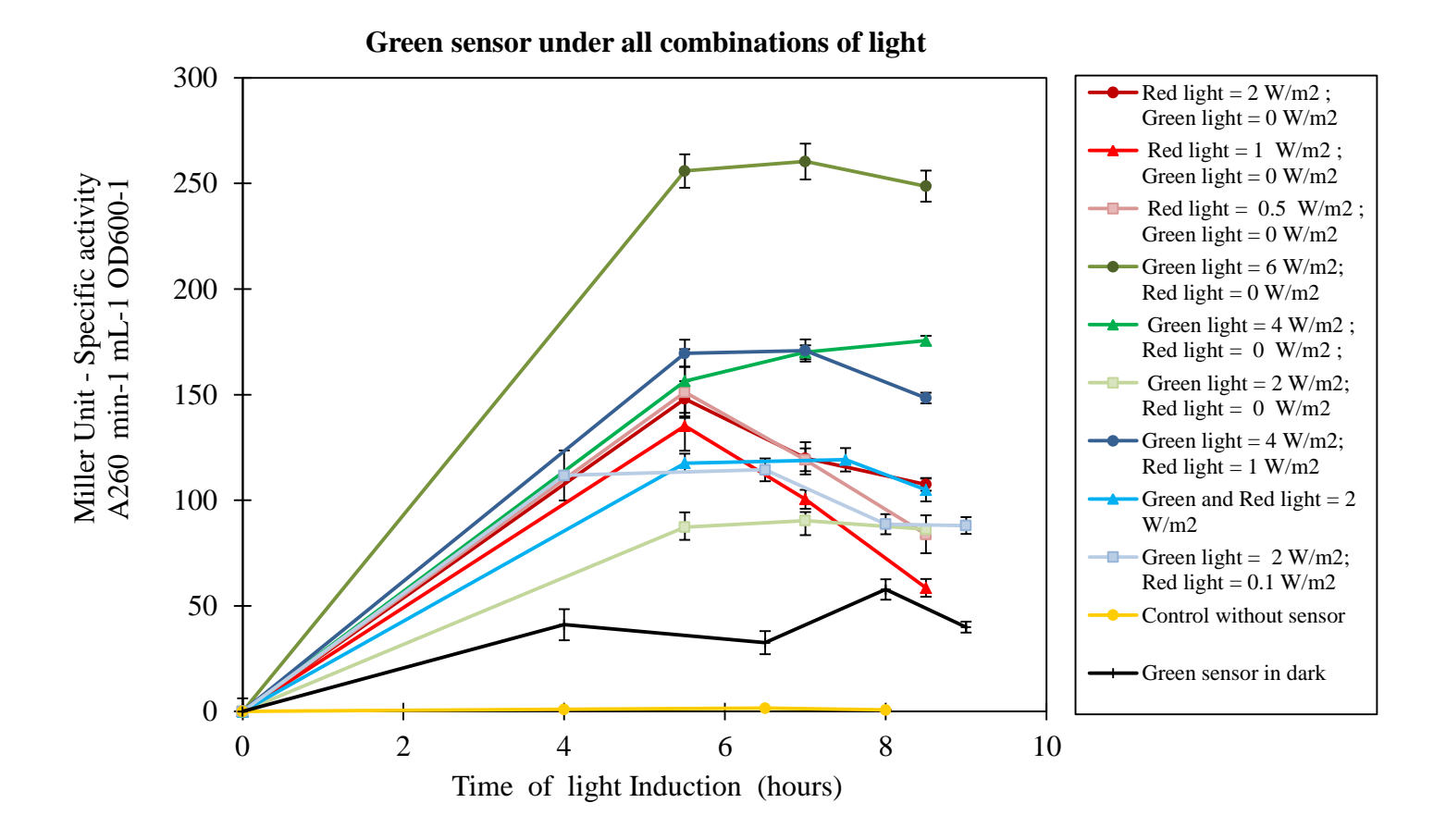






4. Integrated Miller assay graphs for red, green and green-red sensor Detailed description is given in Section 3.4.





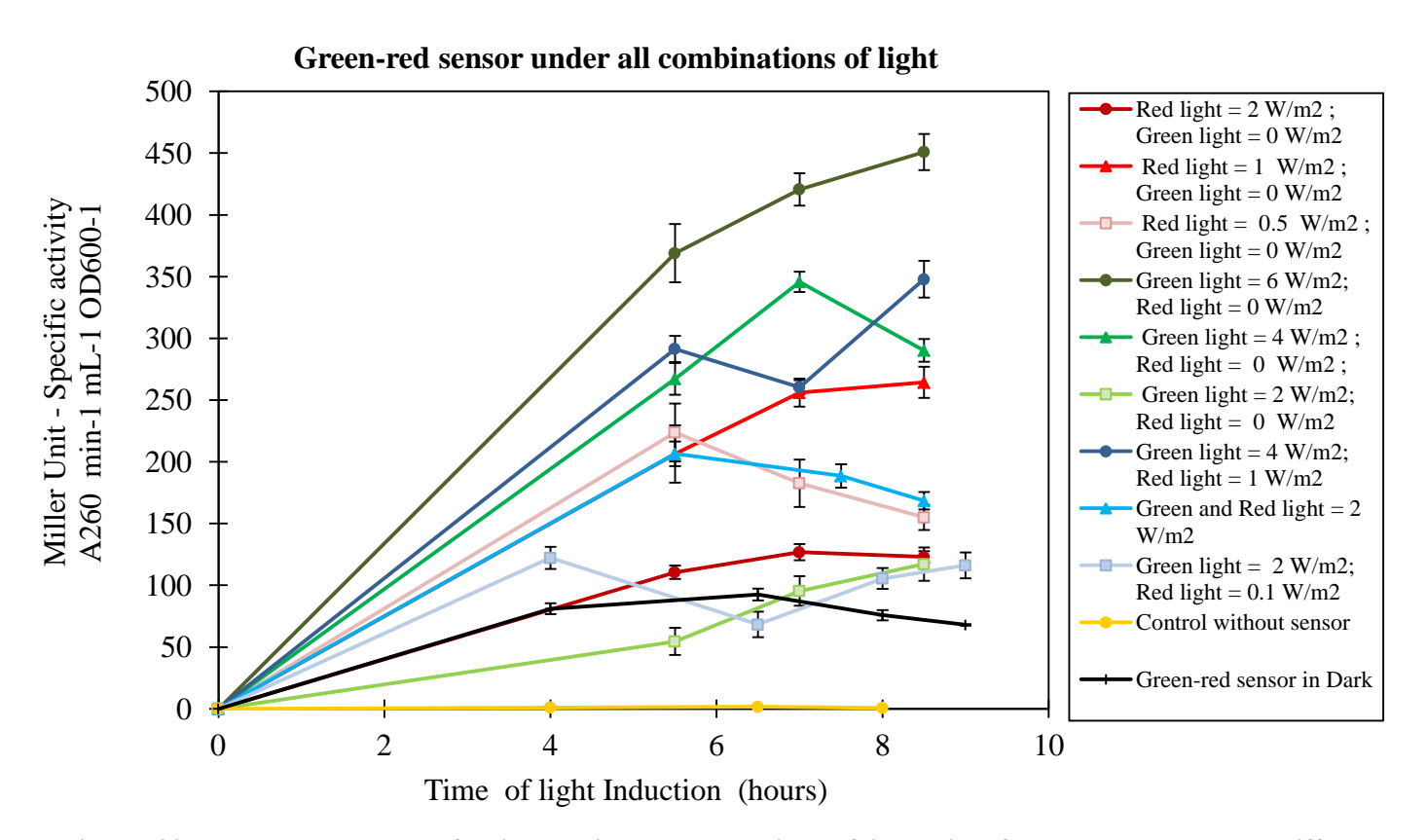


Figure 39 Integrated graphs of Miller unit output vs. time of induction for all sensors under different intensities of light

5. Spectral transfer function in *E. coli*

Figure 40 shows the spectral transfer function in *E. coli* with green and red sensors as shown by Tabor et al., 2010. The cells were exposed to different wavelengths of light and the fold induction over dark-exposed cells was recorded. This was calculated by dividing the Miller unit value of the light induced cells by value of the cells grown in dark. Each data point is an average of four separate cell cultures grown and measured in parallel on a single day.

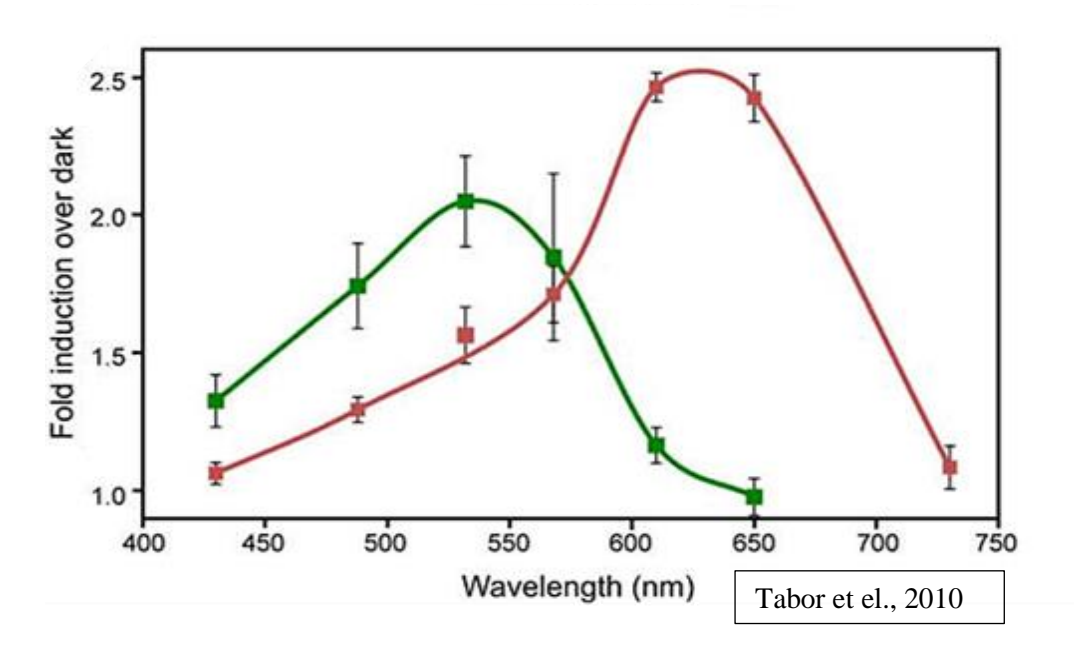


Figure 40 Fold induction over dark for red and green sensor exposed to different wavelengths of light

Figure 41 was shown in Tabor et al., 2010 to characterize the green and red sensors with and without the chromophore PCB. The Miller unit of green and red sensor systems were shown with respect to dark, green and red light. Under both red and green light, the red sensor showed Miller unit outputs. Also output under dark was observed for both green and red sensors. But under the conditions without the PCB molecule, very low Miller units were observed for both green and red sensor. This proved that increase in Miller unit was due the presence of the sensor system and more importantly due to the presence of the light sensing molecule PCB.

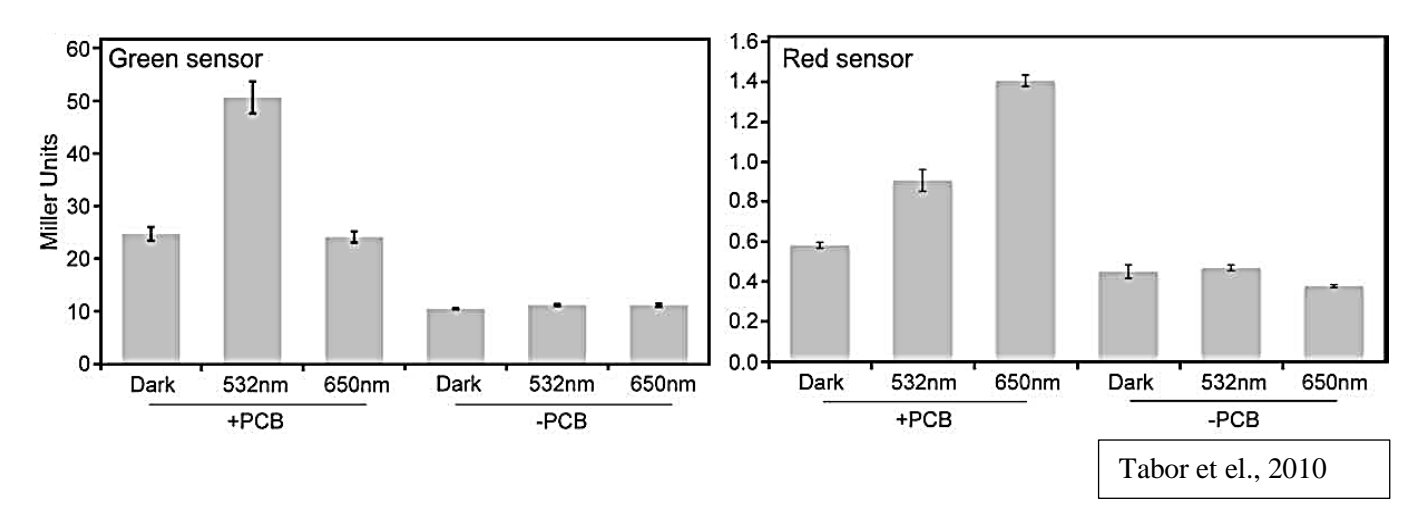
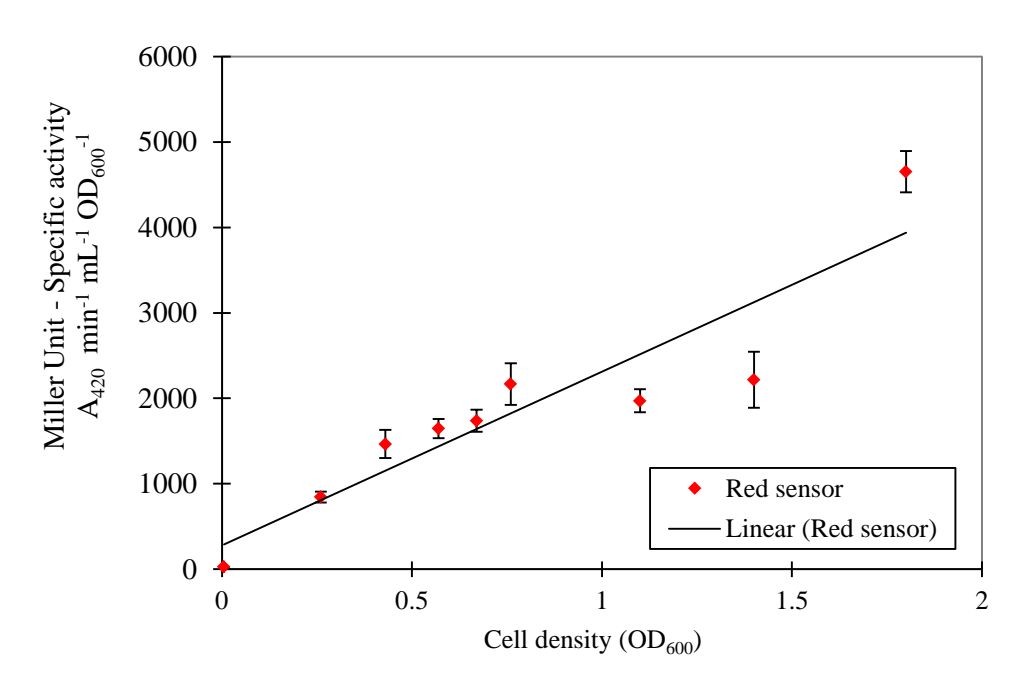


Figure 41 Miller units for green and red sensors under dark, green and red light with and without presence of PCB molecules.

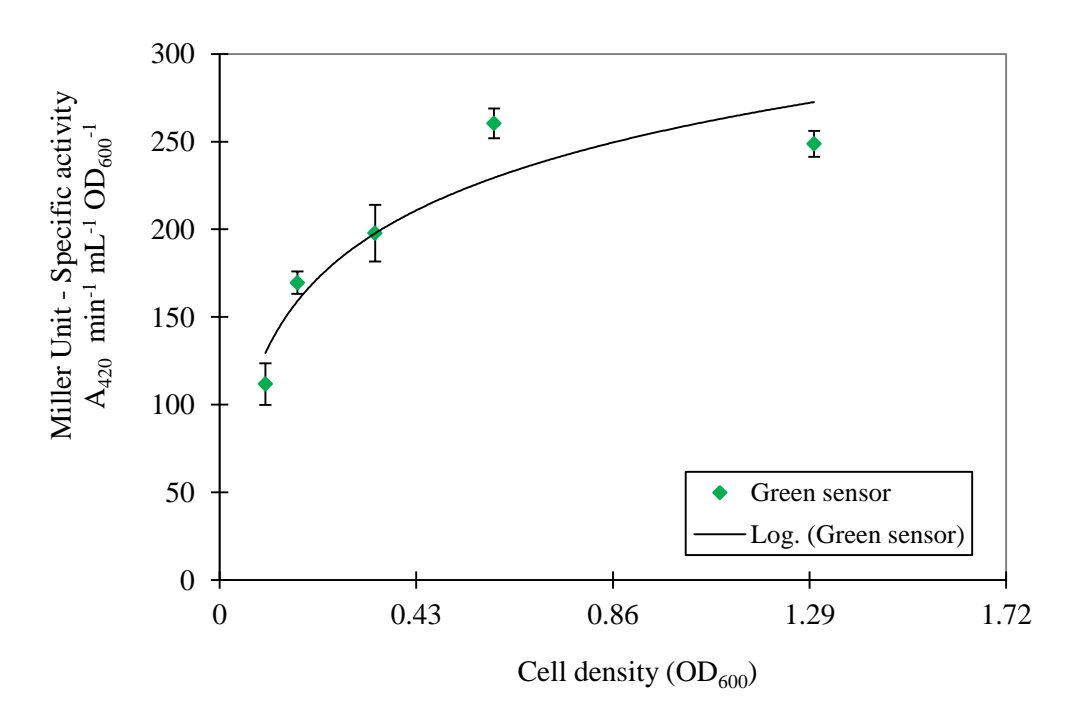
6. Calibration curve for Miller assay

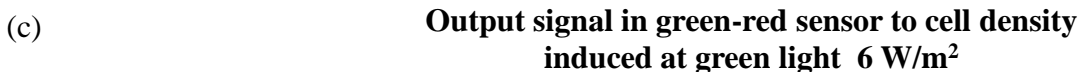
Miller assay was calibrated for each sensor system used in this project. The red sensor was quantified for LacZ at different cell densities shown in Figure 42 (a). There is a linear trend as the number of cells increase. For the green sensor shown in (b), as the number of cells increase an saturation level is reached for the output LacZ. Similarly, for green-red sensor system, a saturate level of output can be seen in (c).

(a) Output signal in red sensor to cell density induced by red light 2 W/m²



(b) Output signal in green sensor to cell density induced at green light 6 W/m²





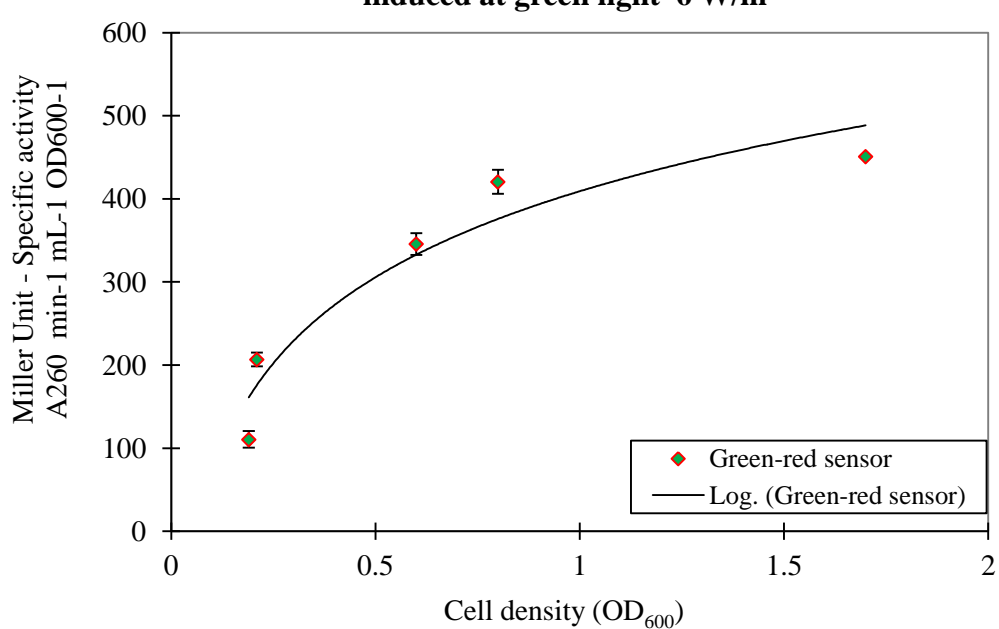
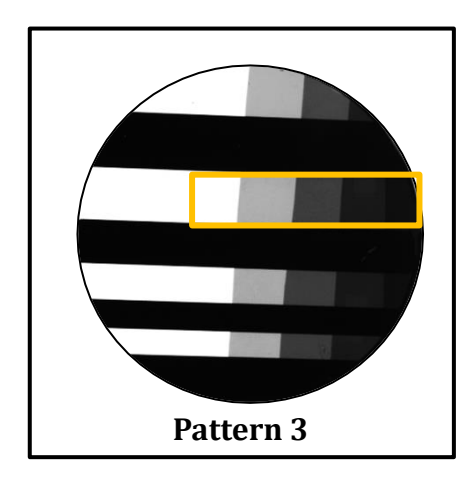


Figure 42 Calibration for each sensor for Miller assay.

7. Calibration curve for ImageJ software



The ImageJ software was calibrated using the pattern 3 shown here. Different intensities of grey on the pattern were analysed using ImageJ. The area without any filter is taken to be 100% light, and then 50%, 25 %, 12.5 % and 6.25 % till the edge of the pattern. The yellow box shown on pattern 3 was quantified and graph was plotted in Figure 43. The value of 100% light was taken as '1' and other values are normalised to it.

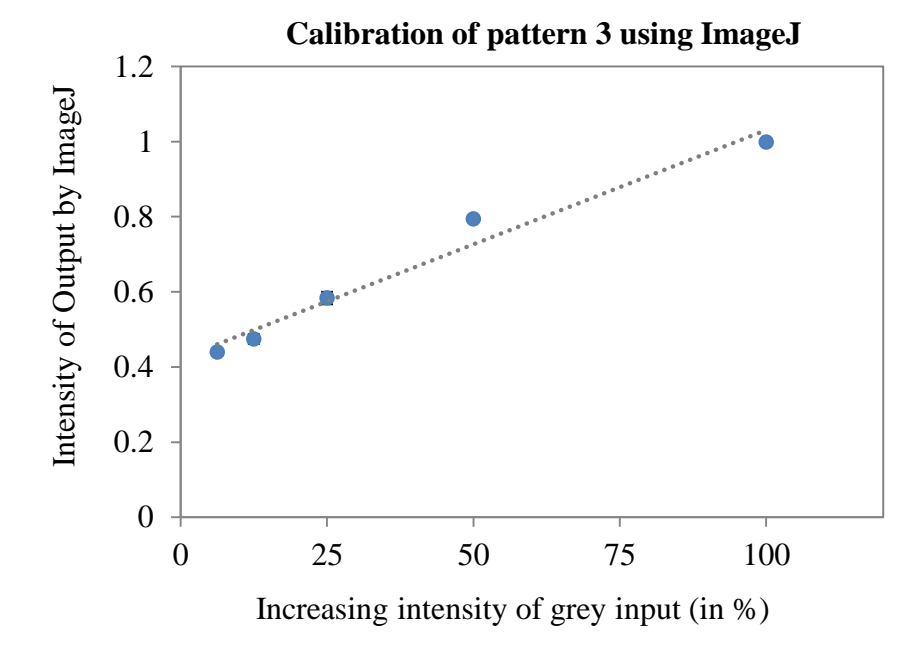


Figure 43 Calibration of pattern 3 using ImageJ software